UNIVERSITAT DE BARCELONA

Identifying new targets to inhibit brat tumour growth in *Drosophila melanogaster* through combined transcriptomics and functional genome-wide analysis

Mª Victoria Méndiz Manero

UNIVERSITAT DE BARCELONA

FACULTAT DE FARMÀCIA I CIÈNCIES DE L'ALIMENTACIÓ

IDENTIFYING NEW TARGETS TO INHIBIT BRAT TUMOUR GROWTH IN DROSOPHILA MELANOGASTER THROUGH COMBINED TRANSCRIPTOMICS AND FUNCTIONAL GENOME-WIDE ANALYSIS

Mª VICTORIA MÉNDIZ MANERO, 2022

UNIVERSITAT DE BARCELONA

FACULTAT DE FARMÀCIA I CIÈNCIES DE L'ALIMENTACIÓ

PROGRAMA DE DOCTORAT: BIOTECNOLOGIA

IDENTIFYING NEW TARGETS TO INHIBIT BRAT TUMOUR GROWTH IN DROSOPHILA MELANOGASTER THROUGH COMBINED TRANSCRIPTOMICS AND FUNCTIONAL GENOME-WIDE ANALYSIS

Memòria presentada per
Mª Victoria Méndiz Manero
per optar al títol de doctor per la Universitat de Barcelona
2022

Director:
Cayetano González Hernández,PhD

Tutor:
Manuel Palacín, PhD

Institute for Research in Biomedicine Barcelona (IRB Barcelona)
Cell Division Laboratory

Abstract

I have used the brain tumours that originate in Drosophila larvae upon depletion of the *brain tumor* (*brat*) gene as a model to study neoplastic malignant growth. I have used genetic analysis to interrogate the Drosophila genome for genes that can be targeted to inhibit the development or arrest the growth of brat tumours. The targetable genome identified through this functional genomics approach includes 80 suppressors of brat tumour growth (brat-SPRs). I have also carried out transcriptomic analysis of brat tumours through which I have been able to define a brat tumour signature that includes 625 and 903 genes that are significantly up- and down-regulated in brat larval brain tumours compared to normal larval brains. From the combined analysis of my functional genomics and transcriptomics data I have concluded that correlation between the extent of gene expression dysregulation and function with regards to tumour development is so low that the former is not a good predictor of the latter. From the combined analysis of my own data on brat tumours and published functional genomics and transcriptomics data on the brain tumours that originate upon depletion of *lethal(3)malignant brain tumor* (*l(3)mbt)*, henceforth referred to as mbt tumours, I have found that nearly 60% (47/80) of the brat-SPRs are tumour-type specific in the sense that they do not suppress mbt tumours. One of the non-tumour specific suppressors (i.e. mbt&brat-SPRs) identified in my study is *Vacuolar protein sorting 26* (*Vps26*). Vps26 had been reported to be a type II neuroblast lineage-specific tumour suppressor. My results show that in addition, Vps26 function contributes to brat tumour growth and is essential for long-term survival of mbt tumours. My results also suggest that unlike its published tumour suppressor function, Vps26 mbt&brat-SPR activity might be independent of its role in the retromer complex.

Resumen

En este trabajo he utilizado los tumores cerebrales que se originan en larvas de Drosophila mutantes para el gen *brain tumor* (*brat*) como modelo para el estudio del crecimiento de neoplasias malignas. Mediante análisis genético he cribado el genoma de Drosophila en la búsqueda de genes cuya inactivación dé lugar a la inhibición de la formación o del crecimiento sostenido de tumores brat. El conjunto de genes diana identificado a través de este enfoque de genómica funcional incluye 80 supresores de tumores brat (brat-SPRs). Así mismo he obtenido el transcriptoma de tumores brat de cuyo análisis he podido definir una "tumour signature" que incluye 625 and 903 genes cuya expresión está significativamente aumentada o disminuida en tumores brat con respecto a cerebros normales. Mediante el análisis combinado de mis resultados de genómica funcional y transcriptómica he podido concluir que la correlación entre el grado de desregulación de la expresión génica y la función del gen en relación con el desarrollo del tumor es tan reducida que el primer factor no puede ser utilizado para predecir el segundo. Del análisis combinado de mis datos sobre los tumores brat y de datos publicados de genómica funcional y transcriptómica de tumores cerebrales causados por la falta de función del gen *lethal(3)malignant brain tumor* (*l(3)mbt*) ("tumores mbt") he observado que cerca del 60% (47/80) de los brat-SPRs son específicos de este tipo de tumor en el sentido de que su falta de función no suprime los tumores mbt. Uno de los supresores comunes para ambos tumores (mbt& brat-SPRs) identificados en mi trabajo es *Vacuolar protein sorting 26* (*Vps26*). Datos publicados previamente demuestran que *Vps26* funciona como supresor tumoral específicamente en el linaje de neuroblastos tipo II. Mis resultados revelan que, además, Vps26 contribuye al crecimiento de los tumores brat y es esencial para la supervivencia a largo plazo de los tumores mbt. Mis resultados también sugieren que a diferencia de su actividad como supresor tumoral, la función de Vps26 como mbt&brat-SPR parece ser independiente de su papel en el complejo del retrómero.

Acknowledgements

I would like to deeply thank my PhD supervisor Dr. Cayetano González, for the opportunity to carry out my PhD Thesis in his laboratory, and for the guidance that help me develop this Project through his wide knowledge and exceptional critical thinking.

I would like to express my sincere gratitude to all my laboratory colleagues for their scientific suggestions, patience and personal support. Thanks to Salud for helping me with Drosophila genetics. I am really thankful to Pepe for all the scientific explanations and unforgettable non-scientific discussions. Thanks to Piet for teaching me to perform complex experiments through his didactic approach. Special thanks to Cristina for helping me with transcriptomic data and her writing advices. I specially thank my bench-mates Anastasia and Serena for their kindly support. I would also like to thank former lab members Ánxela, Fabrizio, Édel, Judit, Andrea, Madhulika, Julia, specially to Giulia and Trini.

I would like to thank the members of my Thesis Advisory Committee (TAC), Jens Lüders, Julián Cerón and TAC member and tutor Manuel Palacín for their useful comments and supervision during the progress this thesis project. I have to thank the members of the IRB administration and facilities for their bureaucratic and scientific support during these years.

I am very thankful to the Spanish Ministerio de Ciencia e Innovación which granted me a fellowship for accomplishing my PhD at IRB Barcelona (Ayudas para contratos predoctorales para la formación de doctores 2016 BES-2016- 079010).

Finally, an incredibly thanks to all my friends and family.

A amebas, AnaRo, Ester A., Ester M., Inés, Marta y Luis. También a Xavi y Mireia por el apoyo, consejos y momentos compartidos desde la carrera tanto en Barcelona como en Zaragoza.

A amigos: Alma, Benja, Diego y familiares: Sonia, Carlos, Carla, Imanol, especialmente a mi tío Chato y mis abuelos por el ejemplo y el amor que me dan. Gracias a mis padres y mi hermana Andrea por inculcarme el gusto por aprender y estar siempre a mi lado.

Contents

List of Abbreviations

The following list describes several abbreviations that will be later used within the body of the document.

AEL	After egg laying
ALH	After larval hatching
aPKC	atypical Protein Kinase C
Ase	Asense
a.u.	arbitrary units
Baz	Bazooka
BDSC	Bloomington Drosophila Stock Center
bHLH	Basic helix-loop-helix domain
BP	Biological Process
Brat	Brain tumor
brat-SPR	brain tumor suppressor
CB	Central brain
CC	Cellular component
cDNA	complementary Desoxi-RiboNucleic Acid
CNS	Central nervous system
CT	Cancer testis
DAPI	4,6-diamidino-2-phenylindole
DAVID	Database for Annotation, Visualization and Integrated Discovery
Dcr	Dicer
Dlg	Discs large
Dpn	Deadpan

DTT	Ditiotreitol
Eag	Ether a go-go
ETC	Electron Transport Chain
FACS	Fluorescence-activated cell sorting
FC	Fold change
FDR	False discovery rate
GFP	Green Fluorescent Protein
GMC	Ganglion Mother Cell
GO	Gene ontology
GSC	Glioblastoma stem cells
Gαi	G protein α i subunit
Hsap	*Homo sapiens*
INPs	Intermediate neural progenitors
Insc	Inscuteable
IPC	Inner Proliferative Center
Klu	Klumpfuss
L(3)mbt	Lethal(3) malignant brain tumor
Lgl	Lethal (2) malignant larvae
MB	Mushroom body
mb-Feret	Maximum brain Feret diameter
mbt	Lethal(3) malignant brain tumor
mbt-SPR	Lethal(3) malignant brain tumor suppressor
mbt&brat-SPRs	Lethal(3) malignant brain tumor and brain tumor suppressors
MBTS	Lethal(3) malignant brain tumor signature
mei-W68	meiotic W68
MF	Molecular function

Mira	Miranda
NB	Neuroblast
NE	Neuroepithelia
NSC	Neural stem cells
OL	Optic lobe
OPC	Outer Proliferative Center
OxPhos	Oxidative Phosphorylation
P	p-value
PcG	Polycomb Group
PBS	Phosphate Buffer Saline
PBST	Phosphate Buffer Saline with 0.3% Triton
PBSTF	Phosphate Buffer Saline with 0.3% Triton and 10% Fetal Calf Serum
Pon	Partner of Numb
Pros	Prospero
RFP	Red fluorescent protein
RT-qPCR	Reat time quantitative polymerase chain reaction
RNAi	RiboNucleic Acid interference
RNAseq	Ribo Nucleic Acid sequencing
SAM	Sterile alpha motif
SD	Standard deviation
SDS	Sex dimorphic signature
SPRs	Suppressors
Tb	Tubby
Tctp	Translationally controlled tumor protein
Tll	Tailless

TRIM	Tripartite motif containing protein
Ubi	Ubiquitin
UAS	Upstream Activation Sequence
VDRC	Vienna Drosophila Resource Center
VNC	Ventral nerve cord
Vps	Vacuolar protein sorting
wg	wingless
wls	wntless
wt	Wild type
Wor	Worniu
Udd	Under development
Zld	Zelda

List of Figures

List of Tables

1.Introduction

1.1. *Drosophila melanogaster* as a model system

Drosophila melanogaster, commonly named as fruit fly or vinegar fly, is a holometabolous that presents four developmental stages: embryo, larva (which includes 3 instars) pupa, and adult. The complete life cycle takes 10 days at 25ºC (Fig. 1.1.).

Drosophila was first used as an experimental model by T. H. Morgan. Morgan himself and his colleagues (notably Sturtevant, Bridges, and Muller) not only carried out the seminal experiments that paved the way for Drosophila to become the paradigm of genetically tractable multicellular organism of choice that it is today but also contributed major landmarks in biology like the demonstration of the chromosomal theory of heredity, the finding of the effect of ionizing radiations on the genome, and the discovery that genes map at fixed distances that can be experimentally measured (Bateson, 1916; Morgan & Bridges, 1916; Muller, 1927, 1928).

Decades after Morgan and colleagues' seminal work, research in Drosophila made it possible to discover the main signaling pathways that orchestrate the design of the body plan in an animal embryo (reviewed in Wieschaus and Nüsslein-Volhard 2016) and made a major contribution to the discovery of the molecular bases of innate immune response (Hoffmann & Reichhart, 2002) and the biological clock (Hardin et al., 1990; Konopka & Benzer, 1971), to cite but a few out of many key discoveries carried out in Drosophila laboratories.

1.1.1. Advantages

Small size, simple husbandry, short generation time, and the highly prolific nature of Drosophila are indeed advantageous. However, in addition to these, Drosophila presents other features that account for its success as an experimental model system. One of the most important ones is that beyond their apparent simplicity, insects are complex metazoan that share many key features with higher organisms like sensory and motor systems, sexual behaviour, the ability to learn and memorise, innate immunity, complex systemic signaling, and a segmented body plan. Also importantly, the Drosophila genome has a high extent of homology to the human genome but a much reduced level of redundancy (Adams et al., 2000), which greatly facilitates gene inactivation.

Other significant advantages of Drosophila as a model for experimental research include the absence of meiotic recombination in males, its very simple karyotype, the presence of giant polytene chromosomes, and the availability of synthetic balancer chromosomes, to cite only those that are particularly relevant from the experimental point of view.

Adding to these "built in features", the extensive research activity carried out in Drosophila for more than a century has resulted in impressive material resources including dozens of cell lines, tens of thousands of fly lines carrying mutants, enhancer and protein traps, and nearly genome-wide double-stranded RNAs for RNA interference (RNAi) (D'Avino & Thummel, 1999; Dietzl et al., 2007; Ni et al., 2009). The same applies to available techniques that include, among many others, high-resolution microscopy of *ex-vivo* and *in-vivo* organs and standardised protocols to inactivate or misexpress almost any gene in a timely and tissue-specific or even cell-specific manner (Brand & Perrimon, 1993; D'Avino & Thummel, 1999; Hales et al., 2015; Rebollo & González, 2000).

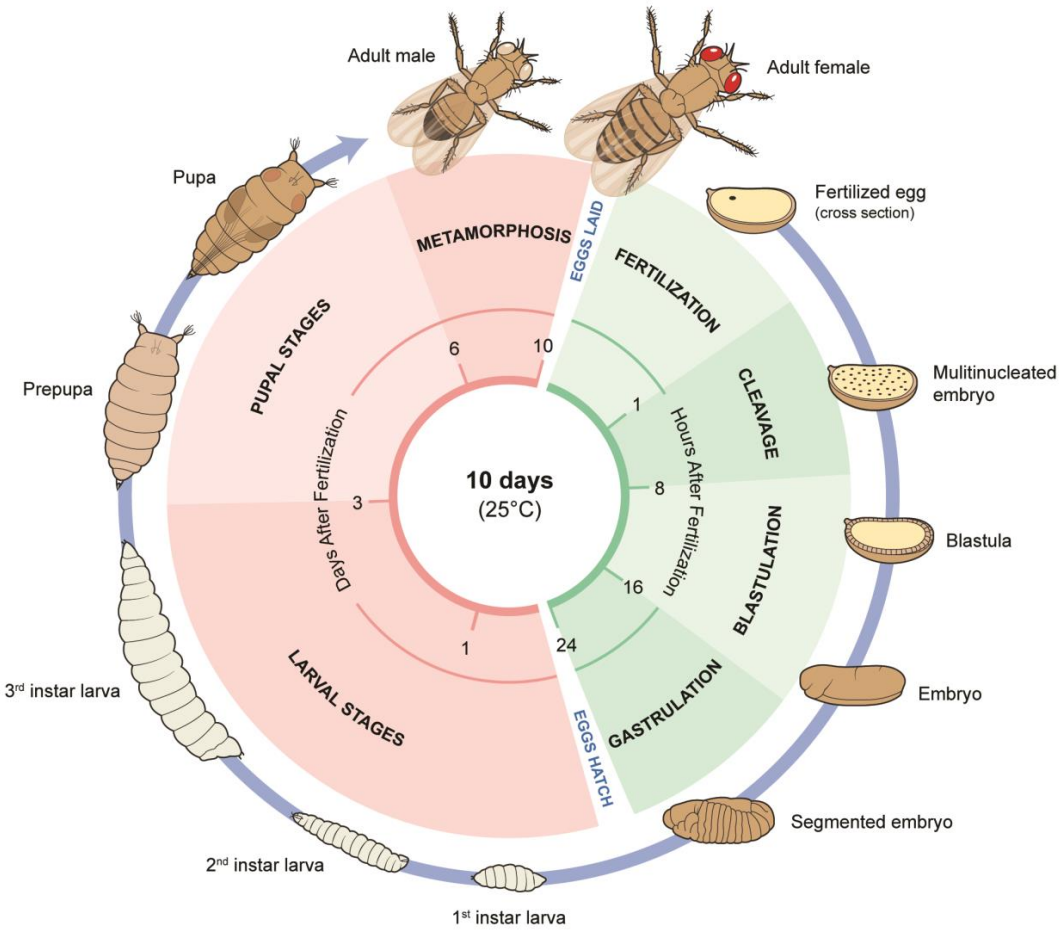

Figure 1.1. Life cycle of *Drosophila melanogaster*. The *Drosophila* life cycle is divided into four stages: embryo, larva, pupa, and adult. The time length of the stages is shown in hours for embryos and days for larvae and pupae. Image from (Shahzad et al., 2021).

1.1.2. Limitations

Like any model system, Drosophila has limitations that must be taken into account when choosing it as experimental model. Thus for instance, flies do not have some tissue types that are present in mammals, such as cartilage, bone and blood. The same goes for certain organs. Drosophila's corpora cardiaca and fat body carry out some of the functions that pancreas, liver and adipose tissue perform in mammals, but are different from these organs in several important regards. Along these lines, Drosophila lacks adaptive immune response and unlike mammals, its circulatory system is opened. This is indeed important for cancer studies because the absence of veins and arteries precludes the modelling of metastatic intravasation and extravasation. Regarding cancer studies, the very simple Drosophila karyotype, made only of four chromosome pairs is a major drawback for modelling the effect of aneuploidy because the gain or loss of a single chromosome affects thousands of genes and is a necessarily lethal event in most cell types. Finally, on a more technical note, it is worth mentioning the lack of protocols to keep Drosophila strains frozen as a current major drawback (Prüßing et al., 2013).

1.1.3. Disease model

The 75% of the genes causing diseases in humans have homologues in Drosophila (Halligan & Keightley, 2006; Ugur et al., 2016). But the extent of homology is even better substantiated by functional data. These can be derived from "humanized" Drosophila strains engineered to carry a human (Hsap) gene instead of the corresponding Drosophila homologue (Bellen et al., 2019). In 2016, Fernandez-Hernandez and colleagues (Fernández-Hernández et al., 2016) reported 135 such genes, but of course this number has been steadily increasing as new Drosophila Hsap lines are constructed and more human genes are put to the test. It is currently impossible to know what the final count of functionally equivalent genes will be, but it is likely to be high taking into account that the corresponding number in *Saccharomyces cerevisiae* is 40%.

Fueled by the conservation of molecular pathways as well as by its advantages as an experimental model discussed before, numerous Drosophila models of different diseases have been implemented in recent years. Included among them are models of aging (Piper & Partridge, 2018), infectious diseases (Harnish et al., 2021), cystic fibrosis (K. Kim et al., 2020), nicotine exposure (Velazquez-Ulloa, 2017), diabetes (Graham & Pick, 2017), anti-viral immunity (J.-H. Wang, 2010) and neurodegenerative diseases (Bolus et al., 2020).

1.1.4. *Drosophila melanogaster* in cancer research

Indeed, Drosophila has also been used to develop a wide variety of cancer models. Through experimental manipulation it is possible to generate tumours in a variety of organs in Drosophila, both in developing larvae and in adult flies (Reviewed in Richardson and Portela 2018; Gonzalez 2013; Mirzoyan et al. 2019; Enomoto, Siow, and Igaki 2018).

These tumours range from hyperplasias to frankly malignant neoplasias that exhibit some of the classic hallmarks of mammalian cancer. Several of these tumour models are being used to investigate specific issues related to malignant growth like genome instability (Castellanos et al., 2008; Clemente-Ruiz et al., 2016), metastasis (Stuelten et al., 2018), or cachexia (Figueroa-Clarevega & Bilder, 2015; Saavedra & Perrimon, 2019). Moreover, Drosophila models of tumour growth have also been implemented to screen for new and to optimise available active compounds to treat the disease (Dar et al., 2012; Fernández-Hernández et al., 2016; Gladstone & Su, 2011; Gonzalez, 2013).

In addition to experimentally induced tumours, natural hyperplasias in testis and gut are frequent in ageing adult flies (Regan et al., 2016; Salomon & Jackson, 2008). Moreover, because haploidy for the strong tumour suppressor *lethal(2)giant larvae* (*lgl)* increases resistance to stress conditions, deficiencies uncovering the *lgl* locus are widespread in wild Drosophila populations, and, thus, larvae affected by lgl tumours must not be infrequent in nature (Golubovsky et al., 2006).

Most of the numerous genes that classify as tumour suppressors (TS) in Drosophila are linked to tumours (overgrowth) that develop in imaginal discs, are not invasive, and undergo terminal differentiation together with the surrounding wild-type tissue thus resulting in an ectopic structure that has little effect in the individual's fitness and lifespan (Bilder, 2004; Watson et al., 1994). Others, however present much greater proliferative capacity. To categorise Drosophila tumours, Gateff applied in flies what is now the golden assay for malignancy in vertebrates: to implant the tissue of interest into a healthy host (allograft culture, also known as 'dauer' culture) (Gateff, 1978; Gonzalez, 2007; Rossi & Gonzalez, 2015). The results from this assay are conclusive. Wild-type tissue never grows; benign hyperplasias grow slowly, do not invade other tissues, and retain the capacity for differentiation; malignant neoplasms, grow limitlessly, colonise distant organs, kill the host, and become immortal such that they can be re-allografted for years.

1.2. Tumorigenesis in the larval central nervous system

The Drosophila larval brain presents three distinct main regions: the ventral nerve code (VNC), which is subdivided in abdominal and thoracic segments; and the two brain lobes, each of which is subdivided in central brain (CB) and an optic lobe (OL) (Hartenstein et al., 2008). For reasons that remain unknown, most of the malignant neoplasms that can be experimentally induced in Drosophila develop in the larval brain. Each tumorigenic condition presents a specific cell-of-origin and therefore brings about tumours that develop in certain brain regions only. Notably, aside from gliomas (Portela et al., 2020; Read et al., 2009; Shohayeb et al., 2020; Witte et al., 2009), all brain malignant neoplasms in the fly develop from the neuroepithelial (NE) region of the OL, the CB and /or the VNC (Bowman et al., 2008; Gateff, 1978; C. Richter et al., 2011; Southall et al., 2014). In particular, the two tumour types that I have analysed in detail, brat and mbt, originate from Type II neuroblasts (NBs) and the NE, respectively.

1.2.1. Larval neuroblasts

Drosophila NBs are neural stem cells that generate the fly's central nervous system through repeated rounds of self-renewing asymmetric divisions. The NBs in the CB and VNC arise from the neuroectoderm of the early embryo. OL neuroblasts are generated in larval stages from the neuroepithelial cells of the optic anlagen (Egger et al., 2008; Kang & Reichert, 2015).

According to the type of lineage, larval NBs can be divided in Type I and Type II. Type I NBs divide to produce another type I NB and a ganglion mother cell (GMC), which divides once to produce two differentiating daughter cells that will become either neurons or glia. In contrast, type II NB division give rise to another type II NB and a, intermediate neural progenitor (INP). INPs can undergo several rounds of asymmetric division generating a self-renewed INP and GMCs (Bello et al., 2008; Boone & Doe, 2008; Bowman et al., 2008). (Fig. 1.2.B). There are approximately 180 type I NBs that are distributed along CB and VNC, and only 16 type II NBs that concentrate on the dorsal side of the CB. (Fig. 1.2.A). Although less abundant than Type I, the transit amplifying compartment of INPs increases exponentially the tissue generating capacity of Type II NBs. Operationally, expression of the transcription factors Asense (Ase) and Deadpan (Dpn) identify these two types of neuroblasts. Type I NBs can be distinguished as Ase+ Dpn+ cells as opposed to Type II that are Ase- Dpn+. New born immature INPs turn off Dpn that is later re-expressed together with Ase in mature INPs (Bello et al., 2008; Boone & Doe, 2008; Bowman et al., 2008; Jiang & Reichert, 2014; Song & Lu, 2011; Xiao et al., 2012).

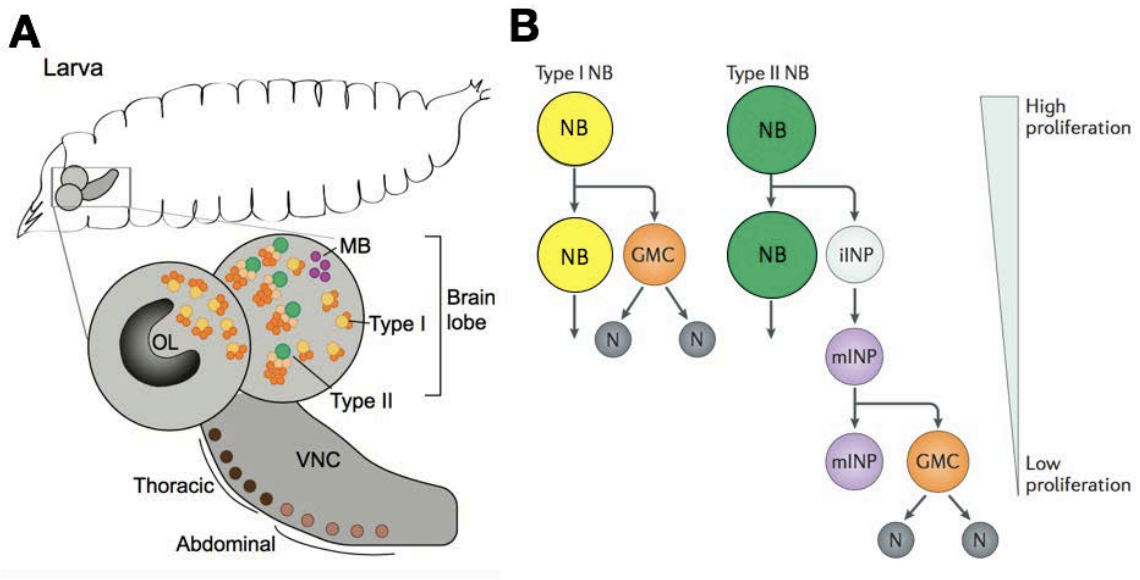

Figure 1.2. Neurogenesis in Drosophila melanogaster larvae. (A) Third instar larval brain. Main brain regions include one ventral nerve cord (VNC) and two brain lobes with optic lobes (OL;black). Colour code: thoracid NBs (dark brown), abdominal NBs (light brown), central brain mushroom body NBs (MB; magenta); type I NBs (yellow); type II NBs (green); ganglion mother cells (GMCs; orange) **(B)** Lineage organization of type I and type II NBs. Type I NBs (yellow) divide to self-renew and to generate a ganglion mother cell (GMC) that divides symmetrically once to form two neurons (N; grey). Type II NBs (green) divide to self-renew and to generate an immature intermediate progenitor (iINP). After a period of maturation, mature (mINPs) undergo several rounds of asymmetric division to self-renew and generate GMCs, each of which divides symmetrically once to form neurons or glia. (A) adapted from (Homem & Knoblich, 2012) and (B) adapted from (Homem et al., 2015)

Self-renewing asymmetric division of Drosophila NBs requires a perfect coordination of the differential sorting of several protein complexes that leads to the generation of cortical asymmetry and the controlled positioning of the plane of cytokinesis that results in the unequal segregation of those cortical protein complexes between the daughter cells (Chia et al., 2008; Gönczy, 2008; Gonzalez, 2007; Knoblich, 2008). Complexes sorted to the apical cortex include the Par (Partitioning defective) and the Pins (Partner of Inscuteable or Rapsynoid) complexes. The core components of the Par complex are Bazooka (Baz/Par3), Par6 and Atypical protein kinase C (aPKC) (Wodarz et al. 1999; Petronczki and Knoblich 2001; Rolls et al. 2003). The main partners complexed with Pins are Gαi, Mushroom body defect (Mud) and Locomotion defects (LOCO) (Parmentier et al. 2000; Schaefer et al. 2000; Yu, Kuo, and Jan 2006; Izumi et al. 2004; 2006; Bowman et al. 2006; Siller, Cabernard, and Doe 2006). The Par and Pins complexes can interact through the bridging protein Inscutable (Insc) (Kraut et al., 1996; Petronczki & Knoblich, 2001; Schaefer et al., 2000; Schober et al., 1999). Proteins sorted to the basal cortex and

inherited by the daughter cell that is primed to enter the differentiation programme, include Staufen (Stau), Prospero (Pros) and Brain tumour (Brat) that are in a complex with the scaffolding protein Miranda (Mira) and the Partner of Numb (Pon)-Numb complex (Betschinger et al., 2006; Caussinus & Hirth, 2007; Doe et al., 1991; Ikeshima-Kataoka et al., 1997; C.-Y. Lee, Wilkinson, et al., 2006; P. Li et al., 1997; Lu et al., 1998; Shen et al., 1997). Other elements that control NB asymmetric division include Cdc2, Polo and Aurora A (C.-Y. Lee, Andersen, et al., 2006; Tio et al., 2001, p. 2; H. Wang et al., 2006, 2007), and the cortical proteins Discs large (Dlg), Lethal giant larvae (Lgl) and Scribbled (Scrib) that mediate in the segregation of basal proteins (Albertson & Doe, 2003; Humbert et al., 2003; Ohshiro et al., 2000; Peng et al., 2000) (Fig.1.3.). Notably *dlg*, *lgl* and *scrib* are tumour suppressor genes (Januschke & Gonzalez, 2008).

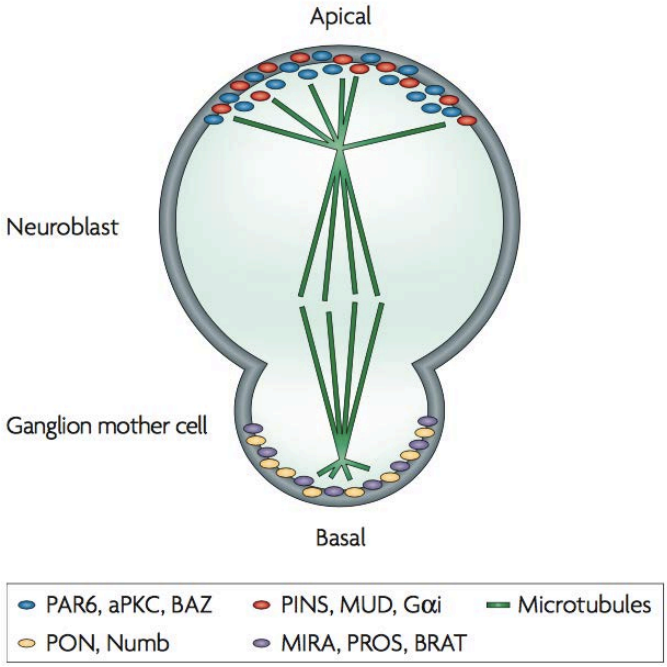

Figure 1.3. Asymmetric division in Drosophila neuroblasts. Segregation of basally localised cell-fate determinants Numb, Prospero (PROS) and Brain tumour (BRAT), and their adaptor proteins Partner of numb (PON) and Miranda (MIRA), into the basal ganglion mother cell (GMC) controls asymmetric division. Apically localised complexes include Bazooka (BAZ or Par3))/PAR6/atypical protein kinase C (aPKC) proteins, Inscuteable (INSC) and Gαi along with their regulators Partner of Inscuteable (PINS), Locomotion defects (LOCO) and a PINS-interacting protein mushroom body defective (MUD). Segregation of basally localised proteins is also mediated by cortically localised tumour suppressors, Discs large (DLG), Lethal giant larvae (LGL) and Scribble (SCRIB). Phosphorylation of LGL by apically localised aPKC leads to LGL inactivation, whereas non- phosphorylated LGL at the basal cortex is active and allows the localization of basal proteins. Interaction of one aster with the apical complex contributes to the alignment of the spindle along the polarity axis. Adapted from (Gonzalez, 2007).

The orientation of the cortical polarity axis has been shown to be dependent upon the position of both the NB's main MTOC and the last GMC (Januschke & Gonzalez, 2010; Loyer & Januschke, 2018).

Controlled positioning of the plane of cytokinesis, which is essential to ensure the unequal distribution of cortical complexes between the two daughter cells, is governed by the orientation of the mitotic spindle (Kaltschmidt et al., 2000; Kraut et al., 1996). At mitosis, spindle orientation is driven by the Pins–Gαi–Mud complex that anchors the aster of one of the spindle poles during mitosis (Bowman et al., 2006; Izumi et al., 2004; Siller et al., 2006). However, spindle orientation is determined from early interphase, before Pins complex assembly (Rebollo et al., 2007; Rusan & Peifer, 2007), through the asymmetric behaviour and function of the NB's centrosomes. At interphase onset, the two centrioles split and one of them stays fixed at the apical cortex organizing an aster that will be the main microtubule network during most of the NB interphase while the other has little or none pericentriolar material (PCM) and moves extensively throughout the cytoplasm. Orientation of the future mitotic spindle can be accurately predicted from the position of the interphase apical aster. The asymmetric partitioning of the self-renewing NB is also controlled by a spindle-independent mechanism for cleavage furrow positioning. This process is controlled by the Pins cortical polarity pathway-dependent localisation of Pavarotti, Anillin, and Myosin to the neuroblast basal cortex at anaphase onset, and can induce a well-positioned furrow even in the absence of a mitotic spindle (Cabernard et al., 2010).

The identification of several known Drosophila TS genes like *lgl*, *dlg*, *scrib* and *brat* as key regulators of NB asymmetry (Wodarz, 2005) provided strong indirect evidence suggesting a tight link between failed NB asymmetry and tumour growth. This hypothesis was first tested and confirmed when loss of many of several elements that regulate NB asymmetry, including all known cell-fate determinants, was shown to cause the growth of malignant tumours when transplanted to the abdomen of adult hosts. The resulting tumours are lethal to the host flies, and they can expand indefinitely through successive rounds of retransplantation (Caussinus & Gonzalez, 2005).

1.2.2. The larval neuroepithelium

The adult OL is the visual processing center of the fly and contains four neuropils: lamina, medulla, lobula and lobula plate. The largest neuropil is the medulla, containing 40,000 neurons belonging to more than 70 cell types (X. Li et al., 2013).

The OL develops during the larval stages from neuroepithelial cells of the outer and inner proliferation centers (OPC and IPC, respectively). OPC and IPC remain in close

contact until the end of second instar larvae when they separate (Nériec & Desplan, 2016). The OPC generates neurons and glial cells in the lamina and outer medulla, whereas the IPC gives rise to the neurons of the lobula complex and inner medulla (Nériec & Desplan, 2016). These proliferative centers consist of two cellular types: a pseudostratified NE in which neuroepithelial stem cells divide symmetrically and expand the pool of proliferative precursor cells (Bate & Martinez Arias, 1993), and a region of medulla NBs and lamina precursor cells which divide asymmetrically to self-renew and generate differentiating ganglion mother cells (GMCs) that after division produce two daughter cells that will differentiate into neurons or glia (Bate & Martinez Arias, 1993; Ceron et al., 2001; Egger et al., 2007; Hofbauer & Campos-Ortega, 1990).

The region placed between NE and NBs is called "Transition zone". Mechanistically, the transition from NE to NBs is driven by the expression of *lethal of scute* (*l'sc*). L´sc expression sweeps across epithelium (the "proneural wave") (Yasugi et al., 2008) inducing the switch from symmetric to asymmetric division, in a process that is controlled by JAK/STAT signalling and involves downregulation of Notch signaling (Egger et al., 2010). Several pathways, such as Fat/Hippo and EGFR pathway have been also identified to play a role in maintenance and differentiation of NE cells. (Egger et al., 2010, 2011; Ngo et al., 2010; Reddy et al., 2010; W. Wang et al., 2011; Weng et al., 2012; Yasugi et al., 2008; Zhou & Luo, 2013) (Fig.1.4.).

Despite notable differences, there are tantalizing similarities between the patterns of neural stem cell pool extension and differentiation in Drosophila and in the developing cortex in mammals (Egger et al., 2010; Götz & Huttner, 2005). Thus, for instance the switch from symmetric to asymmetric stem cell division in the Drosophila larval NE is reminiscent of the transition from NE cells to radial glial cells in the developing mammalian cerebral cortex where the radial glial cells divide asymmetrically producing a NSC and either an inmature neuron or a basal progenitor cell that divides once more to produce postmitotic neurons (Egger et al., 2010; Götz & Huttner, 2005).

Besides mbt tumours, which will be discussed in detail in section 1.4.2., different overproliferation conditions originated in the NE have been reported. Thus for instance, *longitudinals lacking (lola)* mutant larvae present ectopic NB-like cells that arise from dedifferentiation of post-mitotic neurons giving rise to tumour formation in the optic lobe of the adult brain (Southall et al., 2014). Likewise, ectopic expression of the germline-specific component of the inner mitochondrial translocation complex *tiny tim 2* (*ttm2*) brings about NE hyperplasia. Interestingly, expression of *ttm2* in the wing disc epithelium leads to non-cell autonomous overgrowth thus showing that a unique tumorigenic event

may trigger different tumour growth pathways depending on the tissular context (Molnar et al., 2020). Ectopic JAK/STAT activity, like overexpression of *upd* or *hopTum-l*, which encodes an activated JAK kinase (Harrison et al., 1995; Luo et al., 1995) results in neuroepithelial overgrowth (Zhou & Luo, 2013).

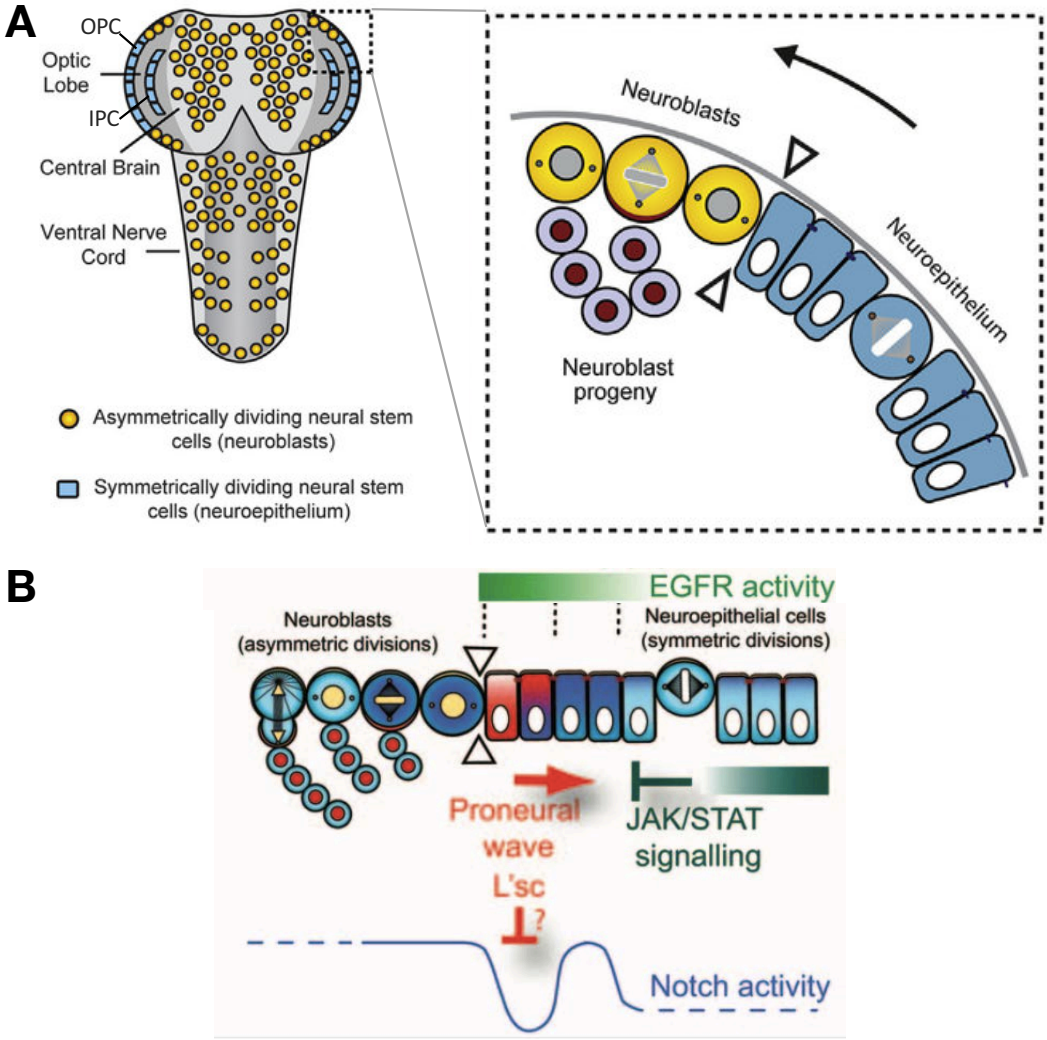

Figure 1.4. Neuroepithelial to neuroblast transition. (A) At the medial edge of the optic lobe columnar neuroepithelial cells disassemble adherens junctions and undergo a transition to neuroblasts. Neuroepithelial cells divide symmetrically with a horizontal spindle orientation to expand the pool of precursors cells. NBs divide asymmetrically with vertical spindle orientation. **(B)** Sequential transition is controlled by the progression of the proneural wave of *lethal of scute (l'sc)*, which is coordinated by orchestrated action of the Notch, EGFR, and JAK/STAT signalling pathways. (A) adapted from (Southall et al., 2013) and (B) adapted from (Egger et al., 2011).

1.3. brat

The *brain tumor* gene (*brat*; a.k.a. *lethal(2)37Cf*) was first identified during a screening for lethal mutations in the dopa decarboxylase region (Wright et al., 1981).

1.3.1. The Brat protein

Upon cloning, *brat* was shown to encode for a 1037 amino acid protein with a modular structure containing several domains (Arama et al., 2000). Brat is a member of the tripartite motif (TRIM) containing superfamily that has a N-terminal TRIM motif followed by variable C-terminal domains. The TRIM motive is defined by the variable presence of RING (Really Interesting New Gene) domain, one or two B-box type zinc fingers, and a coiled-coiled domain. The RING domain is defined by a regular series of Cys and His residues and can act as an E3 ubiquitin ligase. The B-Boxes, which are also zinc binding have not been assigned a clear function yet, but they may be involve in substrate binding. The coiled-coiled domain allows the formation of homo or heterodimers and of protein complexes (Connacher & Goldstrohm, 2021; Hatakeyama, 2017; Marín, 2012).

Brat is mainly cytoplasmatic and regulates mRNAs by binding to the 3´-UTR and repressing translation and increasing degradation of bound targets (Cho et al., 2006; Laver et al., 2015; Loedige et al., 2014; Reichardt et al., 2018; Sonoda, 2001).

Brat is an atypical member of a subset of the TRIM proteins (TRIM-NHL) that miss the RING and contains in the C-terminal an NHL domain. The crystal structure of Brat NHL domain consists in six blade propellers of approximately 44 amino acids forming four beta sheets in a similar way to others beta propellers domains (Edwards, 2003; Kumari et al., 2018; Loedige et al., 2015). Most of the identified mutations in Brat affect the NHL showing the importance of this domain in the function of the protein (Arama et al., 2000; Sonoda, 2001). The NHL domain directly binds RNA and this interaction is essential for its function. Crystalisation of the Brat domain in the presence of its substrate RNA has shown that they form a complex with single stranded RNA with 1:1 stoichiometry. The RNA is recognised by a positively charged channel on the surface of the NHL domain that presents a preference for some nucleotides in certain positions. The domain recognises a core 5´UGUU-3´ sequence flanked by U/A-rich sequences (Kumari et al., 2018; Laver et al., 2015; Loedige et al., 2014, 2015). In addition to its binding to RNA the NHL domain of Brat binds to the adaptor protein Miranda (C.-Y. Lee, Wilkinson, et al., 2006) and the translation inhibitor d4EHP (Cho et al., 2006).

The strong alleles of *brat* are female sterile and have more germ line stem cells (GSCs) than wild type, indicating that Brat plays a role in the differentiation of the stem cells (Harris et al., 2011). The fate of the GSCs is regulated by a niche created by the secretion of Decapentaplegic (Dpp) from the somatic cells (Slaidina & Lehmann, 2014). The Dpp (in human BMP) signal activates the transcription factors Mad, Medea (Med) and Schnurri (Shn) that inhibit the transcription of the differentiation factor *bag of marbles (bam)*. Brat promotes differentiation by reducing the BMP signal by post transcriptionally repressing Mad, Med and Shn (Harris et al., 2011; Newton et al., 2015). Repression of these mRNA is mediated by the 3´UTRs, suggesting that these mRNAs are direct targets of Brat. The role of Pumilio (Pum) in repressing these mRNAs is essential but not well understood. The proposed model calls on Brat recruiting the CNOT deadenylase complex to the mRNAs, shortening the polyA and reducing the transcription of BMP signal. The reduction the Dpp signaling allows the increase of the *bam* transcription inducing the differentiation of GSCs to cystoblast (Slaidina & Lehmann, 2014).

In the early embryo Brat is required for the establishment of the anterior-posterior axis by repressing translation of the posterior determinant *hunchback (hb)* (Sonoda, 2001). Translational control of *hb* is mediated by a complex of Brat, Nanos (Nos) and Pum that binds to the 3'UTR of *hb* mRNA. This complex acts by a dual mechanism: shortening the polyA of *hb* mRNA and by the recruiting 4EHP to reduces the translation (Cho et al., 2006). Notably, Brat alone is able to regulate mRNAs that have the Brat binding motif (Laver et al., 2015).

1.3.2. Brat tumours

Several of the first isolated brat alleles (Stathakis et al., 1995; Wright et al., 1981) were noticed to present enlarged OLs but normal-sized VNCs (Fig.1.5.A.). Overgrowth in the OL was found to result from uncontrolled NB divisions. These early studies also showed that brat tumours can "metastasize" and are lethal to allografted host (Gateff, 1994; Kurzik-Dumke et al., 1992; Woodhouse et al., 1998).

Later studies confirmed these observations and showed that brat tumours arise from Type II NB lineages (Fig.1.5.B.). The specific cell-of-origin appears to be the INP. In *brat* mutants, immature INPs fail to reinitiate *Ase* and *Dpn* expression thus entering a transient cell cycle block and ultimately reverting to type II NB-like tumour cells (Bowman et al., 2008; Janssens et al., 2014; Jiang & Reichert, 2014; Reichardt et al., 2018; Xiao et al., 2012). In normal NBs, Brat blocks INPs dedifferentiation in multiple ways. One that is well studied is negative regulation of Dpn and Zelda-B (Zld-B), two proteins that promote the identity of neuroblast and proliferation (Komori et al., 2018; Reichardt et al., 2018).

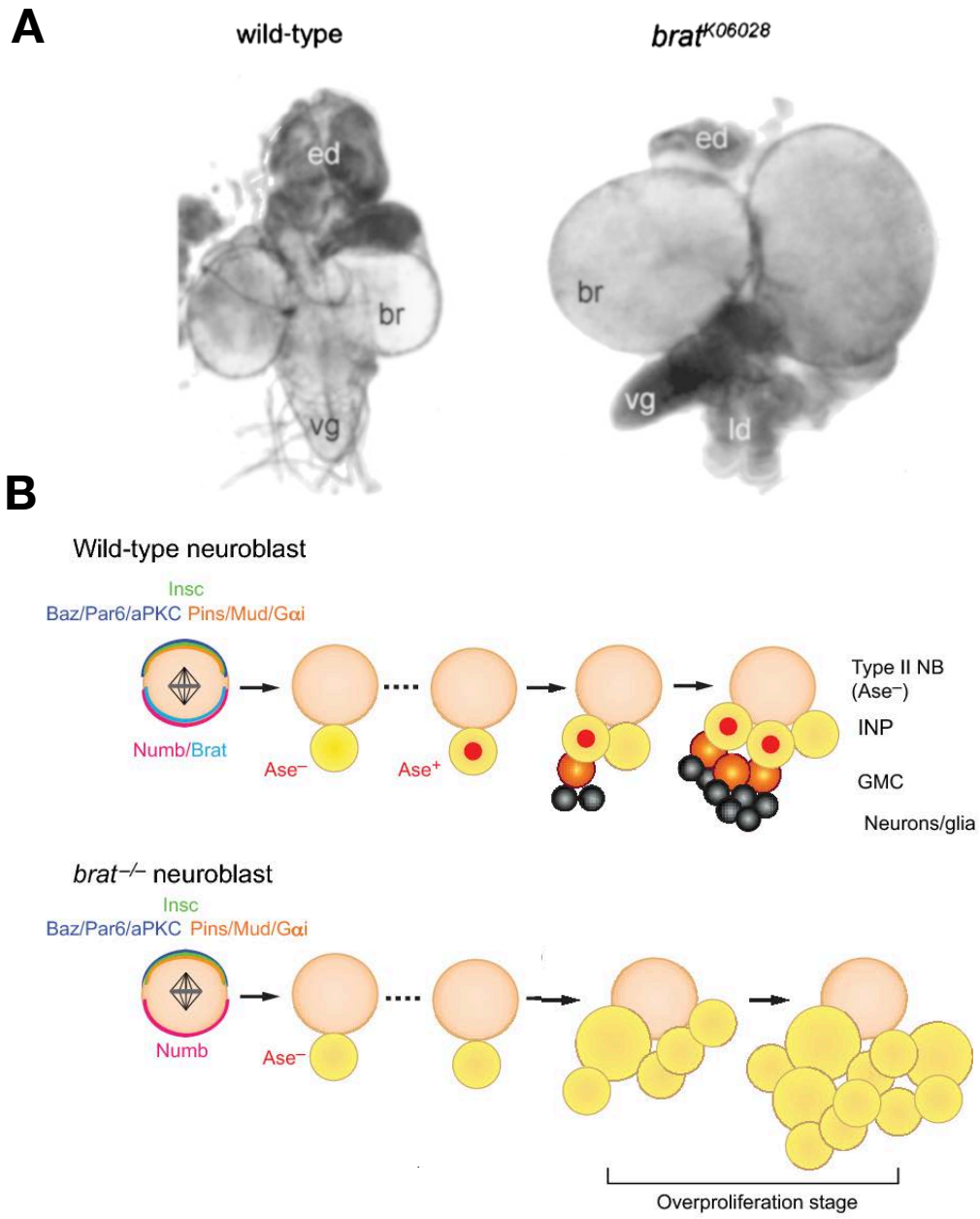

Figure 1.5. Brat tumour phenotype and cellular origin. (A) Central nervous system of crawling third instar larva from wild-type (left) and brat mutant allele *K06028* caused by P-element insertion (right). The brat mutant brain hemispheres are highly enlarged in comparison to the wild-type counterparts. br, brain hemispheres; vg, ventral ganglion; ed, eye-antennal imaginal disc; ld, leg imaginal disc. **(B)** Wild-type central brain type II neuroblasts (NBs) divide asymmetrically, segregating the cell fate determinants Numb (pink) and Brat (light blue) into the differentiating daughter cell. Type II NBs divide to self-renew and generate an immature, Asense-negative (Ase–), intermediate progenitor (INP; yellow). After maturation, INPs start expressing the transcription factor Ase (red; Ase+) and divide to generate ganglion mother cells (GMCs, orange). In brat mutant individuals INPs revert to NB-like cells that overproliferate. (A) adapted from (Arama et al., 2000) and (B) adapted from (Homem & Knoblich, 2012).

This effect is driven by the binding of Brat to the 3´UTR of the mRNA of *dpn* and *zld-B*. In addition to Dpn and Zld, Brat repress the transcription factor dMyc (Betschinger et al., 2006; Reichardt et al., 2018). Both *dMyc* and *eukaryotic translation initiation factor 4E (eIF4E)* are growth regulators that become unscheduled up-regulated in *brat* mutant dedifferentiating INP and removal of either of them strongly inhibits overproliferation in *brat* mutant brains (Betschinger et al., 2006; Q. Deng & Wang, 2022; Song & Lu, 2011). Indeed, it is through dMyc that loss of *brat* promotes the enhanced ribosome biogenesis and rRNA synthesis observed in brat tumours (Betschinger et al., 2006; Neumüller et al., 2013; Reichardt et al., 2018). This effect is conserved in *C. elegans* where the removal of *brat* homolog *ncl-1* results in the increase of rRNA transcription and enlarged nucleolus (Frank et al., 2002b).

Also important in the mechanisms of action through which loss of *brat* triggers tumorigenesis is brat's function in antagonizing both Klumpfuss (Klu) and β-catenin/Armadillo (Arm), which are required to specify the identity of the INPs and to suppress the reversion of these progenitors into ectopic NB-like tumour cells. Consistently, reducing the activity of Klu or Arm can largely suppress the formation of supernumerary neuroblasts in *brat* mutant brains (Komori et al., 2014; Xiao et al., 2012).

A final important point regarding brat tumours is their "metabolic state". In wild-type animals, metabolic pathways are critical to trigger the onset and the end of NB proliferation in Drosophila larval brains (Homem et al., 2014; Otsuki & Brand, 2018). Normal NB asymmetric division is associated with aerobic glycolysis, whereas differentiation is associated with increased glucose oxidation in the tricarboxylic acid (TCA) cycle. In contrast, brat NB-like tumour cells are tightly dependent on the electron transport chain (ETC) and oxidative metabolism. Loss of function for different genes required for the ETC or TCA cycle stops cell proliferation on brat tumours (Bonnay et al., 2020; van den Ameele & Brand, 2019).

There are two human orthologs to Drosophila Brat, TRIM3 and TRIM2, of which TRIM3 has the highest homology. TRIM3 loss is a frequent event both in low grade as in grade IV gliomas and is thus regarded as an early neoplastic step. As Brat and dMyc in Drosophila, TRIM3 directly regulates the expression of the human *c-Myc* proto-oncogen in human glioma cell lines (G. Chen et al., 2014).

1.4. l(3)mbt

The Drosophila gene *lethal (3) malignant brain tumour (l(3)mbt)* was identified by E. Gateff as a temperature sensitive mutant that caused malignant brain tumours and hyperplastic imaginal discs in larvae reared at 29ºC (Gateff et al., 1993).

1.4.1. The L(3)mbt protein

The *l(3)mbt* gene encodes seven transcripts of 5.8 kb, 5.65 kb, 5.35 kb, 5.25 kb, 5.0 kb, 4.4 kb and 1.8 kb. *In situ* hybridizations of whole mount embryos and larval tissues reveal *l(3)mbt*+ RNA ubiquitously present in stage 1 embryos and throughout embryonic development in most tissues. In third instar larvae *l(3)mbt* RNA is detected in the adult optic anlagen and the imaginal discs, the tissues directly affected by *l(3)mbt* mutations, but also in other tissues, showing normal development in the mutant, such as the gut, the goblet cells and the hematopoietic organs (Wismar et al., 1995).

The L(3)mbt protein is 1477 amino acid in size, is proline rich, and is characterised by the presence of Malignant Brain Tumor (MBT) repeats named after the name of the gene (Bornemann et al., 1996; Wismar et al., 1995). MBT repeats recognise differentially methylated histone tails and have been suggested to participate in chromatin compaction (Francis et al., 2004; Klymenko et al., 2006; Trojer et al., 2007). Structurally, MBT repeats consists of a three-blade propeller-like structure. Each blade is composed of an arm attached to a globular structure that contains a ligand-binding pocket (W. K. Wang et al., 2003) forming a structure that resembles Tudor and Chromo domains (Bannister et al., 2001; Cao et al., 2002; Lachner et al., 2001; Maurer-Stroh et al., 2003; Nakayama et al., 2001; Sprangers et al., 2003; W. K. Wang et al., 2003). Consistently, MBT repeats have been shown to physically interact with core Drosophila histones and full length L(3)mbt has high affinity for essentially all of the H3–H4 tetramers present in 0- to 12-h Drosophila embryos (Georlette et al., 2007). The functional relevance of these repeats in underpinned by the fact that the genetic lesion linked to the $l(3)mbt^{GM79}$ and $l(3)mbt^{ts1}$ alleles maps within the MBT domains.

L(3)mbt also presents a Sterile Alpha Motif (SAM) (Bornemann et al., 1996; Wismar et al., 1995). SAM motifs are protein interaction modules that are widespread in signaling and nuclear proteins. A classic example of SAM domain is the one present in the human TEL oncoprotein, an ETS class transcription factor, where the SAM has been referred to as a helix-loop-helix (HLH) domain. This domain mediates self-binding and oligomerization of TEL protein and of TEL fusion protein derivatives (Peterson et al., 1997). In EPH-related tyrosine kinases, the SAM domain appears to mediate cell-cell

initiated signal transduction via the binding of SH2-containing proteins to a conserved tyrosine that is phosphorylated. In Drosophila, SAM domains have been shown to mediate heterotypic and homotypic protein-protein interactions in Polycomb Group (PcG) proteins Sex comb on midleg (Scm) and Polyhomeotic (Ph) (Peterson et al., 1997). For that reason, the high-homology domain subgroup of SAM motifs that is common to Scm, Ph, and l(3)mbt is also known as SPM (ScmPhMbt) (Ponting, 1995). There is a weak homology of the SPM domain to a domain found in members of the ETS family of transcription factors such as the TEL oncoprotein (Boccuni et al., 2003; DeCamillis et al., 1992; Golub et al., 1994; Wasylyk et al., 1994).

Finally L(3)mbt also contains putative Cys_2-Cys_2 zinc fingers (Bornemann et al., 1996; Wismar et al., 1995) of a distinct subclass defined by the conservation of residues that flank the cysteines and the identical spacing between the cysteine pairs, which are different from the Cys2-Cys2 fingers of other DNA-binding proteins such as the nuclear hormone receptors (Coleman, 1992).

L(3)mbt is known to be part of two different repressive chromatin complexes: as a substechiometric member of the dREAM-MMB complex that contains Drosophila retinoblastoma proteins (RBF and E2F2) and Myb-MuvB complex (Blanchard et al., 2014; Lewis et al., 2004), and as a stechiometric component of the tripartite LINT complex together with Lint-1 and CoREST (Coux et al., 2018; Meier et al., 2012; Mačinković et al., 2019).

On the basis of sequence homology and the domain structure of the protein L(3)mbt is considered as a PcG related gene. Indeed, abundant evidence demonstrates that L(3)mbt function is to change chromatin structure to ensure the stable silencing of specific developmental genes thus establishing and maintaining the differentiated state (Boccuni et al., 2003).

L(3)mbt closest homologs are two members of the PcG in Drosophila, Scm and Scm-related gene containing four mbt domain (Sfmbt) with which it shares the zinc fingers, MBT repeats and SAM motifs (Bornemann et al., 1996; Wismar et al., 1995). Scm is a component of PcG complex, PRC1 and Sfmbt is a subunit of PhoRC, a distinct PcG complex. Both complexes function to maintain tissue specific repression of genes throughout *D. melanogaster* development. Sfmbt binds to histone H3 tails mono- or dimethylated at K9 (H3K9me1 and H3K9me2) and H4 tails mono- or dimethylated at K20 (H4K20me1/2) (Klymenko et al., 2006).

The human genome encodes a L3MBTL protein family (named after the Drosophila genes) that includes L3MBTL1 (formerly known as L3MBTL), L3MBTL3 and L3MBTL4, all of which function as chromatin-interacting transcriptional repressors

(Bonasio et al., 2010). L3MBTL1 is the closest homologue to Drosophila L(3)mbt (Meier et al., 2012). L3MBTL1 contains a very similar domain structure to that of its Drosophila orthologue including three MBT repeats, a putative Cys_2-Cys_2 zinc finger, the SPM domain, which is equivalent to the SAM, and a similar C-terminal alpha-helical structure (Bonasio et al., 2010). L3MBTL functions as a histone deacetylase-independent transcriptional repressor and interacts physically and functionally with TEL (or ETV6) (Boccuni et al., 2003; Dura et al., 1987; Koga et al., 1999; J. Li et al., 2004; Usui et al., 2000; Wismar et al., 1995).

1.4.2. l(3)mbt tumours

The collection of *l(3)mbt* alleles include *l(3)mbt*^{ts1}, l*(3)mbt*^{E2}, the P-element insertional allele *Df(3R)mbt*^{P} (a 29 kb deletion) (Gateff et al., 1993) and others that were identified as mutants without germ-cells (Yohn et al., 2003). In addition, there are deficiencies that uncover *l(3)mbt* like *Df(3R)D605* and *Df(3R)mbt*^{PE3}. Indeed, *l(3)mbt* depletion can also be achieved by RNAi technology (C. Richter et al., 2011). Remarkably, the temperature dependence of the tumorigenic phenotype described in the first *l(3)mbt* allele, *l(3)mbt*^{ts1} is a common feature of all other allelic combinations. This unexpected result- temperature sensitive mutants are rare in Drosophila -strongly suggests that temperature sensitivity is a feature of the process L(3)mbt function is required for, rather than an property of each mutant allele (Yohn et al., 2003). Temperature shifting experiments carried out in the Gateff laboratory with the original *l(3)mbt*^{ts1} allele revealed that the first 6 h of embryonic life are essential for tumour suppression (Gateff et al., 1993).

Loss of *l(3)mbt* function in larvae reared at 29°C results in malignant brain tumours and hyperplastic imaginal discs. *l(3)mbt* brain tumours (henceforth referred to as mbt tumours) originate in the larval neuroepithelium (E. Gateff, Löffler, and Wismar 1993; E. Gateff 1994), and present a derepression of target genes in the Salvador-Warts-Hippo (SWH) pathway (C. Richter et al., 2011).

One distinct feature of mbt tumours is that they upregulate dozens of germline genes (Janic et al., 2010). This trait is also common in some human somatic cancers. Such genes are referred to in the literature as cancer-testis (CT) or, more appropriately, cancer-germline (CG) genes (Simpson et al., 2005). The potential interest of CG genes stems from their possible role in cell robustness and fitness. Unlike the soma, which is fated to die, the germline can be passed from one generation to the next, endlessly, and is in this regard an essentially immortal lineage that can outlive the individual. This is made possible by germline-specific mechanisms that inhibit aging and protect from deleterious insults like transposable element mobilisation and exposure to free radicals (Curran et al., 2009;

Simpson et al., 2005). Germline cells are also endowed with conspicuous traits like the ability to migrate and implant themselves in another tissue, demethylation, angiogenesis induction, and immune evasion (Simpson et al., 2005). Because these traits, like immortality, are often associated to cancer cells, it has long been suspected that co-option of CG genes may contribute to malignancy.

Remarkably, some of the CG genes upregulated in mbt tumours are orthologues of known human CG genes and at least four of them are essential for mbt tumour growth. This observation provided the first experimental evidence substantiating a function for CG genes in malignant growth (Janic et al., 2010). Altogether, these observations established mbt tumours as an experimental model to investigate the molecular mechanisms by which germline functions ectopically active in the soma may contribute to the acquisition of neoplastic characteristics, which, indeed, may have both relevant implications for our understanding of cancer as well as therapeutic and diagnostic potential. A remarkable validation of the value of mbt as a model to study cancer is the identification of new human CG genes on the bases of their homology to the germline genes that we found to be ectopically expressed in Drosophila mbt larval brain tumours (Feichtinger et al., 2014).

A second remarkable feature of mbt tumours is that they present strong sex-linked dimorphism they are much more invasive and lethal in males than in their female siblings (Fig.1.6.) (Molnar et al., 2019). This is an important finding because cancer susceptibility and mortality rate are also sex-dependent. Therefore, mbt could serve as a genetically tractable model to investigate the molecular basis of sex-linked differences in malignant growth.

Quantitative proteomics and RNAseq analysis of sexed mbt tumour samples has shown that phenotypic sex dimorphism correlates tightly with sex-link molecular signatures that include genes expressed at significantly different levels in male than in female tumours. Importantly such sex-linked signatures overlap only partially with the corresponding mbt tumour signatures (i.e. differences between tumour and control samples). Prominent component of the mbt sex-linked male signature (expressed at a higher rate in males) are histone code reader Phf7, and thioredoxins TrxT and Dhd. Phf7 plays a fundamental role in sex-linked molecular differences bringing about sex-linked molecular disparities by dysregulating dozens of genes in male tumours. Moreover, it also plays a critical role in sex-linked phenotypic differences: loss of Phf7 suppresses both the anatomy traits and the greater growth potential that make mbt tumours more aggressive in males than in females. These results suggest that proteins that belong to sex-linked

tumour signatures could be targeted to eliminate sex-linked enhanced malignancy (Molnar et al., 2019).

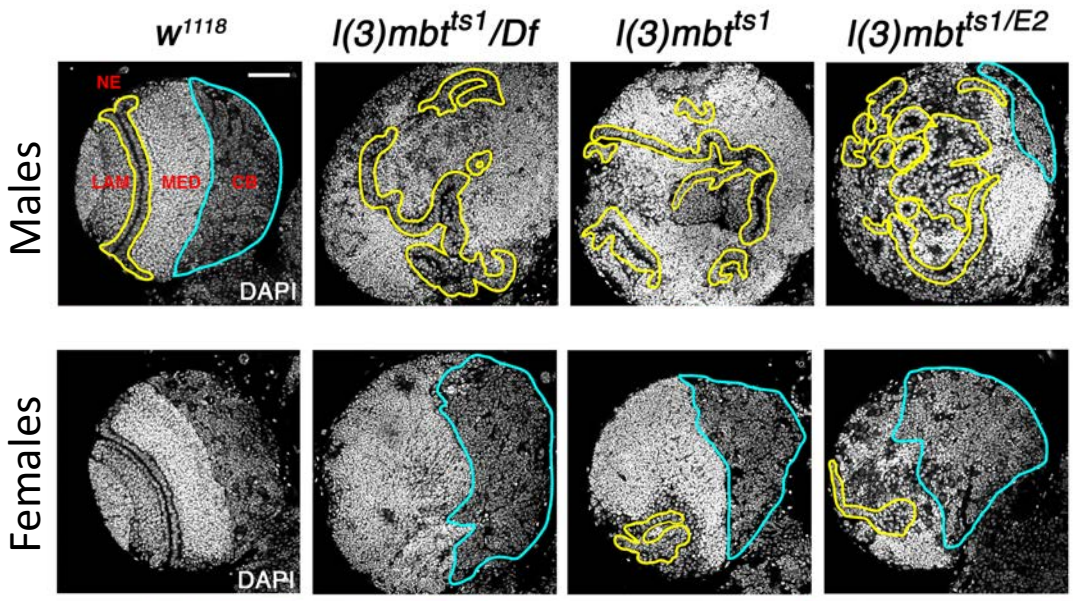

Figure 1.6. Sexual dimorphism in mbt tumours. Larval brain lobes from male and female control (w^{1118}) and mbt mutant [$l(3)mbt^{ts1}/Df$, $l(3)mbt^{ts1}$, and $l(3)mbt^{ts1/E2}$] larvae stained with DAPI (grey). Male mbt lobes present reduced central brains (CBs; blue) and overgrown neuroepithelia (NE; yellow) that invade medial regions. In contrast, in female mbt lobes, the NE do not overgrow and CBs remain as distinct as in wild-type larvae. Scale bar, 50 mm. Adapted from (Molnar et al., 2019).

Abundant correlative evidence suggest that human L3MBTL proteins are also relevant in certain cancer types. L3MBTL1 maps to region 20q12 which is frequently disrupted in myeloid malignancies (Dewald et al., 1993; Gurvich et al., 2010) and CNS germinomas (D. T. Schneider et al., 2006). L3MBTL2 maps to region 22q13 that is associated with medulloblastoma (Northcott et al., 2009). L3MBTL3 maps to chromosomal region 6q23, which is often deleted in acute leukemia (Sundareshan, 2003) and in some cases of medulloblastoma (Northcott et al., 2009). However, studies carried out in L3MBTL1 mutant mice lacking exons 13–20 argue otherwise because they develop and reproduce normally and do not present any increased incidence of tumours (Qin et al., 2010).

2. Objetives

2. OBJETIVES

The rationale behind my thesis project is to advance in the understanding of the molecular mechanisms that drive malignant growth using *Drosophila melanogaster* as a experimental model system. My work has focused on the tumours caused by loss-of-function conditions for the gene *brain tumour (brat)*.

The long-term objective of this project is to identify the molecular circuitry required for the malignant transformation that occurs in the brains of larvae that are mutant for the gene *brat*.

My specific objectives were:

1) To identify genes required for brat tumour growth.
2) To identify the transcriptional signature of brat tumours.

3. Materials and Methods

3.1. Fly stocks

We used the GAL4/UAS system to drive the expression of the RNAi lines (Brand et al., 1994). To induce brat tumours, a stock was generated with line #28590 from Bloomington Drosophila Stock Center (BDSC) that carries a *UAS-brat-RNAi* transgene (Perkins et al., 2015). *UAS-brat-RNAi* expression was driven with *Ubi-GAL4* (#32551 BDSC)(Rossi et al., 2017). To enhance RNAi expression, *UAS-Dcr2* (#24650 BDSC) was also introduced. To repress UAS-transgenes expression in the parental flies we used a balancer that carries TUB GAL80 (#9490 from BDSC). The genotype of the resulting stock used in the screen was: *Ubi-GAL4 UAS-Dcr2; UAS-brat-RNAi/TM6, Tb, tub-GAL80, Tb.*

The RNAi lines used in the screen (Excel sheet: High-content_Brat-screen_n=4300 in Appendix D1) were obtained from the Vienna Drosophila Resource Center (VDRC) (Dietzl et al., 2007). UAS-RNAi lines inserted in the X chromosome and lines that were not homozygous viable were not used in our screen. We used *wor-GAL4 ase-GAL80; UAS-mCD8-GFP* (Neumüller et al., 2011) to genetically label type II NBs. *UAS-Tctp-RNAi* line was a gift from Hsu (Hsu et al., 2007). *UAS-Vps-RNAi* line was obtained from VDRC (#18396); TRiP lines for *Vps29* and *Vps35* (B. Li et al., 2018) were obtained from BDSC (#38963 and #38944, respectively). For allograft tests mbt tumours were obtained from Tb+ larvae from outcrosses using the stock *Ubi-GAL4 UAS-Dcr2; UAS-l(3)mbt-RNAi, DsRed, l(3)mbt^{ts1}/TM6B, tubP-GAL80, Tb* raised at 29ºC (Rossi et al., 2017).

Transcriptomic studies were carried out with mutants samples from *brat^{K06028}* individuals (Arama et al., 2000) raised at 25ºC. All samples for transcriptomic studies were sexed by visual inspection of larval gonads.

3.2. Screen strategy

Males from a *Ubi-GAL4, UAS-Dcr2; UAS-brat-RNAi/TM6, Tb, tub-GAL80, Tb* stock were crossed to virgin females from each UAS-RNAi line to be tested. Eggs collected 0 – 24 h after egg laying (AEL) were allowed to develop for up to 8 days (180 + 12 h AEL), except for the wild-type control, where strain *w^{1118}* was used and larvae were dissected at 5 days AEL. Egg collection and larvae development took place at 29ºC. For the first round of the high-content screen (4300 lines) about 4 brains were dissected per each condition and classified upon visual inspection as (1) smaller than wild-type (2) wild-type size (3) brat tumour size and (4) larger than brat tumour, as previously described for the screening of suppressors of mbt tumours (Rossi et al., 2017). UAS-RNAi lines in which three or more brains were smaller than brat tumours (groups 1 and 2) were tagged as potential

suppressors and re analysed in a second round of screen in which results were quantitated my measuring brain diameter (Fig. 3.1.).

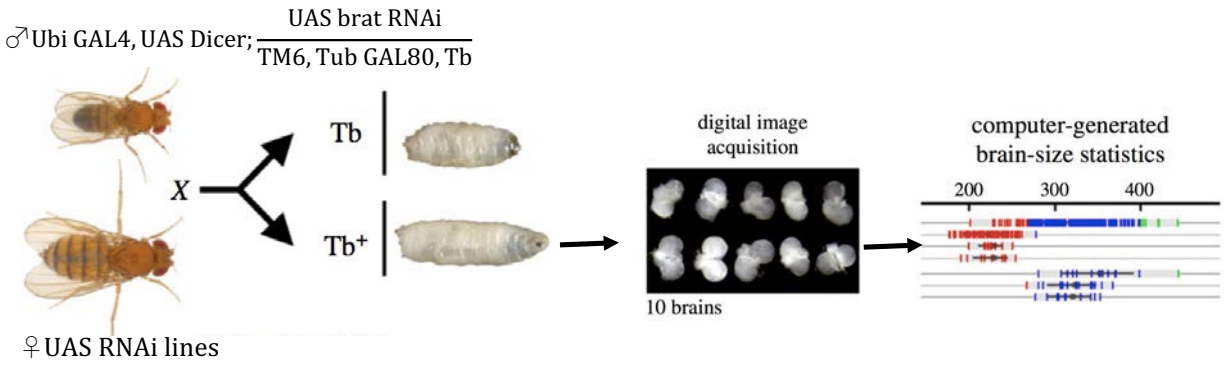

Figure 3.1. Screen strategy. *UbiGAL4, UAS-Dcr2; UAS-brat-RNAi/TM6, Tb, tub-GAL80, Tb* males are crossed to females carrying each of the transgenic *UAS-RNAi* lines. Brains from Tb+ larvae are dissected and subjected to an automated classification procedure based on image analysis of low magnification micrographs. Adapted from (Rossi et al., 2017).

3.3. Brain size measurement

Images of around 10 larval brains from each genotype were acquired using a LEICA EC3 camera coupled to a NIKON SMZ800 stereoscope. Images were analysed by a purpose-made macro written by C.González in IMAGEJ software (C. A. Schneider et al., 2012) that measures maximum brain Feret (mbFeret) diameter of the optic lobes pair and works out statistics from mbFerets for any given RNAi. Ventral ganglions were either cut out prior to image acquisition or digitally masked before measurement. The strain w^{1118} was used as a control to determine wild type brain sizes. From the analysis of brat and w^{1118} larval brains we were able to define the following thresholds: smaller than 190 arbitrary units (a.u.) brains were significantly smaller than wild type; samples in which the fraction of brains smaller than wild type is lower than 0,6 are tagged as grey. Between 190 and 270 a.u. brains are within wild type size and tagged red. Samples with size above 270 a.u. were classified as tumour-like (blue) (Rossi et al., 2017).

3.4. Immunohistochemistry and antibodies

Immunostaining of whole larval brains was performed as described in (Gonzalez and Glover, 1993). In summary, brains were dissected in PBS, fixed for 20 minutes in 4% Formaldehyde in PBS, rinsed 30 minutes in PBS with 0.3% Triton X-100 (PBST) and blocked for 1 hour in PBSTF (0,3%Triton X-100, 10% Fetal Calf Serum (FCS) in PBS) at room temperature. After overnight incubation with primary antibody diluted in PBSTF

at 4ºC, brains were washed three times with PBST (0,3% Triton X-100 in PBS) for 20 min, and incubated with secondary antibody in PBSTF in the dark at room temperature for 2 hours. DNA was stained with 2 µg/ml 4,6-diamidino-2-phenylindole (DAPI) for 20 minutes and washed with PBS. Stained brains were mounted in Vectashield (Molecular Probes) dorsally or ventrally depending on the tumour type to be analysed. We used 1:500 Rabbit anti-Mira 4699 (Caussinus & Gonzalez, 2005; Mollinari et al., 2002) and Alexa Fluor secondary antibodies (1:1000, Life Technologies) (Molnar et al., 2020).

3.5. Microscopy

Immunostaining images were acquired with a Leica TCS SP8 scan unit coupled to a microscope and managed by Leica Application Suite X (LAS X) software.
The objective used was HC PL APO CS2 40x/1.30 OIL and images were acquired at zoom 0.75, unless specified otherwise. Fluorophores 405 and 488 were excited with lasers Diode and Argon, respectively. Image processing was carried out with FIJI. All shown immunofluorescence images correspond to a single Z, Miranda levels enhanced by FIJI. Panels were prepared with FIJI and Adobe Photoshop 2017.

3.6. Statistical analysis

Two-tailed p-values were calculated using Unpaired t-test (web application of GraphPad) for all the experiments regarding brain size. Pairwise Fisher's exact test (web application of GraphPad) was used for tumour growth rate and host lethality in allograft assay (Molnar et al., 2020). For P-value of overlap between gene lists an online tool (http://nemates.org/MA/progs/overlap_stats.html) was used (Lund et al., 2002).

3.7. GO analysis

Functional annotation of Gene Ontology (GO) terms was performed using the online tool Database for Annotation, Visualization and Integrated Discovery (DAVID; http://david.abcc.ncifcrf.gov/) (Huang et al., 2009; Sherman et al., 2022). DAVID (version 6.8.) and GO terms for biological process (GOTERM_BP_DIRECT), cellular component (GOTERM_CC_DIRECT) and molecular function (GOTERM_MF_DIRECT) with a p-value of <0.05 were accepted as a significant enrichment for brat suppressors analysis. For GO analysis of differentially expressed genes, DAVID (version 2021) was used. We accepted GO terms for biological process (GOTERM_BP_DIRECT) with more restrictive p-value ($p<0.001$) in order to filter out the redundant terms that generally appear with input of hundreds of genes.

3.8. Allografts assays

To test the tumorigenic potential of different tissues, allograft assays were performed according to standard procedure (Rossi & Gonzalez, 2015). Briefly, optic lobes were dissected in PBS, injected into the abdomen of 3-4 days old adult mated females and kept at 29ºC. Injected flies were inspected when catatonic or right after their death to check for the presence of an overgrown tumour mass (Fig. 3.2.).

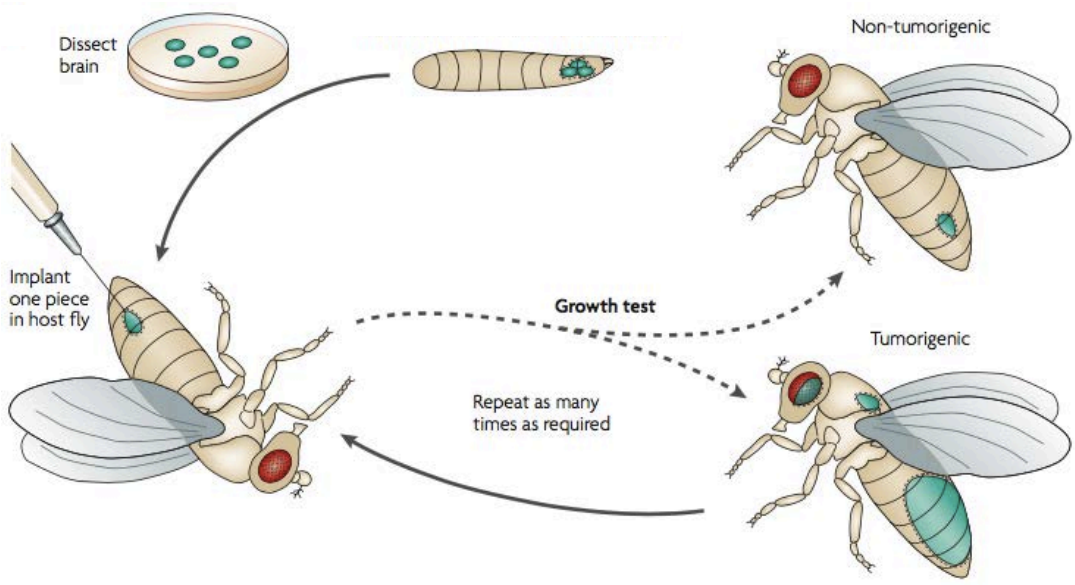

Figure 3.2. Tissue allograft into adult hosts. The tissue of interest from a donor larvae is dissected, cut into pieces, loaded into a fine glass needle and implanted into an adult host. The culture period is typically a few weeks. Upon implantation, non-transformed tissues do not overgrow. In contrast, malignant neoplasias grow without limit, expanding over the abdomen and eventually killing the host. Malignant tumors can be dissected into pieces and injected again into new hosts. Adapted from (Gonzalez, 2007).

3.9. Venn diagrams

Venn diagrams were obtained using the web application BioVenn (http://www.biovenn.nl/; Hulsen, de Vlieg, and Alkema 2008).

3.10. Transcriptomics

3.10.1. Microarray sample preparation

Dissected Drosophila larval brains were collected in 45 µl of a lysis buffer containing 20 mM DTT, 10 mM Tris-HCl pH 7.4, 0.5% SDS, and 0.5 µg/µl proteinase K, incubated at 65 ºC for 15 minutes and immediately frozen until processing. Each sample contained one brain. RNA extraction and cDNA generation was carried out at the IRB Barcelona Functional Genomics Core Facility. Briefly, RNA was treated with DNAse I and purified using magnetic beads (RNAClean XP, Beckman Coulter). RNA was quantitated with Qubit RNA HS Assay kit (Invitrogen), and RNA integrity was assessed with the Bioanalyzer 2100 RNA Pico assay (Agilent). 25 ng of RNA were reverse transcribed and amplified using the Whole Transcriptome Amplification method (WTA2, Sigma Aldrich) with 17 cycles of amplification. cDNA was further purified using a spin column (PureLink Quick PCR Purification Kit, Invitrogen) and quantified using a microvolume spectrophotometer (Nanodrop ND-1000, Thermo-Fisher Scientific) (Janic et al., 2010).

3.10.2. Microarray processing

For microarray processing, 8 µg of cDNA were fragmented and labelled according to the manufacturer instructions (GeneChip Mapping 250K Nsp Assay Kit, Affymetrix). Array hybridization was performed using the GeneChip Hybridization, Wash, and Stain Kit (Applied Biosystems). Briefly, libraries were denatured at 99°C for 2 min prior to incubation into the Affymetrix GeneChip® Drosophila Genome 2.0 Arrays (Applied Biosystems) (Janic et al., 2010). Libraries were hybridized on the arrays for 16 h at 45 °C for 60 rpm at GeneChip Hybridization Oven 645 (Affymetrix/ThermoFisher Scientific). Washing and Stain steps were performed using a GeneChip Fluidics Station 450 following the Drosophila Genome 2.0 protocol (Affymetrix/ThermoFisher Scientific). Finally, arrays were scanned with a GeneChip Scanner GCS3000 (Affymetrix/ThermoFisher Scientific).

3.10.3. Microarray data analysis

The CEL files containing the microarray data were generated with the Command Console software (Affymetrix/ThermoFisher Scientific), and were used for probeset-based gene expression measurements using robust multichip average (RMA) normalization. Results were analysed using the Transcriptome Analysis Console 4.0 (TAC) software.

To identify differentially expressed genes pairwise comparisons between each experimental condition of interest were carried out. Genes with fold change (F.C.) > 2 and false discovery rate (FDR) <0.05 were considered to be differentially expressed (Janic et al., 2010).

3.10.4. Volcano and scatter plots

For visualization of gene expression levels, volcano and scatter plots were generated with GraphPad Prism 9 for MacOS X (GraphPad Software, La Jolla, CA, USA; www.graphpad.com).

4. Results

4.1. A high-content, *in vivo* RNAi screen identifies 68 genes required for brat tumour growth

Drosophila tumour models provide a unique mean to investigate the complex network of cellular and systemic functions that sustain malignant growth through high content genetic screens (Gonzalez, 2013). The first study of this kind, carried out in our laboratory, included two screens that were carried out in parallel using the same collection of RNAi lines to identify suppressors of mbt and brat neoplastic malignant growth (mbt-SPRs and brat-SPRs, respectively). A total of 4300 randomly selected RNAi lines from the VDRC collection that correspond to 4275 genes, 30,6% of the 13969 protein coding genes reported in *Drosophila melanogaster* (FlyBase release FB2021_06) were analysed.

In the case of mbt, once the initial high content screen was finalised, the study was carried out to completion. This included validation of suppressor activity of all identified hits, phenotypic characterization of larval brains from *l(3)mbt* mutant individuals reared at 29ºC and expressing each of the RNAi suppressing lines corresponding to all suppressors, and in-depth characterization of one selected suppressor: *mei-W68* (Rossi et al., 2017).

During the first part of my Thesis I have taken over the brat screen and carried it out to completion myself.

In the initial high content screen, brat-SPRs were identified as RNAi lines that upon visual inspection reduced the size of the tumour down to that of wild-type larval brains in at least 3 out of 4 individuals in two independent assays. Like in the mbt screen, the *Ubi*-GAL4 driver was chosen to drive RNAi expression in the brat screen. The rationale behind this choice is to force the ubiquitous expression of the RNAi under investigation so that RNAi conditions that have an essential cytostatic effect and do not allow for larvae to develop would be filtered out and not considered as hits, as they could be if tumour tissue-specific GAL4 drivers were used. 74 RNAi lines out of the total 4300 RNAi lines that were screened met the criteria to classify as brat-SPRs.

To validate these results, I set up the same screening crosses used during the initial screen *Ubi-GAL4 UAS-Dcr2; UAS-brat-RNAi/TM6 tubGAL80 Tb* males x *UAS-RNAi* line females), obtained micrographs of *Ubi-GAL4 UAS-Dcr2; UAS-brat-RNAi* for each of the screened RNAi lines (in Appendix A), and quantified larval brain size using image processing software developed to this end in the laboratory (Fig. 4.1.). Analysis of the resulting larval brain size distribution confirmed that 68 out of the total 74 RNAi lines identified in the initial screen cause a statistically significant reduction of brain tumour size ($p<9x10E-4$) thus validating the corresponding 68 genes as brat-SPR.

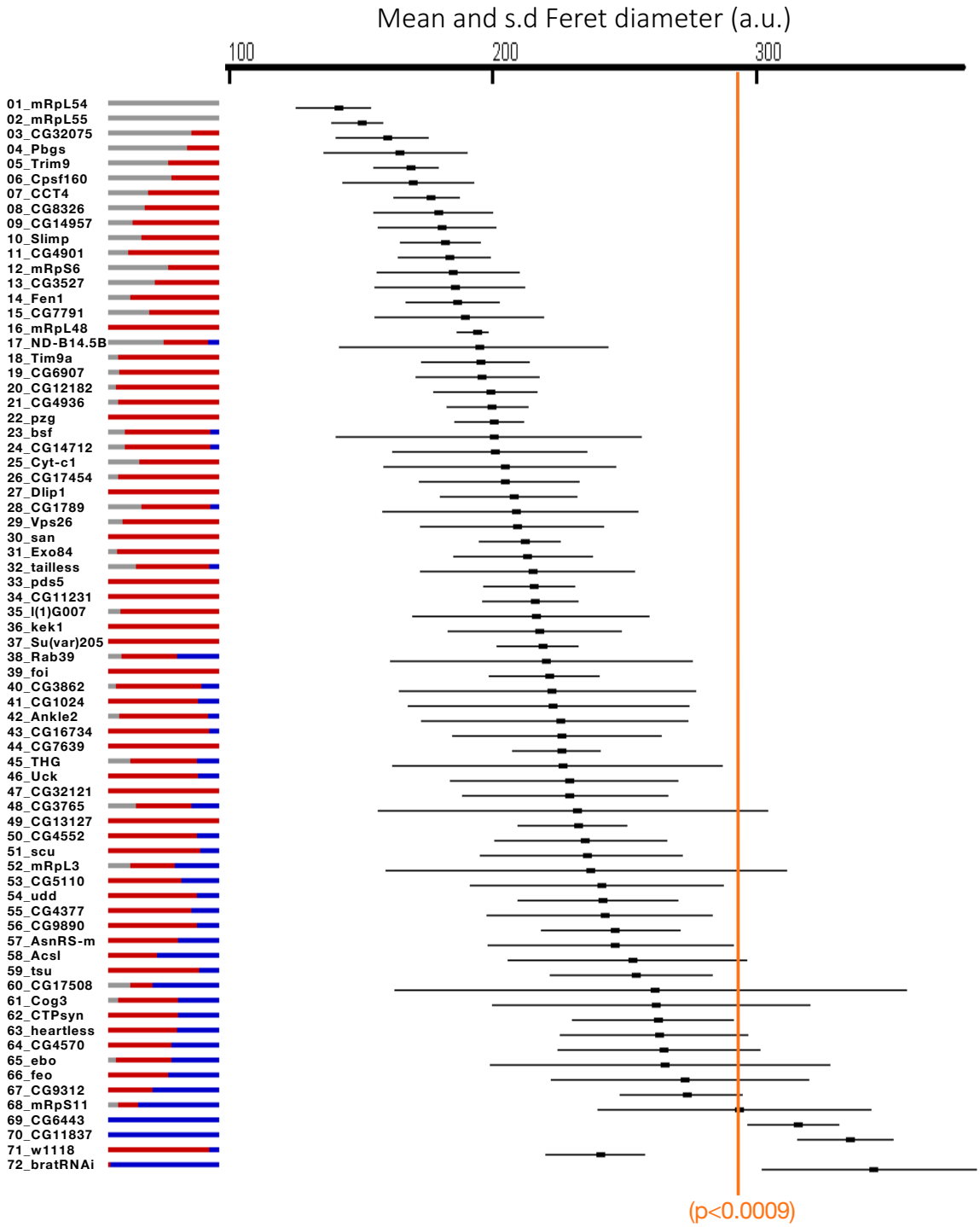

Figure 4.1. Results from high-content screen hits for brat-SPRs. Plot showing maximum mbFerets (mean and standard deviation, s.d.) from brat larvae expressing each of the screened UAS-RNAi lines. A condensed plot of brain-size variation in each sample is shown on the left. Colour code indicates brain size range: brains smaller than wt (grey), wt size (red) or tumour size (blue). The orange line indicates the significance of p<0,0009 below which all have been classified as brat-SPRs. Controls samples (wt and brat) are at the bottom of the table. wt=w^{1118}. Larval brains analysed to generate the plot are in Appendix A.

The remaining six non-validated genes correspond to lines that unlike in the initial screen, either caused early onset lethality and did not reach third instar larval stage (*CG4661, Rab7, l(2)k09022, Tom40*) or did not affect brat brain growth (*CG6443, CG11837*). Out of the six validated brat-SPRs that result in brat larval brains that are smaller than wild type, four had been reported to affect the growth of wild-type larval brains (*Cpsf160*, *CG32075*, *CCT4*, *Trim9*), but two were not reported not to do so (*mRpL55*, *mRpL54*) (Neumüller et al., 2011).

Altogether these results show that 68 out of 4.300 genes (1,6%) randomly selected from the Drosophila genome can be depleted to levels that suppress brat tumorous growth without significantly compromising larval development.

None of the 68 brat-SPRs that we have identified was known as suppressor of brat tumour growth before, but many of them had been linked in different ways to brat or, in more general terms, to neuroblast functions (Table 4.1.).

Regarding genes involved in NB proliferation, a quarter (17 of our 68) brat-SPRs have been identified in a genome wide RNAi screen as required for wild type NB proliferation (Neumüller et al., 2011). Notably, *Acyl-CoA synthetase long-chain* (*Acsl*), was identified as such in (Jia et al., 2019) study but not in the (Neumüller et al., 2011) study. A further 7 brat-SPRs have been reported to bring about defective central nervous system development as they produced lethality in neuroblast-specific RNAi screen by (Carney et al., 2012).

Thirty-nine of our brat-SPRs correspond to NB-specific/enriched genes defined as transcripts overexpressed in brains carrying ectopic NBs or enriched in NBs compared to neurons or newly formed GMCs (Berger et al., 2012; Carney et al., 2012; Wissel et al., 2018).

None of the brat-SPRs is among the *brat* interactors (physical or genetic; n=26 and n=35, respectively) reported in FlyBase (Gramates et al., 2022), but 6 brat-SPRs have been reported to interact with proteins that are well known targets of one or more of the neural transcription factors like *Ase, Dpn, Sna,* and *Pros:: tll, CG1024, CCT4, Su(var)205, htl,* and *Trim9* (Choksi et al., 2006; Hakes & Brand, 2020; Southall & Brand, 2009).

FlyBase ID	Symbol	Underproliferation Neumuller (2011)	Lethality (RNAi screening) Carney (2012)	Neural TF interactors Southall (2009)	specially expressed in NB Carney (2012)	specially expressed in NB Wissel (2018)	specially expressed in NB Berger (2012)	Upregulated in brat versus wt Loop (2004)	Upregulated in brat versus wt Landkron (2018)	Upregulated in brat versus wt Reichardt (2018)	Neurogenesis GO (DAVID 6.8)
FBgn0263120	Acsl								X		X
FBgn0028343	Ankle2	X						X			X
FBgn0034177	AsnRS-m					X	X				
FBgn0284256	bsf		X							X	
FBgn0032444	CCT4	X		X		X	X	X			X
FBgn0027514	CG1024	X		X							X
FBgn0039939	CG11231										
FBgn0028504	CG12182					X					
FBgn0032176	CG13127										
FBgn0037924	CG14712	X							X		X
FBgn0035412	CG14957										
FBgn0037667	CG16734				X	X	X				
FBgn0039977	CG17454										
FBgn0039970	CG17508					X	X				
FBgn0030063	CG1789	X					X				X
FBgn0052075	CG32075	X				X	X				X
FBgn0052121	CG32121										
FBgn0029714	CG3527	X					X				X
FBgn0031657	CG3756				X		X				
FBgn0031286	CG3862					X					
FBgn0034664	CG4377										
FBgn0031304	CG4552										
FBgn0037844	CG4570				X	X	X	X			
FBgn0032194	CG4901	X	X		X	X	X				X
FBgn0038768	CG4936										
FBgn0032642	CG5110					X					
FBgn0031711	CG6907						X				
FBgn0033989	CG7639		X		X	X	X				
FBgn0033038	CG7791										
FBgn0030851	CG8326	X	X		X	X	X				X
FBgn0038179	CG9312										
FBgn0034814	CG9890				X						
FBgn0031536	Cog3	X									X
FBgn0024698	Cpsf160	X				X					X
FBgn0266452	CTPsyn					X					X
FBgn0035600	Cyt-c1						X				
FBgn0040467	Dlip1										
FBgn0266572	ebo					X					
FBgn0266668	Exo84										
FBgn0025832	Fen1	X	X		X	X	X				X
FBgn0030241	feo	X					X	X			X
FBgn0024236	foi	X	X		X	X		X			X
FBgn0010389	htl			X							
FBgn0015399	kek1	X							X		X
FBgn0026713	l(1)G0007						X				
FBgn0030686	mRpL3					X					
FBgn0031357	mRpL48										
FBgn0034579	mRpL54		X		X	X	X				
FBgn0038678	mRpL55						X				
FBgn0038474	mRpS11						X				
FBgn0035534	mRpS6										
FBgn0031505	ND-B14.5B						X				
FBgn0036271	Pbgs					X					
FBgn0260012	pds5								X		
FBgn0259785	pzg							X			X
FBgn0029959	Rab39					X					
FBgn0024188	san						X				
FBgn0021765	scu					X	X				
FBgn0051133	Slimp				X	X	X				
FBgn0003607	Su(var)205	X		X			X	X			X
FBgn0283659	THG										X
FBgn0030480	Tim9a						X				
FBgn0003720	tll			X	X	X	X	X			
FBgn0051721	Trim9	X		X							X
FBgn0033378	tsu										
FBgn0263398	Uck					X					
FBgn0033261	udd										
FBgn0014411	Vps26										

Table 4.1. Summary of bibliography on brat-SPRs. Table summarizing the reports in literature regarding functions in NB development or brat-related function for each brat-SPR. Genes for which no data was available are coloured in grey. Genes whose depletion in a brat mutant background produced brains that are smaller than wild type appear in in red.

4.2. None of the identified suppressors of brat tumour growth (brat-SPRs) allows for wild-type larval brain development

Genetically labelling with mCD8-GFP driven by *wor-GAL4 ase-GAL80* in wild-type brains specifically marks Type II NBs and their progeny (Neumüller et al., 2011), including INPs and GMCs, that appear as isolated clusters located in the dorsal side of the central brain. There are 8 Type II NBs on each brain lobe in wild-type larvae (Fig. 4.2.A.). Labelling with *wor-GAL4 ase-GAL80; UAS-mCD8-GFP* in brat mutant larvae demonstrates the unrestricted overgrowth of the type II NBs lineage cells that account for most of the tumour mass (Fig. 4.2.A.). Consistently, while Mira staining in the dorsal side of the central brain is restricted to a relatively small number of cells (Fig. 4.2.B.), most of the brat tumour mass is accounted for by Mira expressing cells (Fig. 4.2.B.) (Betschinger et al., 2006; Caussinus & Gonzalez, 2005; C.-Y. Lee, Wilkinson, et al., 2006; Reichardt et al., 2018).

To investigate the effect in tumour development brought about by depletion of the brat-SPRs identified in the screen I analysed the gross anatomy of larval brains from *Ubi-GAL4 UAS-Dcr2; UAS-brat-RNAi* for each RNAi line (in Appendix B). Taken individually, each of the 639 brain lobes from the entire collection of RNAi-suppressed brat tumour conditions that I have analysed can be assign to one of two classes. Importantly, however, most of the suppressed tumour conditions result in a mix of class 1 and class 2 brain lobes (Table 4.2.).

An example of class 1 suppressor is *ebo-RNAi* (Fig. 4.2.C.). This class includes brain tumours that although smaller, closely resemble brat tumours in that (i) they are largely accounted for by Mira-positive cells and (ii) the tumoral mass spreads over the entire dorsal side, well beyond of what would be the central brain region in a wild-type brain. Suppressed tumours in this class resemble under-grown brat tumours that do not present any evidence of recovery of normal brain anatomy.

A representative example of class 2 is *Cog3-RNAi* (Fig. 4.2.C.). Larval brains within this class are not only smaller, but also histologically quite different from brat tumours in that a significant fraction of the suppressed tumour is accounted for by large clusters of cells that do not express Mira.

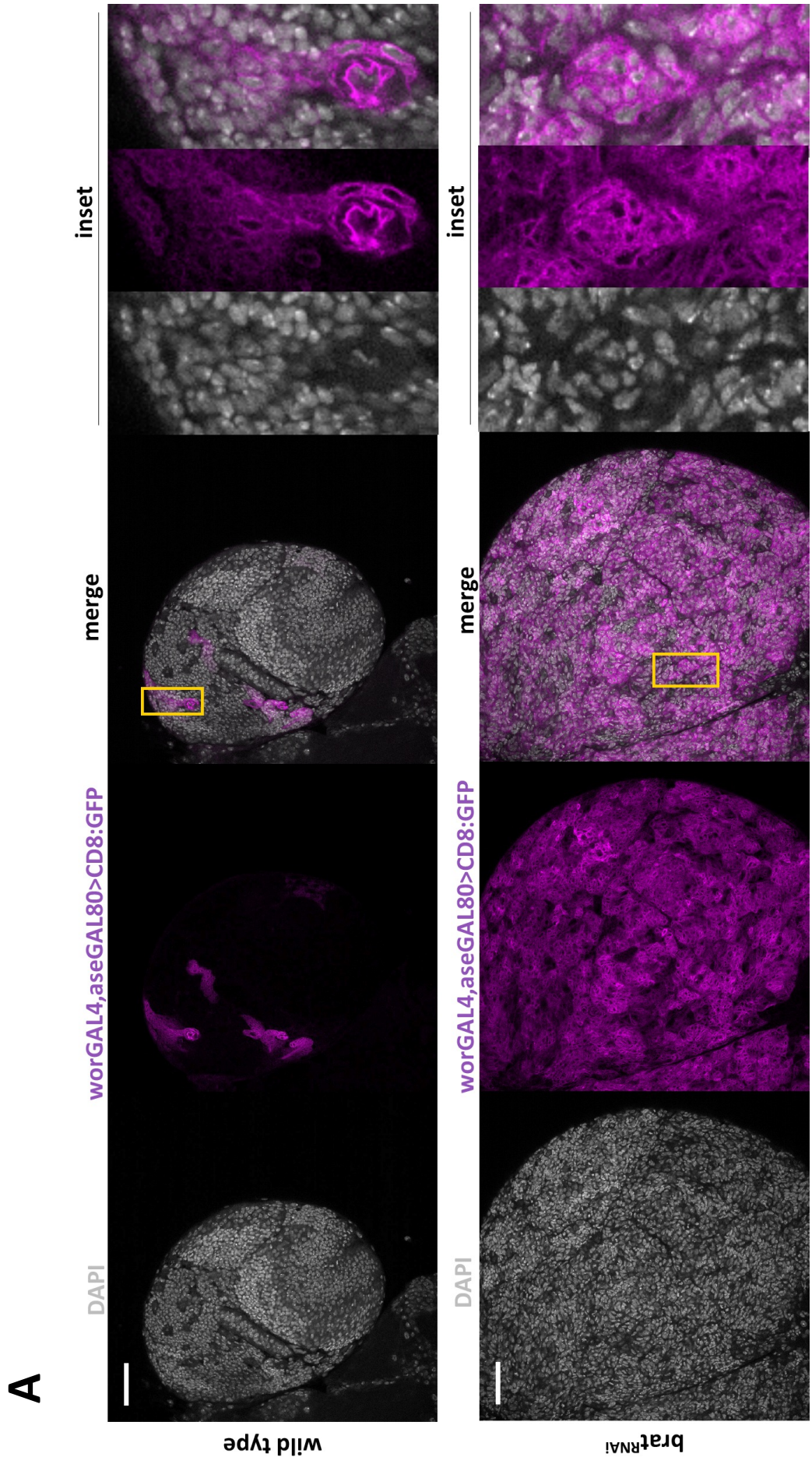
A
wild type
brat^RNAi
DAPI
worGAL4,aseGAL80>CD8:GFP
merge
inset

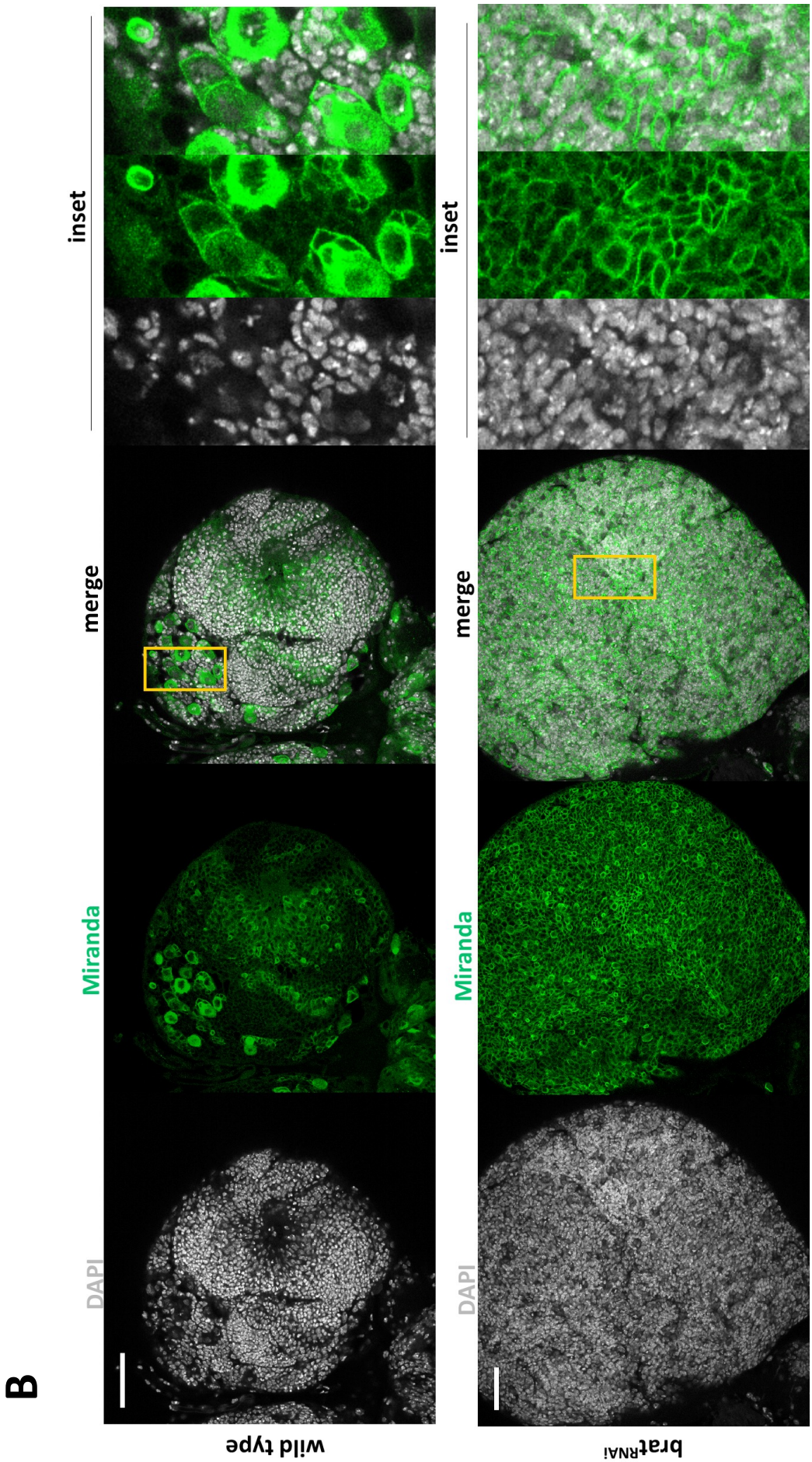
B
wild type
brat^RNAi
DAPI
Miranda
merge
inset

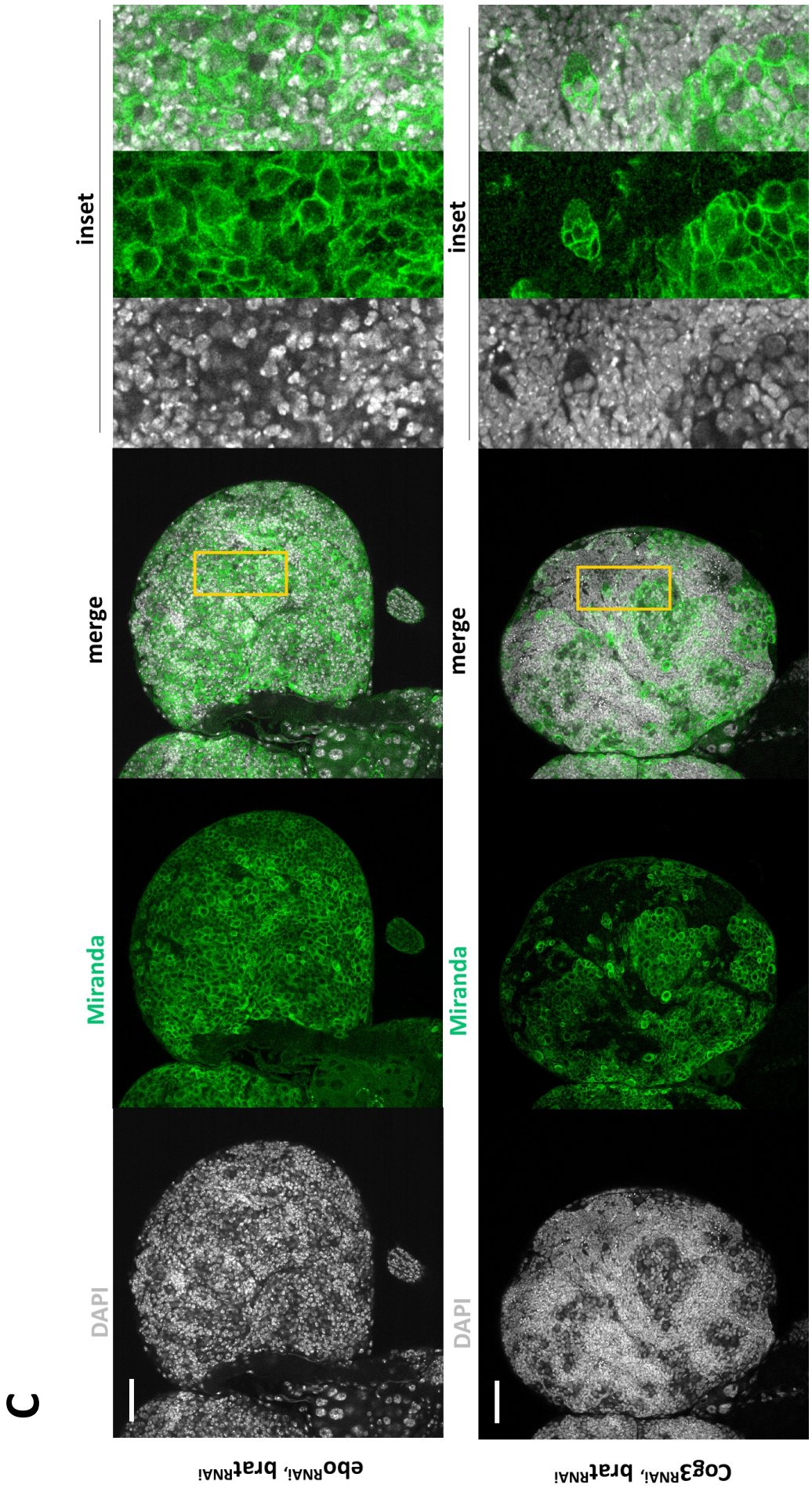
C
inset
merge
Miranda
DAPI
Cog3RNAi, bratRNAi
eboRNAi, bratRNAi

Figure 4.2. The phenotype of suppressed brat tumours. (A) Panels showing confocal dorsal sections of brain lobes from control wt (top) and brat (bottom) expressing *wor-GAL4 ase-GAL80; UAS-mCD8-GFP* that specifically labels type II NB and their progeny (purple). Brain morphology can be observed with DAPI staining (grey) in left panels. Only a small number of type II NBs-like are found in wt brains, restricted to the central brain (CB) region. In contrast, in brat, cells labelled as type II NBs are abundant and invade the whole dorsal side. Insets show high magnification views of the areas outlined in yellow in merged panels. A similar observation can be made from **(B)** panels showing dorsal sections of wt (top) and brat (bottom) brain lobes stained with NB-marker Miranda (Mira; green). In wt brains, NBs outside the CB (such as smaller NBs from optic lobe medulla) are also stained. **(C)** Panels showing dorsal sections of suppressed brat tumour brain lobes with ebo^{RNAi} (top) and $Cog3^{RNAi}$ (bottom), selected as representatives for phenotypic class 1 and class 2 respectively, stained with DAPI (grey) and Mira (green), to reveal morphology and NB distribution. ebo^{RNAi}, $brat^{RNAi}$ brains present mostly Mira-positive cells resembling brat brain while $Cog3^{RNAi}$, $brat^{RNAi}$ brains present clusters of Mira-negative cells. Scale bar of 50 μm.

Such cells, which indeed are very rare in brat tumours, suggest that the corresponding tumour suppressing condition allows for a certain extent of differentiation. It is also possible, however that differentiated cells that do not express Mira may be non-tumoral cells that are not displaced by tumour cells under the suppressed condition. If so, class 1 SPRs morphology might be caused by the combined effect of reduced tumour growth and lethality in surrounding non-tumoral cells. Published brat tumour suppressors *zld, cherub* and *klu* can also be classified within this phenotypic class 2 (Berger et al., 2012; Landskron et al., 2018; Reichardt et al., 2018).

Out of the total 68 brat-SPRs analysed, only 7 (10%) and 15 (22%) result in brain lobes that are exclusively class 1 or class 2, respectively. The remaining 68% of brat-SPRs result in brain lobes of both kinds although for about 2/3 of them class 1 lobes are less frequent than class 2 (Table 4.2. and Fig. 4.3.).

Remarkably, against our expectations I found no cases of suppressed brat growth that resulted in phenotypically wild-type-like brains. Suppressors that allow for the development of brains that present wild-type anatomy in individuals mutant for a tumour suppressor can be interpreted as functions that might be involved in the initial steps of tumorigenesis: upon depletion of such tumour-SPRs, the onset of tumour development cannot take place. The absence of brat-SPRs of this kind was unexpected because 7 (*Nipped-A, Tctp, mei-W68, stil, sunn, TrxT, dhd*) such suppressors were identified in the mbt screen that was carried out in parallel (Rossi et al., 2017).

FlyBase ID	Symbol	Mostly Mira-positive cells	Clusters of Mira-negative cells	Ratio Mostly Mira-positive cells/Total	Main function
FBgn0263120	**Acsl**	0	4	0	lipid metabolism
FBgn0034177	**AsnRS-m**	0	9	0	mitochondrial
FBgn0032444	**CCT4**	0	4	0	protein folding
FBgn0032176	**CG13127**	0	5	0	uncharacterised
FBgn0052121	**CG32121**	0	4	0	transcription
FBgn0031657	**CG3756**	0	7	0	transcription
FBgn0034664	**CG4377**	0	4	0	uncharacterised
FBgn0032194	**CG4901**	0	8	0	transcription
FBgn0030851	**CG8326**	0	13	0	transcription
FBgn0031536	**Cog3**	0	10	0	Transport/Golgi
FBgn0024698	**Cpsf160**	0	8	0	translation
FBgn0038474	**mRpS11**	0	6	0	mitochondrial
FBgn0260012	**pds5**	0	17	0	DNA repair
FBgn0029959	**Rab39**	0	4	0	Transport/Golgi
FBgn0003607	**Su(var)205**	0	8	0	chromatin modifier
FBgn0034814	**CG9890**	1	11	0,083	uncharacterised
FBgn0031505	**ND-B14.5B**	1	11	0,083	mitochondrial
FBgn0029714	**CG3527**	1	9	0,1	response to bacterium
FBgn0037924	**CG14712**	1	7	0,125	nuclear pore
FBgn0051721	**Trim9**	1	7	0,125	development
FBgn0266668	**Exo84**	2	12	0,143	Transport/Golgi
FBgn0284256	**bsf**	2	10	0,167	mitochondrial
FBgn0037844	**CG4570**	2	10	0,167	transposition
FBgn0033989	**CG7639**	2	10	0,167	mitochondrial
FBgn0037667	**CG16734**	3	12	0,2	uncharacterised
FBgn0039977	**CG17454**	3	11	0,214	splicing
FBgn0028504	**CG12182**	2	7	0,222	uncharacterised
FBgn0030063	**CG1789**	2	6	0,25	nucleolus/rRNA processing
FBgn0052075	**CG32075**	2	6	0,25	nucleolus/rRNA processing
FBgn0030241	**feo**	4	11	0,267	cytokinesis
FBgn0031304	**CG4552**	3	8	0,273	Transport/Golgi
FBgn0028343	**Ankle 2**	2	5	0,286	nuclear envelope
FBgn0039939	**CG11231**	4	10	0,286	uncharacterised
FBgn0032642	**CG5110**	3	6	0,333	TOR signalling
FBgn0025832	**Fen1**	2	4	0,333	DNA repair
FBgn0036271	**Pbgs**	4	8	0,333	porphobilinogen synthetic process
FBgn0030480	**THG**	2	4	0,333	translation
FBgn0033378	**tsu**	8	14	0,364	splicing
FBgn0040467	**Dlip1**	4	6	0,4	Nucleus/nucleic acid binding
FBgn0033038	**CG7791**	3	4	0,429	mitochondrial
FBgn0024236	**foi**	6	8	0,429	ion transport
FBgn0283659	**tailless**	4	5	0,444	cell fate
FBgn0027514	**CG1024**	7	8	0,4667	transcription
FBgn0035412	**CG14957**	5	5	0,5	chitin metabolism
FBgn0026713	**l(1)G0007**	3	3	0,5	splicing
FBgn0263398	**Uck**	5	5	0,5	ATPbinding/nucleoside kinase activity
FBgn0038768	**CG4936**	8	7	0,533	transcription
FBgn0010389	**heartless**	4	3	0,571	Fibroblast Growth Factor Receptor
FBgn0266452	**CTPsyn**	7	5	0,583	CTP metabolism
FBgn0259785	**pzg**	7	5	0,583	chromatin modifier
FBgn0031286	**CG3862**	3	2	0,6	uncharacterised
FBgn0031357	**mRpL48**	5	3	0,625	mitochondrial
FBgn0003720	**Tim9a**	9	5	0,643	mitochondrial
FBgn0031711	**CG6907**	4	2	0,667	transcription
FBgn0035534	**mRpS6**	8	4	0,667	mitochondrial
FBgn0035600	**Cyt-c1**	7	3	0,7	mitochondrial
FBgn0030686	**mRpL3**	5	2	0,714	mitochondrial
FBgn0039970	**CG17508**	7	2	0,778	uncharacterised
FBgn0021765	**scu**	9	2	0,818	mitochondrial
FBgn0051133	**Slimp**	8	1	0,889	mitochondrial
FBgn0014411	**Vps26**	8	1	0,889	Transport/Golgi
FBgn0038179	**CG9312**	4	0	1	uncharacterised
FBgn0266572	**ebo**	7	0	1	Mushroom body development
FBgn0015399	**kek1**	4	0	1	Epidermal Growth Factor Receptor
FBgn0034579	**mRpL54**	6	0	1	mitochondrial
FBgn0038678	**mRpL55**	6	0	1	mitochondrial
FBgn0024188	**san**	4	0	1	chromatid cohesion
FBgn0033261	**udd**	8	0	1	nucleolus/rRNA processing

Table 4.2. Phenotypic classification of brat-SPRs. Table classifying each brain lobe to a phenotypic class. Colour code highlights cells where all brain lobes belong to the same class. Brat-SPRs are ranked according to the ratio of mostly Mira-positive cells/total. Highlighted in red are the 3 brat-SPRs that have the same amount of brains belonging to each class (ratio=0,5). Column on the right indicates the main function (grouped by colour) for each brat-SPRs.

4.3. Enriched Gene Ontology terms among the collection of brat-SPRs identified in our screen

Making use of the online Database for Annotation, Visualization and Integrated Discovery (DAVID v6.8) we identified Gene Ontology (GO) enriched terms among the identified brat-SPRs (Fig. 4.4.).

As far as biological processes are concerned there are 3 enriched GO terms: "neurogenesis" (p=5x10E-12), "mitochondrial translation" (p=9,9x10E-05), and "gonadal mesoderm development" (p=4,2x10E-02), that account for 30% (21/68), 9% (6/68), and 3% (2/68) of the brat-SPRs, respectively. The two genes annotated in the GO term "gonadal mesoderm development" are *fear-of-intimacy* (*foi*) and *heartless* (*htl*), that are also known to play roles in glia development (Pielage et al., 2004; Stork et al., 2014). Regarding cellular components, the 4 enriched terms are: "mitochondrial large ribosomal subunit" (p=2,6x10E-03), "mitochondrion" (p=3,7x10E-03), "mitochondrial small ribosomal subunit" (p=1,3x10E-02), and "nucleolus" (p=1,3x10E-02). These account for 6% (4/68), 13% (9/68), 4% (3/68) and 7% (5/68) of the brat-SPRs, respectively. Finally, 3 molecular functions were found to be enriched including "protein transporter activity" (p=2,7x10E-02): "structural constituent of ribosome" (p=3,2x10E-02), and "small ribosomal subunit rRNA binding" (p=3,9x10E-02) that account for 4% (3/68), 9% (6/68) and 3% (2/68) of the brat-SPRs, respectively (Fig. 4.4.).

Altogether DAVID's results reveal a high enrichment of mitochondrial related functions among the brat-SPRs identified in our screen. This observation substantiates published results suggesting that inhibition of respiratory complex activity can suppress brat tumour growth (van den Ameele & Brand, 2019). These authors found that oxidative phosphorylation (OxPhos) dysfunction causes wild-type neural stem cells to fail to undergo terminal differentiation and brat tumour cells to slow down proliferation rate. Similarly, Bonnay and colleagues (Bonnay et al., 2020) reported that neural stem cells increase OxPhos during immortalization and blocking OxPhos -or mitochondrial fusion- stalls tumour cells in quiescence and prevents tumorigenesis. Interestingly, published results from our lab showed that mbt tumours are also more sensitive than wild-type tissues to loss of mitochondria-related functions (Rossi et al., 2017).

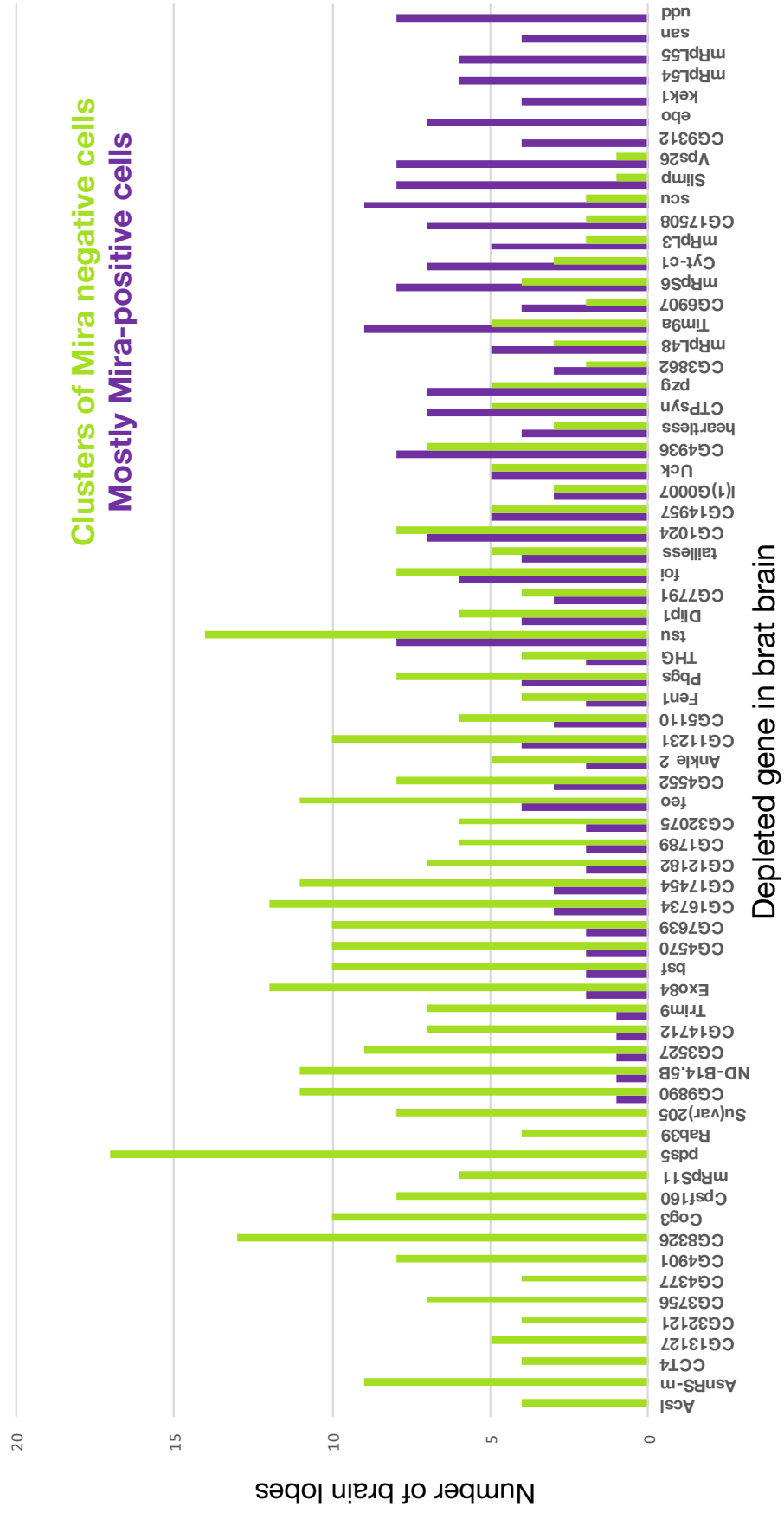

Figure 4.3. Distribution of the phenotypic classes. Histogram showing the number of brain lobes (Y-axis) associated to phenotypic class 1 (Mostly Mira-positive cells; purple) or class 2 (Clusters of Mira negative cells; green) for each brat-SPRs (X-axis).

A

Enriched G.O. for 68 brat-SPRs (high content)

	term	p-value	count
BP	neurogenesis	5,00E-12	21
	mitochondrial translation	9,90E-05	6
	gonadal mesoderm development	4,20E-02	2
CC	mitochondrial large ribosomal subunit	2,60E-03	4
	mitochondrion	3,70E-03	9
	mitochondrial small ribosomal subunit	1,30E-02	3
	nucleolus	1,30E-02	5
MF	protein transporter activity	2,70E-02	3
	structural constituent of ribosome	3,20E-02	6
	small ribosomal subunit rRNA binding	3,90E-02	2

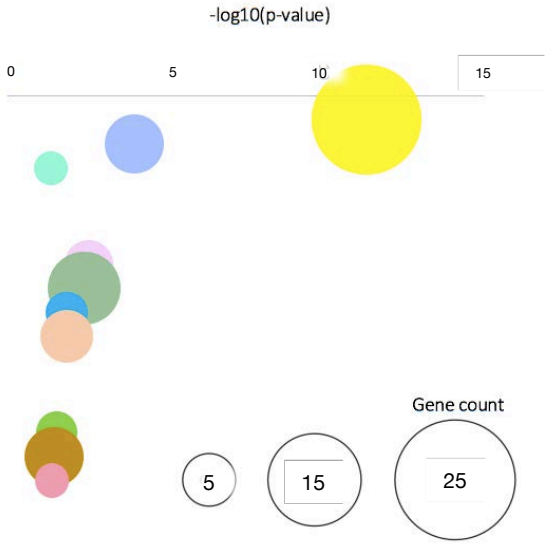

B

Category	Term	Ankle 2	Acsl	CG1024	CG14712	CG1789	CG32075	Cog3	CG3527	CG4901	CG5525 (CCT4)	CG8326	CTPsyn	Cpsf160	Fen1	Su(var)205	Trim9	feo	foi	kek1	l(2)35Bc -THG	pzg	mRpL3	mRpL48	mRpL54	mRpL55	mRpS11	mRpS6	htl	Tim9a	CG6796	CG7791	Cyt-c1	Slimp	bsf	scu	udd	Vps26
BP	neurogenesis	X	X	X	X	X	X	X	X	X	X	X	X	X	X	X	X	X	X	X	X	X																
	mitochondrial translation																						X	X	X	X	X	X										
	gonadal mesoderm development																		X										X									
CC	mitochondrial large ribosomal subunit																						X	X	X	X												
	mitochondrion														X											X				X	X	X	X	X	X	X			
	mitochondrial small ribosomal subunit																						X				X	X										
	nucleolus					X			X	X					X																						X	
MF	protein transporter activity							X																						X								X
	structural constituent of ribosome																						X	X	X	X	X	X										
	small ribosomal subunit rRNA binding																										X	X										

Figure 4.4. Gene Ontology enrichment in the collection of brat-SPRs. (A) Table and bubble plot showing the p-values (-log10) for each enriched Gene Ontology term (Y-axis) for the group of 68 brat-SPRs. The diameter of each circle represents the number of brat-SPRs belonging to each term. **(B)** Table showing the 37 brat-SPRs that belong to any of the enriched G.O. terms. Table cells are colour-coded according to circles in bubble plot. BP=biological process, CC=cellular component, MF= molecular function.

Surprisingly, however, enrichment of nucleolar functions is very small (Fig. 4.4.). This is unexpected because *brat* mutant cells are known to present enlarged nucleoli both in absolute terms and in terms of the ratio between nucleolar and cellular diameter, thus strongly suggesting that Brat might directly regulate the size of the nucleolus, most likely by downregulating dMyc expression (Betschinger et al., 2006). Indeed, brat overexpressing cells contain less ribosomal RNA than control cells. These results suggest that the tumorous phenotype of brat mutants may be due to excess cell growth and ribosome synthesis (Frank et al., 2002).

Besides the brat-SPRs referred to above that are linked to enriched GOs (n=37), there is a further 31 brat-SPRs that although belonging to GOs that are not significantly enriched in our gene set, identify functions that are certainly essential for brat tumour growth. The main function for each of these genes is detailed in (Table 4.2.). These include genes that play key roles in mitosis (*san*) (Pimenta-Marques et al., 2008), Golgi transport (*Exo84* and *Rab39*) (Blankenship et al., 2007; Lakatos et al., 2021) and DNA repair (*pds5*) (Dorsett et al., 2005; Gaudet et al., 2011).

4.4. Tumour-specific suppressors outnumber those that inhibit both brat and mbt tumours

One very important issue regarding malignant growth is the extent to which different tumours require different functions (Chang et al., 2021), i.e. which gene set is greater: tumour-SPRs that can be targeted to inhibit any type of tumour or tumour type-specific tumour-SPRs? The first gene set would be expected to include "tumour housekeeping" functions which may be expected to be more abundant than the second which would be accounted for by genes related to the specific function of the corresponding tumour suppressor gene. The differences in terms of both cell-of-origin of each tumour and molecular function of each tumour suppressor makes brat and mbt tumours ideally suited for this purpose.

I have addressed this issue by comparing the results from this study to those published by our laboratory reporting the screen for mbt-SPRs that was carried out with the same RNAi collection (Rossi et al., 2017).

The first interesting comparison between the mbt and brat datasets regards synthetic interactions. Out of the 4151 lines analysed in common for both tumours, there are 288 RNAi lines that cause lethality in both the brat and mbt background (Excel sheet: Screens_mbt_&_brat_Lethal_lines in Appendix D1). In addition to these, there are 192 lines causing lethality in mbt, but not in brat, and 186 lines that cause lethality in brat, but not in mbt (Excel sheet: Screens_mbt_&_brat_Lethal_lines in Appendix D1). These genes, whose depletion allows for survival in one mutant background but causes lethality on the other background represent putative tumour specific synthetic lethal genetic interactions.

The second relevant comparison regards the brat-SPRs and mbt-SPRs gene sets.
I found that four brat-SPRs (*CG32121, Rab39, CCT4, Cpsf160*) are lethal in a mbt mutant background, and seven of the mbt-SPRs (*Zip99C, l(1)sc, nito, CG8005, mRpL21, RtcB, ND-49*) are lethal in a brat mutant background. These must correspond to genes that are

required for both brat and mbt tumour growth but for which the depletion level achieved by the corresponding RNAi is tolerable for one of these mutant backgrounds but not for the other.

Among the remaining SPRs (those that do not cause lethality in either mutant background) there are 21 genes in common between the 68 brat-SPRs reported here and 92 mbt-SPRs identified in the high-content screen carried out by Rossi and colleagues (brat&mbt-SPRs) (Fig. 4.5.A.). This result reveals that, rather counterintuitively, tumour-specific suppressors largely outnumber those that inhibit both types of tumours.

In addition to slowing tumour growth, ubiquitous knockdown of "tumour housekeeping" genes might also cause larval lethality. That might be a trivial explanation for why fewer mbt&brat-SPRs were recovered than tumour-specific-SPRs and a proof of the setup of the screen, which actually was designed to filter out RNAi lines whose ubiquitous expression is lethal.

Like for the brat-SPRs identified before, GO enriched terms by DAVID in the mbt&brat-SPRs gene set are mostly accounted for by "neurogenesis" and "mitochondria" functions. Enrichment levels, however, are only moderate.

Enriched GOs as revealed by DAVID among the set of 21 brat&mbt-SPRs are "neurogenesis" (p=1,3x10E-03), "mitochondrial translation" (p=7,8x10E-03), and "mitotic sister chromatid cohesion" (p=1,7x10E-02) for biological process; "mitochondrial small ribosomal subunit" (p=4,4x10E-02) for cellular component and "small ribosomal subunit rRNA binding" (p=1,1x10E-02) for molecular function (Fig. 4.5.B.).

In addition to the high-content screen for mbt-SPRs referred to before (Rossi et al., 2017), our laboratory carried out a candidate screen of 233 RNAi lines corresponding to genes that were expected to be related to mbt function based on a series of criteria. Through this targeted screen they identified another 46 mbt-SPRs, of which 7 produce underproliferation. I have tested these mbt-SPRs and found that 12 (26%) classify as mbt&brat-SPRs (p<0,015) (Fig. 4.6.). These are *rept, pont, Mcm5,* and *Tctp* involved in meiotic recombination; *Rbm13,* and *CG32694*, which are upregulated in mbt; the mbt signature genes *eIF4E-6, swa, sunn,* and *gnu*; *Cul2* (Janic et al., 2010) and *Hop* which is required for the piRNA pathway. From these, *rept, Rbm13,* and *Cul2* produce very small (much smaller than wild type brains) brat and mbt tumours and *Dom*, *Nipped-A*, and *Ercc1* cause lethality in the brat tumour background.

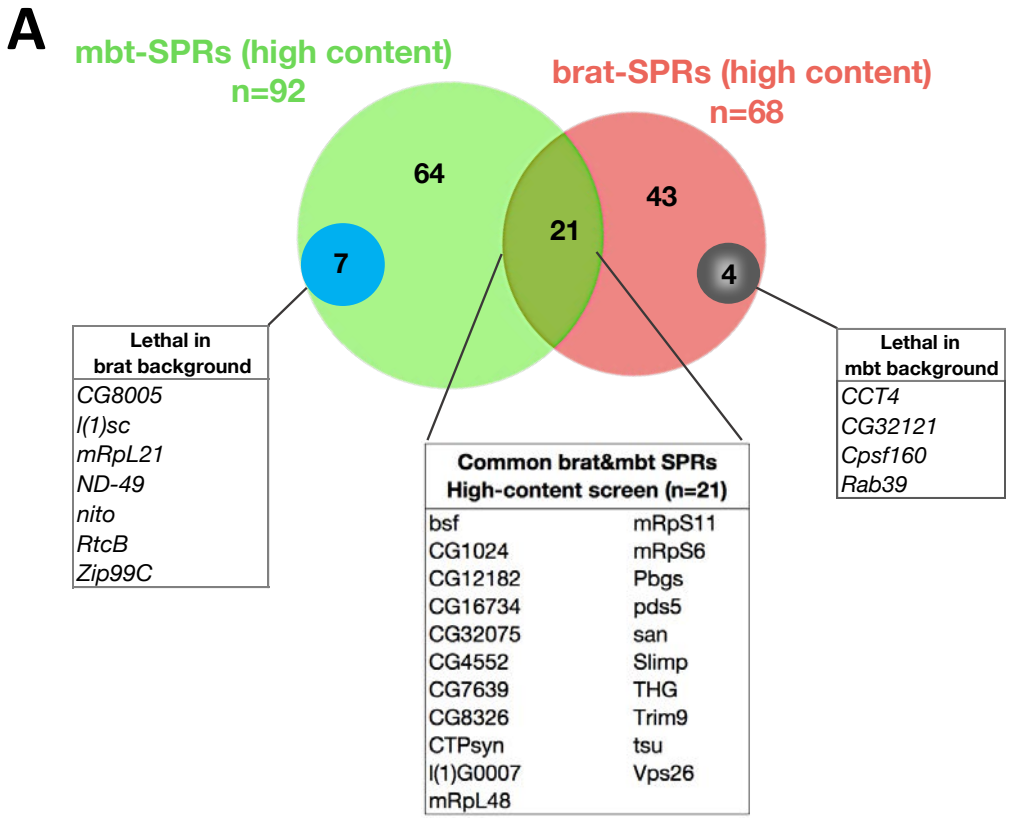

B

Enriched G.O. for unbiased common brat & mbt SPRs (n=21)			
	term	p-value	count
BP	neurogenesis	1,30E-03	6
BP	mitochondrial translation	7,80E-03	3
BP	mitotic sister chromatid cohesion	1,70E-02	2
CC	mitochondrial small ribosomal subunit	4,40E-02	2
MF	small ribosomal subunit rRNA binding	1,10E-02	2

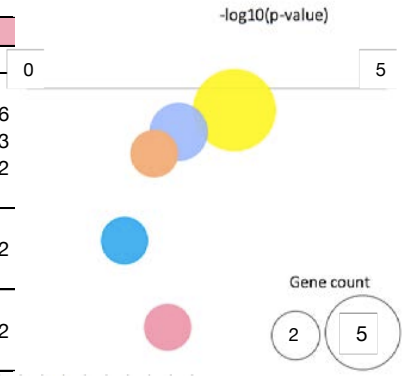

Category	Term	CG1024	CG32075	CG8326	CTPsyn	Trim9	l(2)35Bc - THG	mRpL48	mRpS11	mRpS6	pds5	san
BP	neurogenesis	X	X	X	X	X	X					
BP	mitochondrial translation							X	X	X		
BP	mitotic sister chromatid cohesion										X	X
CC	mitochondrial small ribosomal subunit								X	X		
MF	small ribosomal subunit rRNA binding								X	X		

Figure 4.5. Overlapping between brat-SPRs and mbt-SPRs. (A) Venn diagram showing the overlap between brat-SPRs (red, n=68) and mbt-SPRs (green, n=92). The 21 genes in common (brat&mbt-SPRs) are listed below the diagramm. Remarkably, depletion of 7 out of the 71 specific mbt-SPRs is lethal in brat background (blue), and depletion of 4 out of the 47 specific brat-SPRs results in lethality in mbt background (grey). **(B)** Gene Ontology enrichment for brat&mbt-SPRs. Upper table and bubble plot show the p-values (-log10) for each Gene Ontology term enriched for the group of 21 brat&mbt-SPRs. The diameter of the circle corresponds to the number of genes in each group. In table at the bottom, cells are colour-coded according to circles in bubble plot. BP=biological process, CC=cellular component, MF= molecular function.

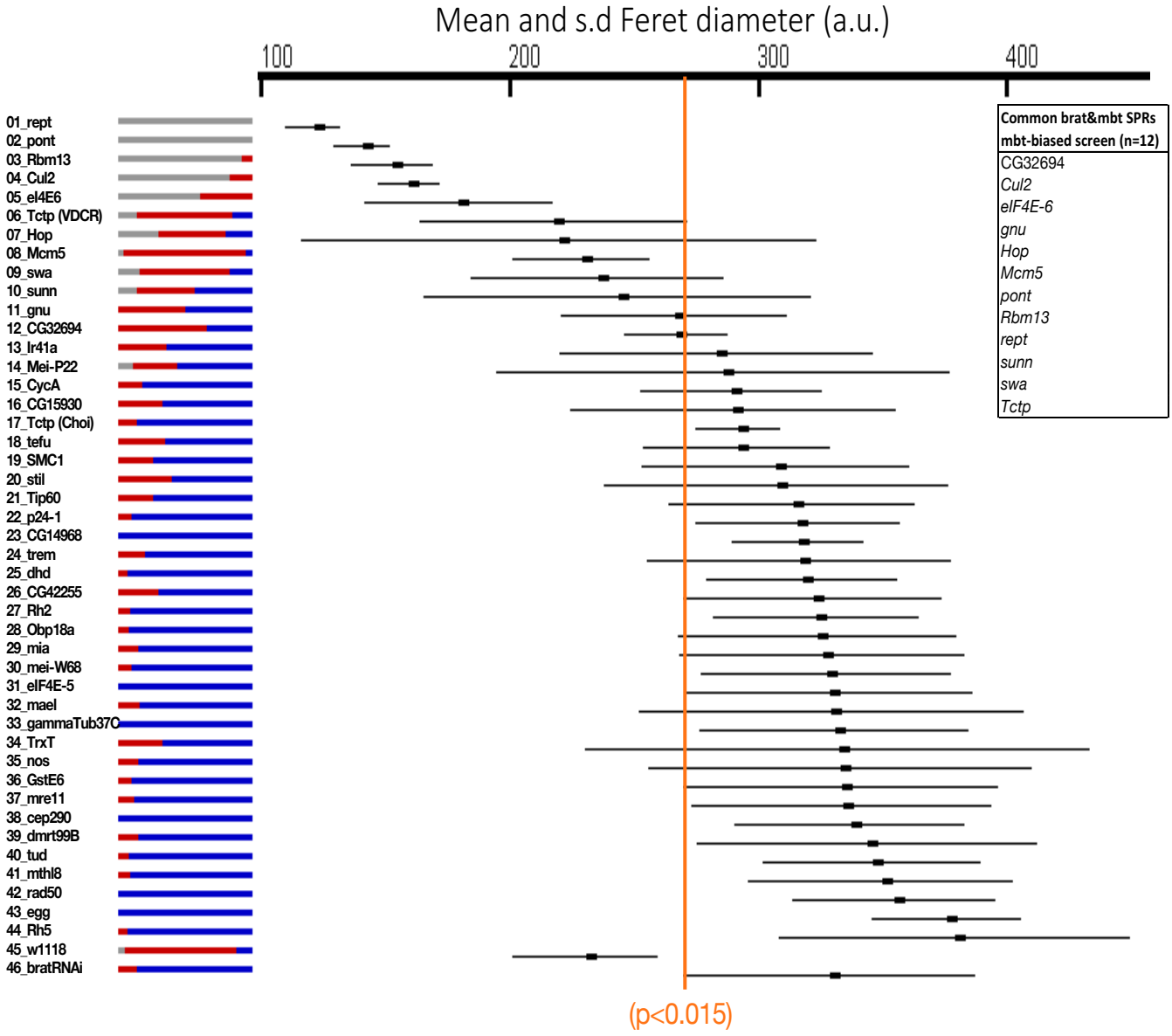

Figure 4.6. Effect of mbt-SPRs genes identified in the mbt targeted screen in brat tumour growth. Plot showing mbFerets (mean and standard deviation, s.d.) from brat larvae expressing each of the screened UAS-RNAi lines. A condensed plot of brain-size variation in each sample is shown on the left. Colour code indicates brain size range: brains smaller than wt (grey), wt size (red), and tumour size (blue). An orange line indicates the significance of p<0,015 below which all have been classified as brat&mbt-SPRs (n=12) which are listed in upper right table. Control samples (wt and brat) are at the bottom of the table. wt=w^{1118}. Larval brains analysed to generate the plot are in Appendix C.

Thus, altogether, we have identified a total of 80 brat-SPRs of which 33 are mbt&brat-SPRs. Interestingly, brat-SPRs are equally abundant among mbt-SPRs identified in the high content screen (23%) than among mbt-SPRs identified in the targeted screen (26%) (Fig. 4.7.).

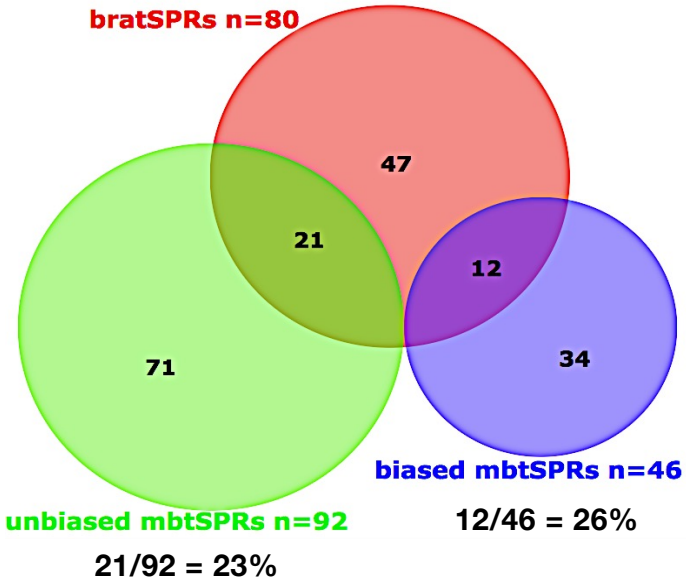

Figure 4.7. Overlapping between brat-SPRs and mbt-SPRs identified in the mbt targeted screen. Venn diagram showing overlap between all brat-SPRs identified (red) with mbt-SPRs identified in the high content screen (green) and in the targeted screen (blue), 21 and 12 genes are in common, respectively.

4.5. Depletion of Vps26 reduces overgrowth of Drosophila mbt and brat larval brain tumours

One of the mbt&brat-SPRs identified in this study is *Vacuolar protein sorting 26* (*Vps26*). Vps26 is a component of the retromer complex which is best known for its role in the Wntless (Wls) traffic loop that encompasses the Golgi, the cell surface, an endocytic compartment and a retrograde route leading back to the Golgi, thereby enabling Wls to direct Wingless (Wg) secretion (Port et al., 2008). However, my interest in this suppressor of brat and mbt tumour growth is that it has been reported to have a tumour suppressor function that is NB type specific: depletion of Vps26 in the larval central brain type II NB lineages (driven by *PntP1*-GAL4 or *erm*-GAL4) results in supernumerary NBs and tumour growth while depletion of Vps26 in type I NBs (driven by *erm*-GAL4 or *ase*-GAL4) does not (B. Li et al., 2018). The finding that *Vps35* behaves likewise led these authors to conclude that the retromer complex itself has a tumour suppressing activity.

Taking these results into account I decided to test whether the mbt&brat-SPR activity of Vps26 is shared by the other members of the retromer complex, *Vps29* and *Vps35*. Through these studies I found that depletion of neither Vps29 (Fig. 4.8.) nor Vps35 (data not shown) has any effect on brat and mbt tumour growth, and confirmed Vps26

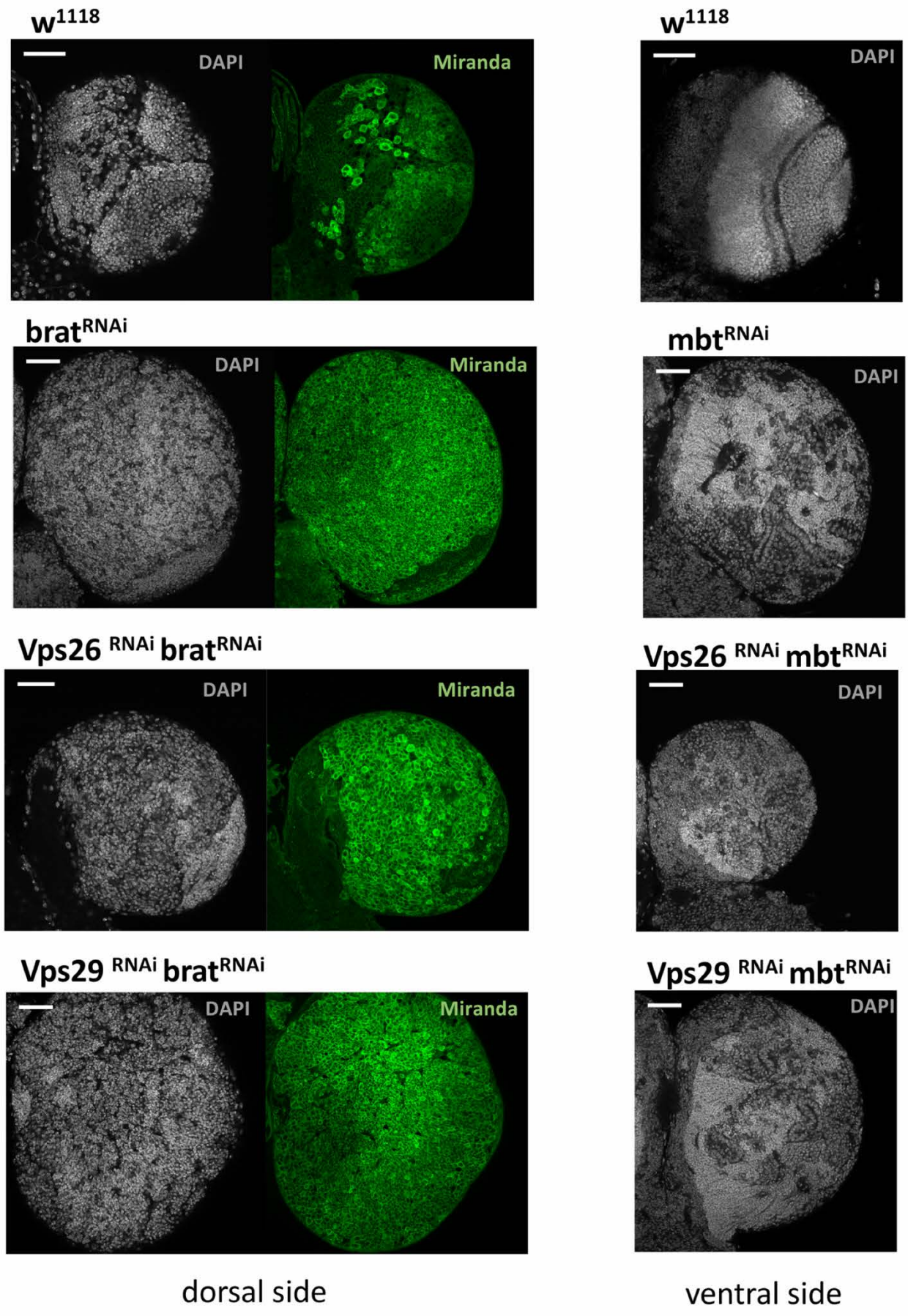
w1118
DAPI
Miranda
w1118
DAPI
bratRNAi
DAPI
Miranda
mbtRNAi
DAPI
Vps26 RNAi bratRNAi
DAPI
Miranda
Vps26 RNAi mbtRNAi
DAPI
Vps29 RNAi bratRNAi
DAPI
Miranda
Vps29 RNAi mbtRNAi
DAPI
dorsal side
ventral side

Figure 4.8. Effect of retromer components depletion in larval brain tumours. Left panels showing dorsal section of brain lobes from wt, brat tumour and brat tumours in which *Vps26* or *Vps29* has been depleted by RNAi, stained with DAPI (grey) and NB-marker Mira (green). wt brain presents type II NBs in the CB, while brat tumour mass is mostly composed by cells expressing Mira. In the case of $Vps26^{RNAi}$, $brat^{RNAi}$ (*Ubi-GAL4 UAS-Dcr2/+; UAS-brat-RNAi/ UAS-Vps26-RNAi*), wt size is observed but the dorsal side presents mutant morphology with mostly Mira-positive cells. $Vps29^{RNAi}$, $brat^{RNAi}$ *(Ubi-GAL4 UAS-Dcr2/UAS-Vps29-RNAi; UAS-brat-RNAi/+*), resembles the brat brain, since reduction of size is not observed and presents mutant morphology with mostly Mira-positive cells. Right panels show ventral section of DAPI-stained brain lobes from wt, mbt tumour and mbt tumours in which *Vps26* or *Vps29* has been depleted by RNAi. wt brain presents typical row of neuroepithelia (NE) in the optic lobe (OL), while mbt presents overgrown NE that invades the OL. $Vps26^{RNAi}$, mbt^{RNAi} (*Ubi-GAL4 UAS-Dcr2/+; UAS-l(3)mbt-RNAi l(3)mbt^{ts1}/UAS-Vps26-RNAi*) brain shows size reduction, but maintains mutant morphology with NE folding, and $Vps29^{RNAi}$, mbt^{RNAi} (*Ubi-GAL4 UAS-Dcr2/UAS-Vps29-RNAi; UAS-l(3)mbt-RNAi l(3)mbt^{ts1}/+*) fully resembles a mbt brain in size and morphology. wt=w^{1118} Scale bar: 50μm.

as an mbt&brat-SPR. Regarding its effect in brat tumour anatomy, Vps26 classifies within class 1, as defined earlier (Fig. 4.2.C.). In mbt tumours, Vps26 depletion slows down growth but does not allow for the recovery of normal anatomy landmarks (Fig. 4.8.).

In situ overgrowth is a direct readout of tumour formation. However, it cannot be taken as evidence for malignancy. The ultimate test to determine malignancy is based on allograft assays (Gateff, 1978). To further analyse the mbt&brat-SPR activity of *Vps26* we carried out allograft assays. To this end, we implanted larval brain tissue from (i) *Ubi-GAL4 UAS-Dcr2/+; UAS-l(3)mbt-RNAi l(3)mbt^{ts1}/+*; (ii) *Ubi-GAL4 UAS-Dcr2/+; UAS-brat-RNAi/+ ;* (iii) *Ubi-GAL4 UAS-Dcr2/+; UAS-l(3)mbt-RNAi l(3)mbt^{ts1}/ UAS-Vps26-RNAi* and (iv) *Ubi-GAL4 UAS-Dcr2/+; UAS-brat-RNAi/ UAS-Vps26-RNAi* individuals. We found that despite the significant reduction in larval brain size, depletion of Vps26 has very little effect on the rate of malignancy of brat tumours in either sex. In mbt tumours, however, loss of Vps26 significantly reduces the malignancy rate in both sexes (Fig. 4.9.).

These results show that in addition to Vps26 published tumour suppression activity (i.e. depletion results in tumour growth) Vps26 is also a suppressor of mbt and brat tumour growth (i.e. depletion inhibits the growth of mbt and brat tumours). They also show that as far as brat tumours are concerned Vps26 depletion appears to slow down growth but have little effect in the malignant potential of the tumour while it seems to affect both growth and malignancy of mbt tumours. Finally, my results show that, unlike the published tumour suppression activity, the mbt&brat-SPR function appears to be specific of Vps26 and not a general function of the retromer complex.

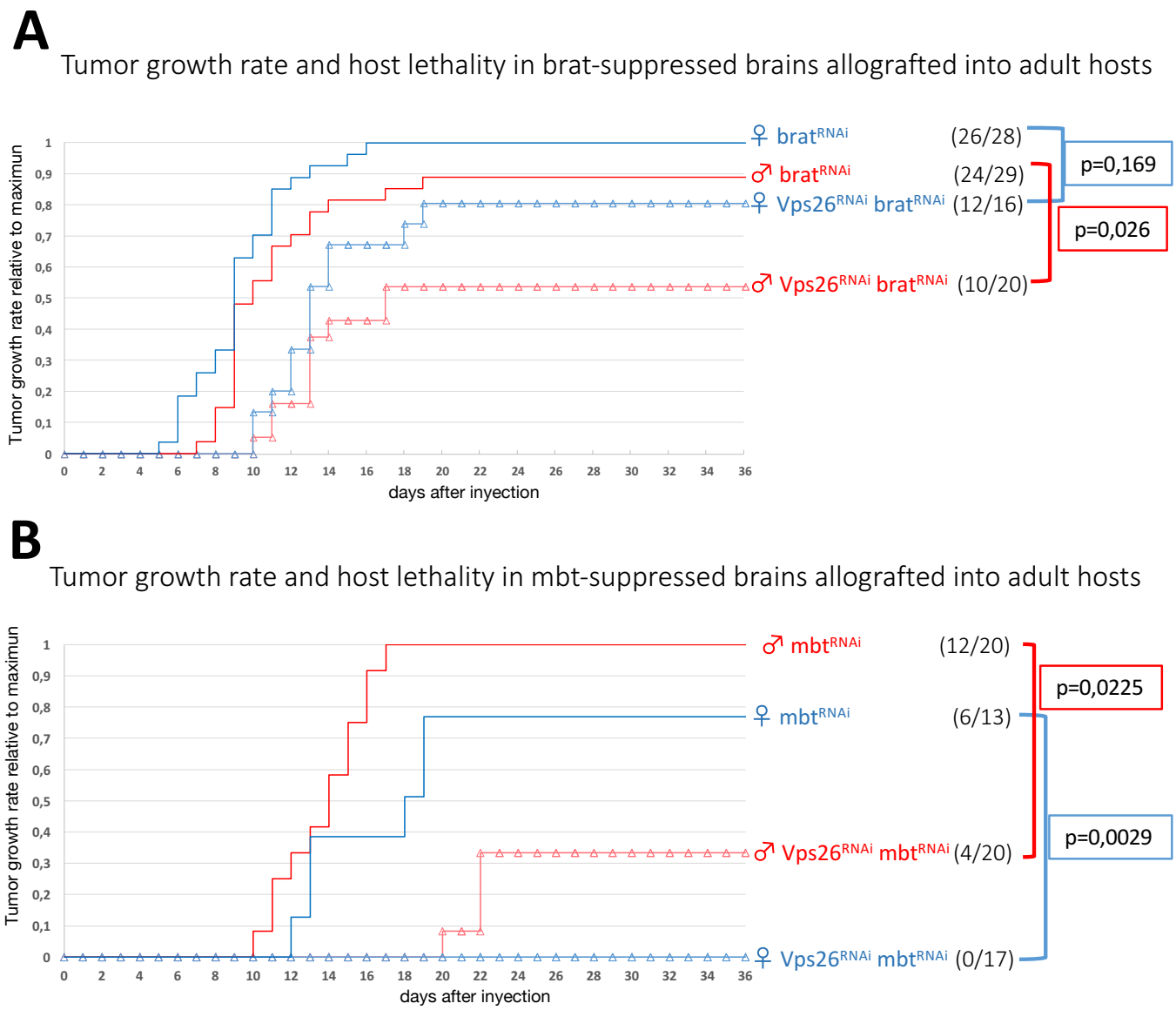

Figure 4.9. Tumorigenic potential of Vps26-depleted tumours. Tumour growth rate and host lethality caused by **(A)** Vps26-depleted brat tumour and **(B)** Vps26-depleted mbt tumours allografted into adult hosts. Implants of *Vps26*^{RNAi}, *brat*^{RNAi} kill similarly to *brat*^{RNAi} in both sexes, while *Vps26*^{RNAi}, *mbt*^{RNAi} kill significantly less than *mbt*^{RNAi} in both sexes. Allografted tissues were dissected from third instar larvae (168 ± 12 hours AEL; 29°C). Pairwise p-values were calculated by Fisher's exact test. Colour code: male samples= red; female samples = blue.

4.6. The transcriptome of brat larval brain tumours

4.6.1. Inconsistencies among published databases

An important standing question in tumour biology is the correlation between the extent of gene expression dysregulation and the functional relevance of the corresponding gene with regards to tumour growth. The importance of this question resides in that tumour gene signatures ("transcriptomic landscapes") are often taken as functionally relevant gene sets in the absence of functional data (Drăghici et al., 2003). This issue must be addressed from two different angles: the proportion of tumour-relevant genes that are dysregulated in tumour cells and the proportion of dysregulated genes that are functionally relevant for tumour growth.

Having identified a validated gene set of brat-SPRs among 4.000 randomly selected genes I decided to tackle the expression/function question by comparing my results to 3 published studies reporting the transcriptome of brat tumours (Loop et al., 2004), (Landskron et al., 2018), and (Reichardt et al., 2018).

The first study (Loop et al., 2004) was carried out on $brat^{K06028}$ adult heads using two different micro-chip platforms, Affymetrix and roDromega full genome, with and without signal amplification methods, respectively. In this study $brat^{K06028}$ mutant adult heads were compared to both wild type Oregon R and $brat^{K06028}$ revertants generated by excision of the P-element that causes the $brat^{K06028}$ mutant allele (bratK *jump-out*). They found 725 genes to be differentially expressed between $brat^{K06028}$ and Oregon R, and 1888 genes to be differentially expressed between $brat^{K06028}$ and bratK *jump-out.* Notably, only 321 genes, 279 and 42 transcripts that showed increased and decreased expression level respectively, are common between these two gene sets. These were classified as consistently differentially expressed in adult neoplastic $brat^{K06028}$ brains.

The other two studies (Landskron et al., 2018) and (Reichardt et al., 2018) were carried out by RNA-seq on FACS-sorted brat NB-like cells using wild-type type II NBs as control. A major difference as far as experimental approaches go between these two studies is that Landskron and colleagues used NBs from wandering third instar larvae expressing brat-RNAi driven by *UAS-Dcr2; wor-GAL4 ase-GAL80; UAS-stinger::RFP* during all development, while Reichardt and colleagues profiled NBs that had been expressing brat-RNAi for only 24 hours. Likely a consequence of such major difference in the timing of onset of the *brat* loss of function condition, the Landskron study found 1372 upregulated and 345 downregulated genes, while the corresponding numbers identified by Reichardt were only 41 and 38, respectively.

Plotting together the results from all three studies I observed that as far as upregulated genes are concerned, the overlap between the Loop and Reichardt, Loop and Landskron and Reichardt and Landskron datasets is only of 4, 26, and 18 genes, respectively (Fig. 4.10.). There are only 2 genes in common among the three studies: *Staufen*, that encodes the RNA binding protein Staufen involved in the localization of diverse mRNA during oogenesis, embryogenesis and nervous system development (Barbee et al., 2006; Irion et al., 2006; Ramos et al., 2000; St Johnston et al., 1991), and the transcription factor dMyc, the Drosophila homologue of human Myc, which is implicated in multiple biological processes related to cell growth (Furrer et al., 2010; Parisi et al., 2011; Teleman et al., 2008). Similar results were observed regarding downregulated genes except that in this case there are no common genes among the 3 studies (Fig. 4.10.).

It is unclear what the reasons for the very poor overlap among the dysregulated gene sets from these three studies might be. Different methods (micro-chip *versus* RNAseq) may play a small part (Moreau et al., 2003; W. Zhang et al., 2015). However, the main reason may be the very different nature of the biological samples and experimental conditions that were used. Adult flies bearing brat tumours are escapers that unlike most of their siblings manage to eclose (Arama et al., 2000; Loop et al., 2004). The very same factors that allowed for these individuals to survive might affect the tumours that they carry. Moreover, unlike brat tumours in larval brains, brat tumours in adult flies have gone through the pupal stage and are likely to having been affected by the hormone-triggered signaling pathways that ultimately reshape the larval body into that of an adult (Noselli & Agnès, 1999; Tennessen & Thummel, 2011; Thummel, 1996). NB-like cells sorted by FACS from brat larval brains, on the other hand, are only part of the cells present in brat tumours that indeed include other cell types. Therefore, the transcriptome of brat NB-like cells is unlikely to provide a bona fide proxy for that of the whole tumour.

4.6.2. The signatures of whole larval brain brat tumour tissue

To circumvent these limitations, I decided to generate my own transcriptomics data. To this end I was able to take advantage of raw data files containing Affymetrix (Drosophila Genome 2.0.) results comparing larval $brat^{K06028}$ tumour tissue to wild-type larval brains. The study was carried out taking sex as a biological variable even though neither anatomy traits, nor malignancy rates upon allograft show any kind of sex-linked dimorphisms (Molnar et al., 2019).

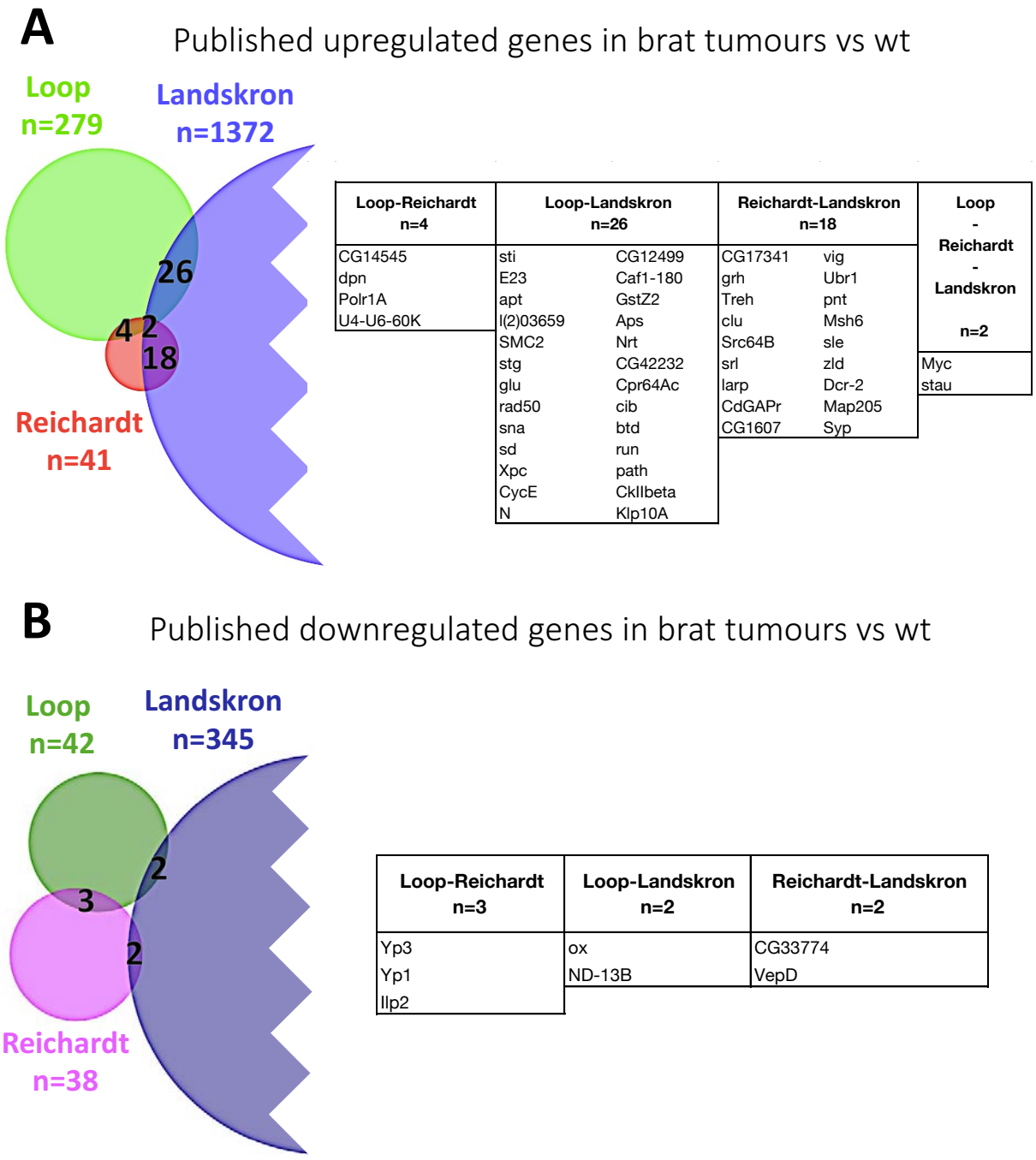

Loop-Reichardt n=4
CG14545
dpn
Polr1A
U4-U6-60K

Loop-Landskron n=26	
sti	CG12499
E23	Caf1-180
apt	GstZ2
l(2)03659	Aps
SMC2	Nrt
stg	CG42232
glu	Cpr64Ac
rad50	cib
sna	btd
sd	run
Xpc	path
CycE	CkIIbeta
N	Klp10A

Reichardt-Landskron n=18	
CG17341	vig
grh	Ubr1
Treh	pnt
clu	Msh6
Src64B	sle
srl	zld
larp	Dcr-2
CdGAPr	Map205
CG1607	Syp

Loop - Reichardt - Landskron n=2
Myc
stau

Loop-Reichardt n=3
Yp3
Yp1
Ilp2

Loop-Landskron n=2
ox
ND-13B

Reichardt-Landskron n=2
CG33774
VepD

Figure 4.10: Comparison between published transcriptomics data on brat. Venn diagrams showing the number of brat dysregulated genes that overlap between transcriptome studies: Reichardt et al., 2018 (red and pink), Loop et al.,2004 (light and dark green), and Landskron et al., 2018 (blue and purple), **(A)** for upregulated and **(B)** for downregulated genes, respectively. Numbers in between circles indicate the number of genes in common, which are listed in tables on the right.

Principal component analysis of these data shows that brat tumour samples, male and female, form a distinct cluster, away from wild-type brain samples and from two other tumour types, included here only as a reference (Fig. 4.11.).

The Affymetrix chip used in this study contained a total of 18952 probes corresponding to 18500 transcripts. Significantly dysregulated genes were identified using a |Fold Change| > 2 and FDR < 0.05. Gene expression values and differential expression results are shown on (Excel file in Appendix D2). From these data I derived both the brat tumour signature (i.e brat tumour compared to wild type) and the brat sex dimorphic signature (SDS) (i.e. male brat tumour *versus* female brat tumour) as originally defined by (Molnar et al., 2019).

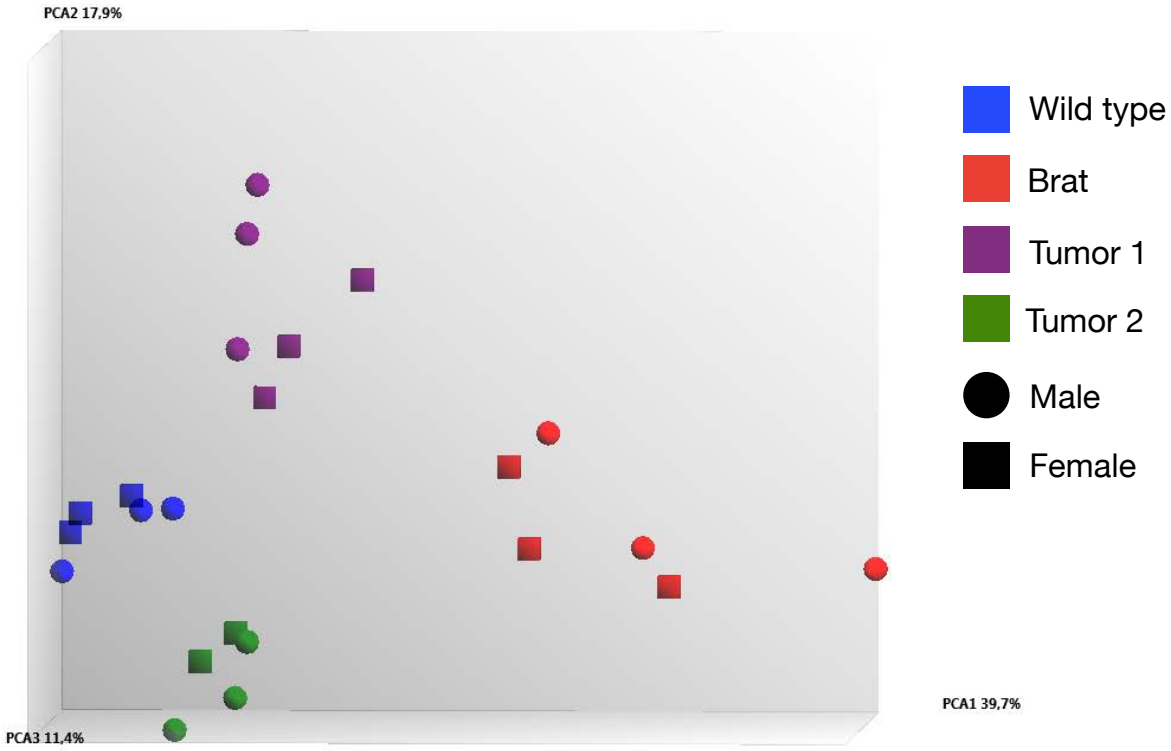

Figure 4.11. Principal Component Analysis Plot showing Principal Component Analysis (PCA) reveals distinct clusters for each condition, wt (blue), brat tumour (red) and other two tumour types analysed within the same microarray for reference (purple and green). Circles and squares indicate male and female samples, respectively.

Regarding the brat tumour signature, I found 516 and 710 genes upregulated and downregulated in male brat tumours compared to male wild-type brains and 375 and 622 genes upregulated and downregulated in female brat tumours compared to female wild-type brains (Fig. 4.12.A.). Most dysregulated genes present fold change values between +5 and -5 (Fig. 4.12.B.). In terms of sex specificity of upregulated genes, we found that 250, 109, and 266 genes were upregulated only in males, only in females, and in both sexes, respectively. Likewise, as far as downregulated genes go, we found 281, 193, and 429 genes downregulated only in males, only in females, and in both sexes, respectively (Fig. 4.12.C.). The completed lists of the dysregulated genes are shown in (Excel file of Appendix D2).

Consistent with the lack of sex-linked differences in terms of anatomy and malignancy rate of larval brain brat tumours (Molnar et al., 2019), the fraction of genes that are differentially dysregulated in brat tumours originated in male and female individuals (brat-SDS) is only marginal (Fig. 4.13.). Grey coloured dots representing genes that are not significantly differentially expressed account for the vast majority of the dataset, and blue (higher expression in males) and red (higher expression in females) genes are only a handful.

Given the notorious disagreement among the published transcriptomes of brat derived from brat adult heads and brat FACS sorted NBs, discussed in section 4.6.1., I decided to find out which of them fits best to my own transcriptomics data derived from whole brain samples from brat mutant larvae (Fig. 4.14.). I found that the extent of overlap with my data is much greater with the Loop et al. and the Reichardt et al. signatures than with that from the Landskron et al. study. I also found that the overlap is greater for upregulated than for downregulated genes. As far as upregulated genes are concerned the extent of overlap between my data and the Loop et al., Reichardt et al., Landskron et al. signatures is 20%, 41% and 7%, respectively ($p<5.5x10E-27$, $p<9.8x10E-15$, $p<7.3x10E-14$) (Fig. 4.14.A.). The corresponding values for downregulated genes are 19%, 16% and 1% ($p<0.001$, $p<0.011$, $p<8.9x10E-05$) (Fig. 4.14.B.). The much lower overlap between downregulated genes may be largely due to the fact that downregulation can only be appreciated for genes that are expressed in the control samples, which indeed are very different in each of these experiments.

Interestingly, although partial, the extent of overlap between my own data set with either the (Loop et al., 2004) and (Reichardt et al., 2018) signatures (20% and 41% for upregulated genes, respectively) is greater than between themselves (overlap *versus* Reichardt, 4/41, 10%; overlap *versus* Loop, 4/279, 1%).

A

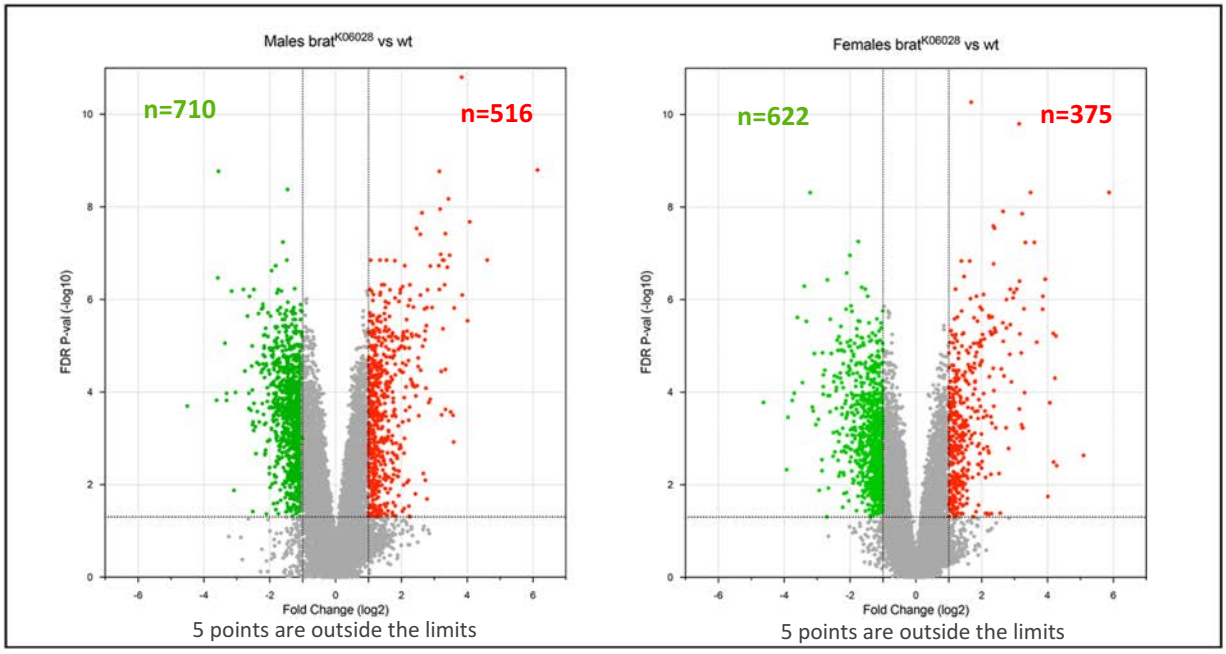
Males bratK06028 vs wt
n=710
n=516
FDR P-val (-log10)
Fold Change (log2)
5 points are outside the limits
Females bratK06028 vs wt
n=622
n=375
FDR P-val (-log10)
Fold Change (log2)
5 points are outside the limits

B

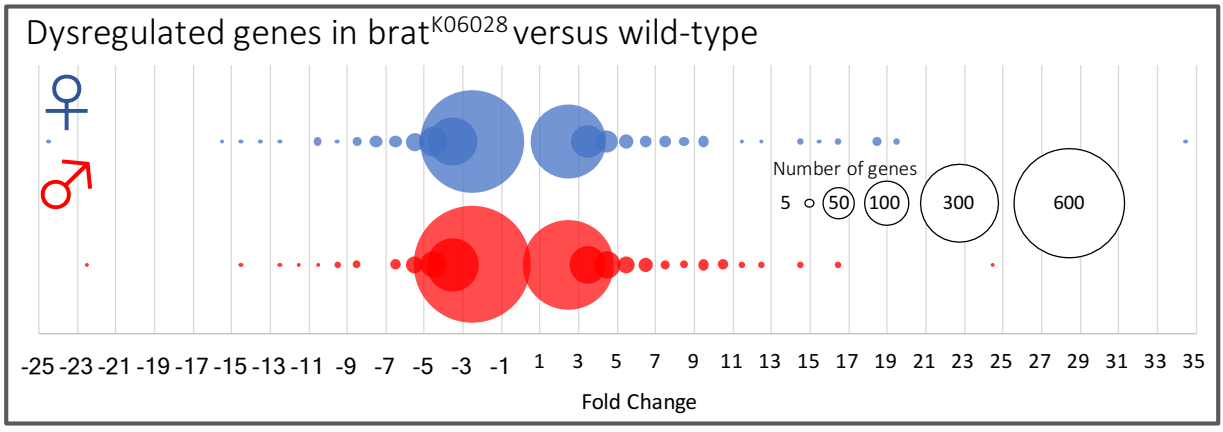
Dysregulated genes in bratK06028 versus wild-type
♀
♂
Number of genes
5
50
100
300
600
-25 -23 -21 -19 -17 -15 -13 -11 -9 -7 -5 -3 -1 1 3 5 7 9 11 13 15 17 19 21 23 25 27 29 31 33 35
Fold Change

C

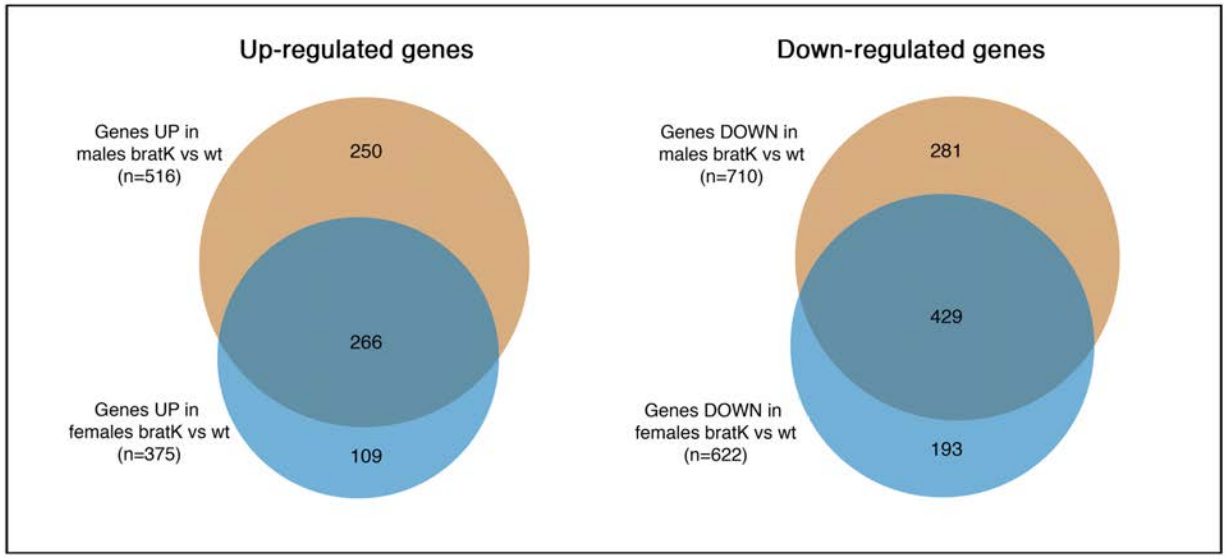
Up-regulated genes
Genes UP in males bratK vs wt (n=516)
250
266
Genes UP in females bratK vs wt (n=375)
109
Down-regulated genes
Genes DOWN in males bratK vs wt (n=710)
281
429
Genes DOWN in females bratK vs wt (n=622)
193

Figure 4.12: The transcriptomic signature of brat tumours. (A) Volcano plots showing changes in gene expression levels in brat tumour (*brat*^{K06028}) compared to control wt (*w*^{1118}) in males (left) and females (right) samples. Red and green dots represent genes that are significantly (FDR=0.05) up (FC>2) and downregulated (FC<2), respectively. **(B)** Plot showing the range of Fold Change (x-axis) for dysregulated genes in brat tumours compared to wild-type samples in female (blue) and male (red) samples. Circle size corresponds to the number of genes whose Fold Change is between the same range (± 0,5). **(C)** Venn diagrams showing the number of brat upregulated (left) and downregulated (right) genes compared with wt, that overlap between males (brown) and females (blue) samples.

Regarding the 5 transcription factors identified in the (Reichardt et al., 2018) study (*grh*, *dMyc*, *dpn*, *pnt* and *zld*) we found *grh*, *pnt*, *zld* to be upregulated in brat tumours from both male and female larvae), *dpn* to be upregulated only in brat tumours from female larvae and *dMyc* not to be significantly dysregulated in either sex.

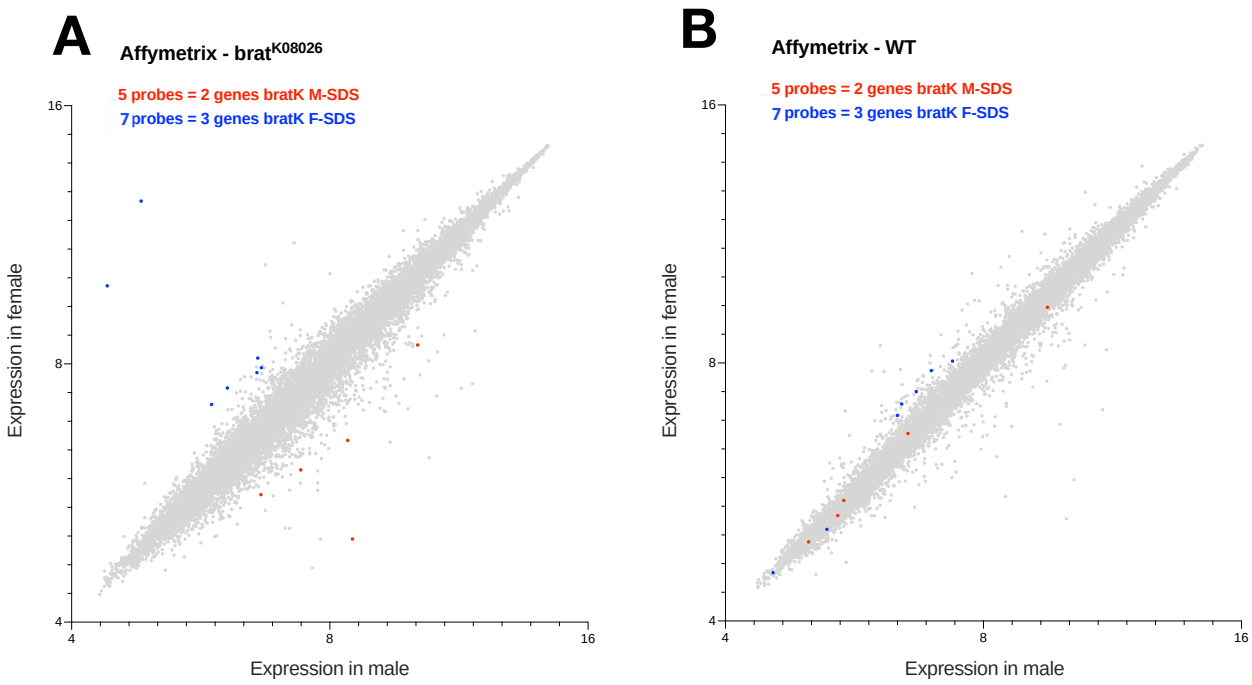

Figure 4.13. The sex-linked brat transcriptomic signature. Scatter plots showing the expression level of the genes in *brat*^{k06028} tumour **(A)** and control wt **(B)** brain lobes in male (x-axis) and female (y-axis) samples. Red and blue dots correspond to probes that are significantly overrepresented in males (M-SDS) and females (F-SDS), respectively, in *brat*^{K06028} samples. Grey dots correspond to genes that are expressed at levels that are not significantly different between male and female in *brat*^{K06028} samples. wt=*w*^{1118}

A Upregulated genes in brat tumours compared to published

Male brat^{k06028} vs wt n=516 Female brat^{k06028} vs wt n=375

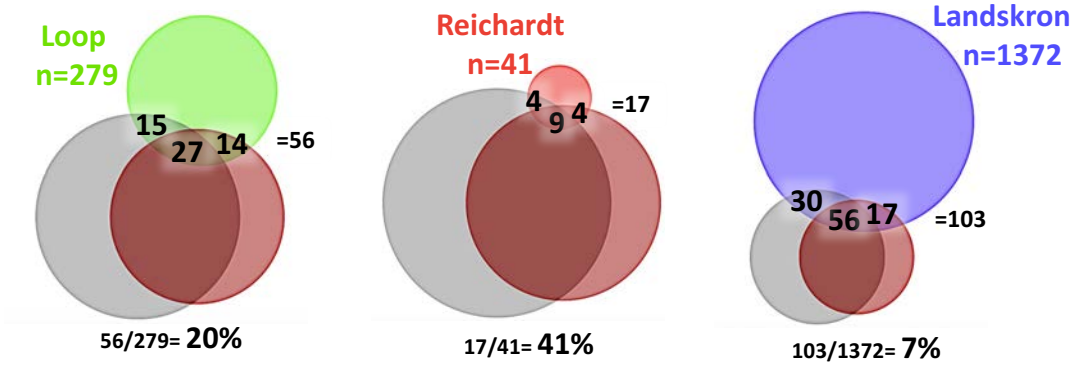

B Downregulated genes in brat tumours compared to published

Male brat^{k06028} vs wt n=713 Female brat^{k06028} vs wt n=623

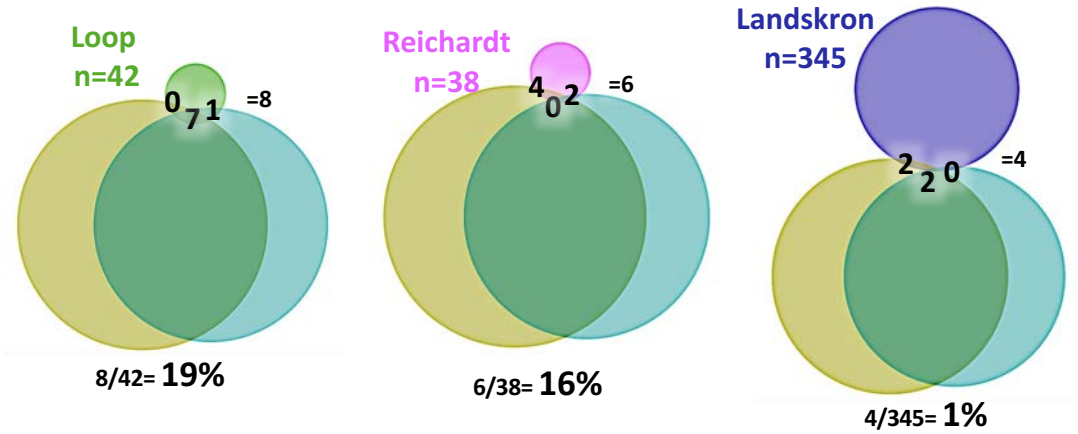

C Brat dysregulated genes compared to brat interactors

Interactors (FlyBase)				
Physical		Genetic		
w	pum	**btd**	Gpdh1	Mfe2
mira	stau	**dpn**	Men	Wwox
zld	piwi	**klu**	mor	Syp
dpn	Tis11	**sgg**	Pepck1	osa
klu	Sirt1	**pros**	sld	Myc
Corin	par-6	**erm**	trx	Mdh1
Sxl	sstn	**Nsf2**	Zw	lncRNA:cherub
aub	eIF4EHP	**ct**	Mad	orb2
bam	chinmo	**gcm**	grb	Imp
hb	elav	arm	Smox	Cklα
kni	Myc	brm	Axn	E(spl)mγ-HLH
nos	AGO1	bsk	Apc2	
Pc	orb2			

Brat dysregulated genes

Figure 4.14: Brat tumour transcriptomic signatures. (A-B) Venn diagrams showing the overlap between brat upregulated (A) and downregulated (B) genes in our transcriptomic study separated by sexes (males, grey and olive; females, maroon and teal blue) compared to those reported in Loop et al. (2004) (light and dark green), Reichardt et al. (2018) (red and pink) and Landskron et al. (2018) (blue and purple), respectively. **(C)** Table showing physical and genetic interactors of brat described in FlyBase. Upregulation of *white (w)* in our study due to genotype of the flies used in our studies and is not dependent on brat.

Only a minority of the genes classified in FlyBase as brat interactors, either physical (n=26) or genetic (n=35) are present among the genes that I have found dysregulated in brat tumours. These are *mira, zld, dpn, klu, Corin,* and *btd* which are upregulated in our dataset, while *Sxl, sgg, pros, erm, Nsf2, ct,* and *gcm* are downregulated (Fig. 4.14.C.). Remarkably, none of the 80 brat-SPRs appears in FlyBase as a brat interactor.

4.6.3. Enriched Gene Ontology terms in the brat transcriptome

Enriched "Biological Process" GOs among genes dysregulated in brat tumours compared to wild-type brains are shown in (Table 4.3.) (DAVID 2021; http://david.abcc.ncifcrf.gov.). Only terms with p-value<1x10E-03 are shown.

As far as downregulated genes are concerned, most GO terms are linked to neurogenesis and cell adhesion without any notable differences between male and female tumour samples. However, differences between sexes are notorious as far as upregulated genes go. In male brat samples, most of the significantly enriched GO terms are linked to DNA recombination and repair. In contrast, most of the enriched GO terms in female brat samples are linked to protein folding and stress response. Common GOs in both sexes are few and linked to ribosome biogenesis/rRNA only.

Genes associated to GOs enriched in male samples (DNA recombination and repair) include: *Blm, Msh6, rad50, spn-A,* and *spn-B*. Genes associated to GOs enriched in female samples (protein folding and stress response) are mostly accounted for by heat-shock proteins including: *Hsp70Aa, Hsp70Ab, Hsp70Ba, Hsp70Bb, Hsp70Bc,* and *Hsp22*.

Enrichment for upregulated genes in males brat [k06028] versus males wild type (n=515)			
Category	Term	P value	count
Biological Process	DNA recombination	6,00E-05	8
	maturation of SSU-rRNA	9,20E-05	6
	DNA repair	1,10E-04	13
	rRNA processing	2,40E-04	10
	karyosome formation	6,10E-04	7
	mismatch repair	6,60E-04	5
Enrichment for upregulated genes in females brat [k06028] versus females wild type (n=374)			
Category	Term	P value	count
Biological Process	regulation of protein serine/threonine phosphatase activity	1,90E-16	13
	heat shock-mediated polytene chromosome puffing	1,60E-06	6
	response to unfolded protein	3,30E-05	5
	cellular response to unfolded protein	6,50E-05	6
	protein refolding	1,80E-04	7
	purine nucleobase biosynthetic process	1,90E-04	4
	response to hypoxia	2,60E-04	7
	response to heat	3,80E-04	9
Enrichment for downregulated genes in males brat [k06028] versus males wild type (n=710)			
Category	Term	P value	count
Biological Process	motor neuron axon guidance	1,60E-14	26
	axon guidance	5,50E-12	35
	regulation of transcription from RNA polymerase II promoter	1,30E-11	76
	homophilic cell adhesion via plasma membrane adhesion molecules	2,40E-10	17
	synapse organization	6,00E-10	19
	ecdysteroid metabolic process	1,70E-08	9
	heterophilic cell-cell adhesion via plasma membrane cell adhesion molecules	7,50E-08	12
	synaptic target recognition	9,40E-07	12
	dendrite self-avoidance	1,10E-06	9
	cell adhesion	4,90E-06	15
	chemical synaptic transmission	5,40E-06	18
	G-protein coupled receptor signaling pathway	7,70E-06	22
	glial cell development	1,60E-05	8
	cell-cell adhesion	9,50E-05	11
	neuromuscular junction development	1,40E-04	11
	synaptic transmission, cholinergic	1,90E-04	6
	signal transduction	3,20E-04	31
	locomotor rhythm	3,70E-04	12
	neuromuscular synaptic transmission	5,80E-04	11
	synaptic target inhibition	6,40E-04	6
	phospholipid dephosphorylation	6,60E-04	5
	neuron differentiation	6,70E-04	10
	negative regulation of transcription from RNA polymerase II promoter	8,50E-04	24
	adult locomotory behavior	8,80E-04	11
	axonal fasciculation	8,90E-04	6

Enrichment for downregulated genes in females brat [k06028] versus females wild typeS (n=622)			
Category	Term	P value	count
Biological Process	motor neuron axon guidance	6,80E-13	23
	axon guidance	3,90E-10	30
	homophilic cell adhesion via plasma membrane adhesion molecules	3,90E-09	15
	synapse organization	2,80E-07	15
	regulation of transcription from RNA polymerase II promoter	1,10E-06	57
	heterophilic cell-cell adhesion via plasma membrane cell adhesion molecules	2,60E-06	10
	ecdysteroid metabolic process	5,10E-06	7
	cell adhesion	5,50E-06	14
	cell-cell adhesion	2,90E-05	11
	G-protein coupled receptor signaling pathway	4,40E-05	19
	synaptic target recognition	1,30E-04	9
	cation transmembrane transport	2,20E-04	5
	neuron differentiation	2,40E-04	10
	transmembrane transport	3,30E-04	25
	intracellular signal transduction	4,80E-04	16
	dendrite morphogenesis	5,00E-04	15
	dendrite self-avoidance	8,50E-04	6

Table 4.3. Gene Ontology enrichment among the list of genes dysregulated in brat tumours. Table showing significantly enriched gene ontology terms for Biological Process of brat dysregulated genes, divided in up and downregulated in male and female samples, respectively. Terms are ranked according to smaller p-value and counts report the number of brat dysregulated genes associated to each term.

Notably, DNA recombination and repair terms are also enriched in the proteomic analysis from (Jüschke et al., 2013), but not in transcriptome from (Loop et al., 2004). Although not explicitly mentioned in the article, my own analysis from the (Landskron et al., 2018) data set shows that it is also enriched for genes related to DNA repair (p=1,5x10E-03), while protein folding and stress response terms are not enriched in any of the published brat signatures. However, terms related to ribosome biogenesis/rRNA were found to be enriched in both the (Loop et al., 2004) and the (Jüschke et al., 2013) studies. These terms are not enriched in the (Landskron et al., 2018) study according to my own analysis of the published dataset. Importantly, unlike mine, none of these studies included sex as a biological variable.

4.7. Gene expression dysregulation is a poor predictor of functional requirement

Gene expression signatures carry very valuable information as they identify specific tumour markers and provide the means to objectively stratify tumour types and grades with high precision. Their diagnostic value is therefore undisputed. A very different issue is their value with regards to identifying genes that are essential for the growth of the corresponding tumours (García-Escudero & Paramio, 2008; Hanash, 2003). Indeed, it is conceivable that as a consequence of the high extent of rewiring of gene expression presented by many tumour types, a fraction of the genes of any given tumour signature are dysregulated by such bystander effect and may not play any significant role in tumour growth (Dopazo, 2009; Lauri et al., 2021; Sara et al., 2009). The question is how big such a fraction is.

This question, which due to obvious technical difficulties remains unanswered for most human cancer types, can be addressed with relative ease in Drosophila tumour models for which both genome-wide transcriptomics and functional studies can be generated (Bangi, 2020; Liang et al., 2014; Richardson et al., 2020). Taking advantage of the screening and transcriptomics results presented in this work I have addressed this issue with regards to brat tumours. The only, relatively minor limitation of this analysis is that while transcriptomics data is genome wide, functional data derived from our screen is "limited" to 4.000 genes, that is about 30% of the Drosophila genes. The present expression/function correlation study is therefore limited to these.

I found that out of the 80 suppressors that I have identified 7 (8,7%) are upregulated, 72 (90%) are not significantly dysregulated and 1 (1,2%) is actually downregulated in brat tumour samples (Fig. 4.15.A.). Conversely, out of the 144 of genes upregulated in brat tumours (n=625) that were included in the screen, 7 (4,8%) were found to be brat-SPRs. In addition, 150 downregulated genes were screened and only 1 (0,7%) of genes downregulated in brat tumours were found to be brat-SPRs (Fig. 4.15.B.).

Similar conclusions were drawn in the published study carried out in our laboratory concerning mbt tumours. In that case, depletion of 86% (117/136) of the top most upregulated genes in mbt tumour samples had no effect upon mbt tumour growth (Rossi et al., 2017).

Altogether, these results reveal that gene dysregulation (i.e. gene expression signatures) is a poor predictor of functional requirement.

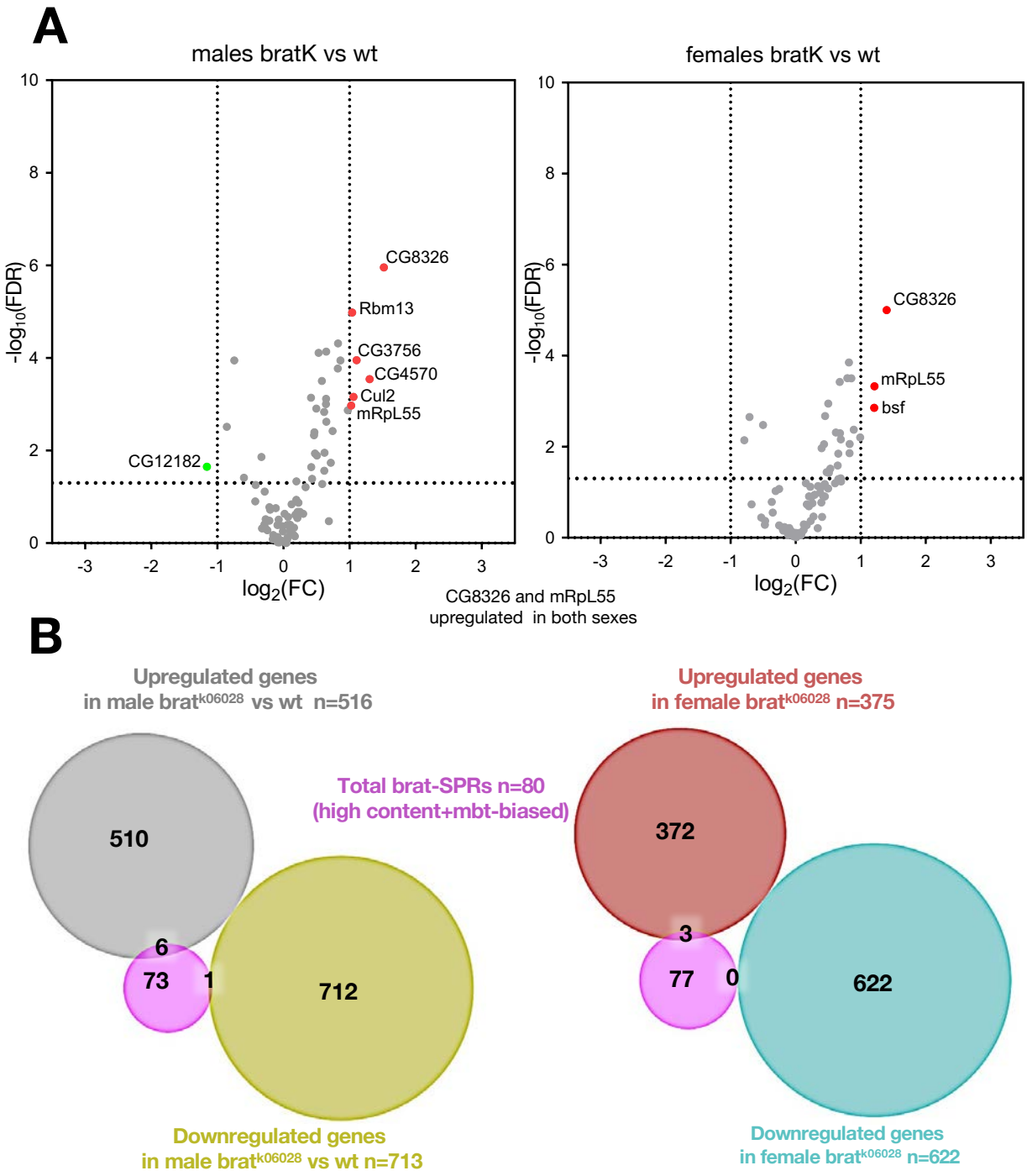

Figure 4.15. Correlation between gene expression and functional requirements in brat tumours. (A) Volcano plots showing changes in gene expression levels of brat-SPRs genes in brat tumour (*brat*^{K06028}) compared to control wt in males (left) and females (right) samples. Red and green dots represent genes that are significantly (FDR=0.05) up (FC>2) and downregulated (FC<2), respectively. Interestingly, only *CG8326* and *mRpL55* are significantly upregulated in brat tumours in both sexes. Grey dots correspond to brat-SPRs genes that are expressed at levels that are not significantly different between *brat*^{K06028} and control wt samples. wt=w^{1118}. **(B)** Venn diagrams showing overlap between brat-SPRs genes (pink) and brat dysregulated genes in males (left) and females (right) samples.

5. Discussion

Drosophila has proven to be a fruitful experimental model to understand some of the molecular mechanisms of tumour growth (Gonzalez, 2013; Sonoshita & Cagan, 2017). In this work, I have combined functional genomics and transcriptomics to investigate a model larval brain tumour caused by the loss of *brat*. I have identified a total of 80 targets to inhibit brat tumour growth (brat-SPRs) which are enriched in genes required for neurogenesis, mitochondria, and several basic cellular functions. Moreover, I have found a low correlation between genes required for brat tumor growth and genes that are upregulated in brat tumour tissue. My functional studies have focused on the initial results from a high content screen that was carried out in parallel with another screen to identify suppressors of brain tumours caused by the loss of *l(3)mbt* (Rossi et al., 2017). Taking advantage of this, I have been able to run comparative analyses of both sets of data (i.e. brat-SPRs and mbt-SPRs). From these studies I have found that 41% (33/80) of the brat-SPRs, are also mbt-SPRs.

5.1. Suppressed tumorous brains in two different models of Drosophila

In order to address which genes are crucial for brat tumour growth, we have performed a functional genomics unbiased screen covering a very significant part of the entire Drosophila genome. Expression of *brat-RNAi* from type II NB-specific driver is sufficient to produce brat tumours (Reichardt et al., 2018). However, we chose the ubiquitous *Ubi-GAL4* driver to filter out RNAi lines that have a detrimental effect on development because the corresponding genes could hardly be considered as putative targets for therapy. This approach worked rather well in a previous, similar screen for mbt-SPRs in which some of the identified genes could be deleted such that mbt mutant brains developed as phenotypically wild-type-like larval brains (Rossi et al., 2017). The filter provided by this approach is nonetheless only partial and does not exclude that a significant part of the identified RNAi suppressor lines corresponds to essential (housekeeping) genes. However, the fact that they qualify as brat-SPRs even when driven from a ubiquitous promoter suggests that there must be a threshold of functional requirement that is different between tumorous and wild-type tissues.

We have found that 68 out of 4300 (1,6%) genes randomly selected from Drosophila genome are brat-SPRs, compared to the 2,2% (n=92) obtained for mbt-SPRs (Rossi et al., 2017). Among the SPRs found for each tumour in the high content screen (more than 4000 genes), only 21 genes are SPRs of both tumours, which seems a low overlapping if we take into consideration the high proportion of housekeeping genes among them.

We have also found that unlike mbt-SPRs, several of which like *mei-W68* or *Tctp,* for instance, fully rescue nearly normal wild-type brain anatomy (Rossi et al., 2017), no such brat-SPRs were found. All the suppressed brat tumour conditions that can be generated with the collection of brat-SPRs identified in this study present phenotypes ranging from brains with small clusters of neuroblasts (such as brains suppressed by inhibition of: *Acsl, AsnRS-m, Cog3, Cpsf160, pds5,* and *Rab39*) to brains that resemble a brat tumorous brain with reduced size (such as brat brains lacking: *ebo, udd, kek1*, *mRpL54,* and *mRpL55*). Previously published studies describing suppressors for brat do not indicate rescue to wild-type morphology either (Landskron et al., 2018; Reichardt et al., 2018).

A possible explanation for the difference between brat-SPRs and mbt-SPRs regarding the phenotype of the suppressed tumour condition derives from the different molecular function of these two tumour suppressors. Brat is an RNA binding protein whose best known function is to repress translation of mRNAs, notably some that encode for proteins that promote NB differentiation (Betschinger et al., 2006; Reichardt et al., 2018). Upon loss of Brat function, tumours develop from INPs that revert to a NB-like state and proliferate without control. This suggests that brat NB-like tumour cells must coopt most of the proteins that are required for normal INPs growth and cell division and, therefore, genes required for brat tumour growth but dispensable for normal brain development are bound to be very rare. In contrast, L(3)mbt is a chromatin protein whose best known function is to repress specific gene programs including germline genes in somatic cells and somatic genes in the germline (Coux et al., 2018; Janic et al., 2010; C. Richter et al., 2011). Consequently, mbt tumours upregulate and use genes that are neither needed nor expressed in normal brains. Such genes are the potential Achilles' heel of the tumour because their inactivation affects tumour tissue without compromising wild-type brain development.

5.2. Synthetic lethal interactions

While forcing the ubiquitous expression of RNAi has the advantage of filtering out conditions that have an essential cytostatic effect, it also has the drawback of filtering out synthetic lethal interactions that have great potential as anticancer therapeutics (O'Neil et al., 2017). To circumvent this drawback, we took advantage of the fact that for the 4151 RNAi lines analysed we have data on lethality on two different mutant backgrounds, *l(3)mbt* and *brat* that can serve as controls of one another to determine if the lethality caused by any given RNAi is "generic" or tumour-type specific. Through this comparison we identified a set of 192 RNAi lines that cause lethality in mbt, but not in brat, and another set of 186 RNAi lines that cause lethality in brat, but not in mbt.

It remains to be determined if knocking down any of these putative synthetic lethals can inhibit proliferation when RNAi expression is limited to the tumorous tissue.

5.3. *Tailless* in brat and mbt tumorous brains

One of the double suppressors (brat-SPR and mbt-SPR) identified in this study is the neural transcription factor Tailless (Tll) (Jürgens et al., 1984; Strecker et al., 1986).
Tll has a key function in proliferation and growth in the OL and is essential for NE cell survival. In particular, loss of *Tll* function affects the transition zone where NE cells transform into NB and results in abnormal NE morphology and reduced OL size (Guillermin et al., 2015). Moreover, *Tll* also plays a main role in NBs and INPs. Together with transcription factors *Hth, Ey, Slp1, and D, Tll* is expressed in five consecutive stripes that correlate with NB age, with *Hth* expressed in newly differentiated NBs, and *Tll* in the oldest NBs (X. Li et al., 2013). These oldest Tll-positive NBs undergo Pros-dependent cell-cycle exit ending their life (X. Li et al., 2013; Maurange et al., 2008).

Recent studies have shown that Tll has an oncogenic function in Drosophila: high Tll levels initiate tumourigenesis by reverting intermediate neural progenitors to a stem cell state in a process that requires the silencing of the proneuronal gene *Ase* (Hakes & Brand, 2020). In Type II neuroblast Tll is activated by the binding of the ETS transcriptional factor Pointed P1 (PntP1) to seven ETS binding sites on the *Tll* promoter and Tll suppress the expression of *Ase* by binding directly to *Ase* promoter. In addition, Tll provides a positive feedback loop that maintains the expression of PntP1(Chen, Den and Zhu, 2022). Thus, It is likely that the suppression of brat tumoral growth is due to the upregulation of *Ase* and downregulation of *PntP1* that in consequence will induce the transformation of type II NBs into Type I NBs, that indeed do not produce INPs and cannot give rise to brat tumours (Hakes & Brand, 2020).

These observations are particularly interesting because overexpression of the human orthologue, TLX, has been reported to correlate tightly with aggressiveness in human primary glioblastoma. Like Drosophila *Tll*, human *Tlx* is involved in maintaining the proliferative state of NSCs by negatively regulating expression of differentiation-promoting genes (Gui et al., 2011; Roy, 2004). Moreover, TLX repress expression of *Pten* in the developing retina and adult brain and it has been proposed that Tlx control of PTEN expression may also be critical to maintains the self-renewing state in NSCs. Indeed, PTEN is often mutated in different human cancers, including gliomas (Gui et al., 2011). Consequently, it has been proposed that counteracting high TLX may have a therapy effect on malignancies derived from intermediate progenitor cells (Gui et al., 2011; Hakes & Brand, 2020).

5.4. Mitochondrial genes in Drosophila tumorous brain

Many of the proteins that are essential components of complexes I, III, IV, and V of the Electron Transport Chain (ETC) are encoded by the mitochondrial genome and therefore are dependent upon mitoribosomes for translation (Boore, 1999). Consequently, one direct effect of mitoribosome downregulation is repression of OxPhos.

A conspicuous group of the brat-SPRs identified in this study includes mitoribosomal proteins mRpL54, mRpL55, mRpL48, mRpS6, mRpL3, and mRpS11. This result is consistent with the metabolic reprogramming towards OxPhos that has been reported in brat tumours as well as with published results showing that depletion of respiratory complex activity, including ETC components, suppresses brat tumour growth (Bonnay et al., 2020; van den Ameele & Brand, 2019). What makes our results more interesting is the fact that while RNAi-mediated depletion of these proteins leads to a significant reduction of brat tumour size, it does not appear to have a major detrimental effect on larval development. These observations suggest that tumour tissue growth is more sensitive than wild-type tissue growth to loss of mitochondria function, thus revealing a threshold of sensitivity that could make selected mitochondrial proteins, like the mitoribosomal proteins identified in this study, suitable for pharmacological inhibition of tumour tissue growth. Similar conclusions were reached by Rossi and colleagues from their work on mbt-SPRs (Rossi et al., 2017), which suggests that enhanced sensitivity to loss of mitochondrial function is not unique to brat tumours.

Increased glucose uptake and fermentation of glucose to lactate in the presence of oxygen (aerobic glycolysis) is a generally acknowledged trait of cancer. This phenomenon is known as the Warburg Effect (Warburg, 1925). However, the contribution of respiration to tumour metabolism is rather variable and many tumours exhibit a substantial amount of respiration (Crabtree, 1929). For decades, it was unclear whether the Warburg effect was a contributing factor or a bystander effect from cancer, but recent genetic and pharmacological studies conclusively show that the Warburg effect is required for tumour growth in a variety of cancer types (Fantin et al., 2006; Shim et al., 1998). However, there is also mounting evidence suggesting that even under Warburg effect conditions, targeting aerobic glycolysis only is not sufficient to arrest those cancer types (reviewed in Liberti and Locasale 2016). Moreover, targeting OxPhos has proved to be an option for some tumours (C.-L. Chen et al., 2021; Criscuolo et al., 2021). Both mbt (Rossi et al., 2017), and brat (my own work) Drosophila brain tumours behave likewise.

The identification of mitochondrial translation as a therapeutic target opens the way to take advantage of the prokaryotic origin of mitochondria and repurposing antibiotics

that target the mitochondrial translation machinery as anti-cancer agents (D'Andrea et al., 2016; H.-J. Kim et al., 2017). For instance, tetracycline analogues doxycycline and COL-3 have been shown to exert anti-proliferative and pro-apoptotic effects caused by inhibition of mitochondrial protein synthesis with a decreased OxPhos and present anti-tumour effects in several human cancers in both pre-clinical and clinical studies (Dijk et al., 2020; Protasoni et al., 2018; Richards et al., 2011; Škrtić et al., 2011).

Similarly, actinonin has been shown to inhibit the proliferation of several human cancer cell lines (Escobar-Alvarez et al., 2010; M. D. Lee et al., 2004; Škrtić et al., 2011). Actinonin mode of action appears to be two-fold: (i) inhibiting the mitochondrial peptide deformylase (HsPDF), a metalloprotease that catalyzes the co-translational removal of the formyl group from N-terminal methionine of newly synthesised proteins and (ii) blocking the mitoribosomal polypeptide exit tunnel, leading to mitoribosome stall which in turn triggers a retrograde signal to the nucleus, that induces degradation of mt-rRNAs, mt-mRNAs and mitoribosomes (U. Richter et al., 2013).

5.5. *Vps26* in larval brain tumour growth

I have found that depletion of *Vacuolar protein sorting 26 (Vps26*) inhibits brat and mbt tumour growth *in situ*, and reduces the malignancy traits as measured by allograft tests, partially in the case of brat and almost entirely in the case of mbt tumours. Interestingly, *Vps26* and *Vps35* have been described before as a type II NB-specific tumour suppressor: *Vps26* down regulation in Type II NBs results in supernumerary neuroblasts and tumour formation (B. Li et al., 2018).

Vps26 and Vps35 are essential component of the retromer complex that mediates retrograde transport of proteins and lipids between endosomes and biosynthetic/secretory compartments such as the Golgi apparatus, a process which is crucial for a wide range of cellular functions (Johannes & Popoff, 2008). In Drosophila NBs, the retromer complex directly and specifically regulates Notch receptor retrograde trafficking to ensure the unidirectionality of Notch signaling. Increased Notch signaling upon loss of retromer complex activity is thought to be the mechanism that triggers dedifferentiation of INPs (B. Li et al., 2018) and accounts for the tumour suppressor activity of *Vps26* and *Vps35*.

I do not know the mechanism by which *Vps26* loss inhibits tumour growth, but my results showing that unlike *Vps26* neither *Vps35* nor *Vps29* (another retromer complex components), behave as suppressors of brat or mbt tumour growth suggest a retromer complex-independent activity as the basis for Vps26 function as brat&mbt-SPRs. A tantalizing possibility is that the ubiquitous knockdown of *Vps26* may trigger a systemic

signal that suppress tumorigenesis. Interestingly, in plants, Vps26 homologs have a moonlighting function in modulating the prototype 7-transmembrane Regulator of G Signaling 1 protein (AtRGS) and GPCR endocytosis (Ross-Elliott et al., 2019).

5.6. Nucleolar genes

An interesting enriched group of brat-SPRs includes nucleolar proteins. This is not unexpected because conspicuous phenotypic traits of *brat* depletion include a net increase in rRNA and enlarged nucleoli (Frank et al., 2002; Neumüller et al., 2013, p. 201; Betschinger et al., 2006). The most straight forward mechanistic interpretation for this phenotype is suggested by the activity of f Brat as a translational repressor of dMyc. Activation of ribosome biogenesis is likely to be a net contributor to tumour growth through its effect in promoting protein synthesis. Indeed, disruption of ribosome biogenesis triggers a stress response that activates JNK and apoptosis in imaginal discs, NB quiescence, and tissue hypoplasia in larval brains in Drosophila (Baral et al., 2020).

In this regard, the finding of *Under-developed (Udd)* as brat-SPR is particularly interesting. Female germline stem cells (GSCs) display high levels of rRNA transcription. In these cells, Udd, together with TAF1B, and a TAF1C-like factor forms a complex that regulates Drosophila RNA polymerase I (Pol I), the polymerase that transcribes rRNA. During GSC asymmetric division, Udd is retained by the self-renewed GSC and is not passed on to the differentiating daughter. Disruption of either Udd or TAF1B arrests GSC proliferation and overexpression of Pol I transcription delays differentiation. Moreover, Udd loss of function forces differentiation of the supernumerary GSCs present in *bam* mutant "tumorous" ovaries. These observations have been taken to suggest that the level of ribosome biogenesis could modulate the expression of proteins that control cell fate decisions (Q. Zhang et al., 2014). If so, the role of the nucleolar proteins in tumour biology could be more complex than simply facilitating protein synthesis for growth.

Importantly, in many cancer types ribosome biogenesis is enhanced and, indeed, some commonly used chemotherapeutic drugs like Cisplatin, Actinomycin D, etc. target ribosome synthesis (Zisi et al., 2022). In humans, abnormal ribosome biogenesis leads to the activation p53 dependent and independent pathways that cause cell cycle arrest or cell death (Zisi et al., 2022). In colon cancer cells presenting notoriously high levels of protein synthesis, depletion of RNA pol I results in irreversible differentiation (Morral et al., 2020). Altogether, available data points at ribosome biology and protein synthesis as potentially effective targets to kill tumour cells.

5.7. Low correlation between functional requirements and dysregulation of gene expression

An important conclusion derived from our functional and transcriptomic data is the rather low correlation between the extent of dysregulation of gene expression and gene function requirement in our tumour models. This is both in the case of brat tumours (this study) as well as in the case of mbt brain tumours (Rossi et al., 2017). Notably, in the latter, transcriptomic profiling of different "suppressed mbt tumour" conditions (i.e., larval brains from individuals that were both mutant for mbt and also depleted for any of several mbt-SPRs) showed that they still present most of the tumour transcriptome signature. This was found to be true even for suppressed mbt tumour conditions that, as far as the main anatomy traits are concerned, develop larval brains that closely resemble those from wild type larvae. These results confirmed that, indeed, unscheduled dysregulation of most of the tumour signature genes is not on its own necessarily tumorigenic (Rossi et al., 2017).

In the case of Brat that functions as a regulator of translation (Frank et al., 2002; Reichardt et al., 2018; Sonoda, 2001) it is to be expected that the transcription level of its direct target genes remains unaffected in the tumour. However, many of those direct target genes are transcription factors themselves and, therefore, the transcriptional regulation of their own target genes is expected to be compromised in brat tumour tissue. Consistently, my transcriptome analysis reveals dysregulation in brat larval brains particularly with regards to reduced expression of neurogenesis and cell adhesion and increased transcription of DNA recombination and repair and protein folding genes. Yet, most of such transcriptionally dysregulated genes appear to be silent as brat tumour growth is concerned and do not qualify a brat-SPRS. Finding targets to effectively inhibit tumour growth on the basis of gene expression dysregulation is therefore unlikely, although exceptions apply (Landskron et al., 2018; Reichardt et al., 2018).

Another possibility that may explain the poor matching between transcriptomics and functional requirement is tumour tissue heterogeneity. This is well characterised in *pros* tumours derived from VNC NBs that have been shown to contain multiple cell types that present notably different transcriptomes (Genovese et al., 2019). Cell heterogeneity can mask transcriptional dysregulation of important transcripts as well as overrepresent less functionally relevant genes. This is especially important for tumours that are maintained by tumour stem cells that may represent a small fraction of the total tumour mass. In this regard, an interesting observation derived from my data on function and expression is that more than half of all brat-SPRs (46/80) correspond to NB-specific or NB-enriched genes but only 4 are enriched in brat tumours (i.e. qualify as brat tumour signature genes).

This observation suggests that brat tumours can hardly be regarded as tissue made of NB-like cells only. It also strongly argues against FACS-sorted NB-like cells as a proxy for brat tumour tissue.

5.8. Future perspectives

Among the different research lines that may derive from this work I would like to underscore two that I find to be of special interest.

The first is to apply single-cell transcriptomic analysis to unequivocally identify and quantify the different cell types that make up the brat tumour mass. Such a study may shed light on the standing issue of low correlation between transcriptional dysregulation and function in tumour growth.

The second is a thorough molecular characterization of the suppressors that cause synthetic lethality with the tumour condition. A first step in this direction would be to combine CRISPR-Cas9 technology, which is now standard in Drosophila (Meltzer et al., 2019), to achieve tissue-specific depletion of a selected list of such suppressors, with single cells transcriptomics, to identify the regulatory networks that might account for synthetic lethality. Synthetic lethal genetic interactions with tumour-specific mutations may be exploited to develop anticancer therapeutics (O'Neil et al., 2017).

6. Conclusions

6. CONCLUSIONS

1) I have identified 80 genes that can function as targets to inhibit the growth of larval brain malignant tumours caused by the loss of function of the gene *brat* (brat-SPRs).

2) None of the brat tumours suppressed conditions brought about by depletion of the brat-SPRs identified in this study allows for normal larval brain development.

3) The collection of identified brat-SPRs is enriched in genes involved in neurogenesis and mitochondrial functions.

4) As far as brat and mbt tumours are concerned, tumour type-specific suppressors outnumber those that function as suppressors for both tumour types.

5) One of the double suppressors (brat&mbt-SPRs) identified in this work is *Vacuolar protein sorting-associated protein 26 (Vps26)*, which appears to exert this function in a retromer complex independent manner.

6) The brat tumour transcriptome signature is enriched in genes involved in DNA repair and ribosome biogenesis, which are upregulated, and neurogenesis and cell adhesion genes, which are downregulated.

7) Unlike the case in mbt tumours, the sex of the tumour bearing larvae affects neither the transcriptome nor the anatomy/histology of brat tumours.

8) Like the case in mbt tumours, the extent of transcription dysregulation is a poor predictor of the functional requirement in brat tumour development.

7. References

7. REFERENCES

Adams, M. D., Celniker, S. E., Holt, R. A., Evans, C. A., Gocayne, J. D., Amanatides, P. G., Scherer, S. E., Li, P. W., Hoskins, R. A., Galle, R. F., George, R. A., Lewis, S. E., Richards, S., Ashburner, M., Henderson, S. N., Sutton, G. G., Wortman, J. R., Yandell, M. D., Zhang, Q., … Venter, J. C. (2000). The Genome Sequence of *Drosophila melanogaster*. *Science*, *287*(5461), 2185–2195. https://doi.org/10.1126/science.287.5461.2185

Albertson, R., & Doe, C. Q. (2003). Dlg, Scrib and Lgl regulate neuroblast cell size and mitotic spindle asymmetry. *Nature Cell Biology*, *5*(2), 166–170. https://doi.org/10.1038/ncb922

Arama, E., Dickman, D., Kimchie, Z., Shearn, A., & Lev, Z. (2000). Mutations in the β-propeller domain of the Drosophila brain tumor (brat) protein induce neoplasm in the larval brain. *Oncogene*, *19*(33), 3706–3716. https://doi.org/10.1038/sj.onc.1203706

Bangi, E. (2020). Strategies for Functional Interrogation of Big Cancer Data Using Drosophila Cancer Models. *International Journal of Molecular Sciences*, *21*(11), 3754. https://doi.org/10.3390/ijms21113754

Bannister, A. J., Zegerman, P., Partridge, J. F., Miska, E. A., Thomas, J. O., Allshire, R. C., & Kouzarides, T. (2001). Selective recognition of methylated lysine 9 on histone H3 by the HP1 chromo domain. *Nature*, *410*(6824), 120–124. https://doi.org/10.1038/35065138

Baral, S. S., Lieux, M. E., & DiMario, P. J. (2020). Nucleolar stress in *Drosophila* neuroblasts, a model for human ribosomopathies. *Biology Open*, bio.046565. https://doi.org/10.1242/bio.046565

Barbee, S. A., Estes, P. S., Cziko, A.-M., Hillebrand, J., Luedeman, R. A., Coller, J. M., Johnson, N., Howlett, I. C., Geng, C., Ueda, R., Brand, A. H., Newbury, S. F., Wilhelm, J. E., Levine, R. B., Nakamura, A., Parker, R., & Ramaswami, M. (2006). Staufen- and FMRP-Containing Neuronal RNPs Are Structurally and Functionally Related to Somatic P Bodies. *Neuron*, *52*(6), 997–1009. https://doi.org/10.1016/j.neuron.2006.10.028

Bate, M., & Martinez Arias, A. (Eds.). (1993). *The Development of Drosophila melanogaster*. Cold Spring Harbor Laboratory Press.

Bateson, W. (1916). *The Mechanism of Mendelian Heredity*. By T. H. Morgan, A. H. Sturtevant, H. J. Muller and C. B. Bridges. Henry Holt and Company, New York. 1915. *Science*, *44*(1137), 536–543. https://doi.org/10.1126/science.44.1137.536

Bellen, H. J., Wangler, M. F., & Yamamoto, S. (2019). The fruit fly at the interface of diagnosis and pathogenic mechanisms of rare and common human diseases. *Human Molecular Genetics*, *28*(R2), R207–R214. https://doi.org/10.1093/hmg/ddz135

Bello, B. C., Izergina, N., Caussinus, E., & Reichert, H. (2008). Amplification of neural stem cell proliferation by intermediate progenitor cells in Drosophila brain development. *Neural Development*, *3*(1), 5. https://doi.org/10.1186/1749-8104-3-5

Berger, C., Harzer, H., Burkard, T. R., Steinmann, J., van der Horst, S., Laurenson, A.-S., Novatchkova, M., Reichert, H., & Knoblich, J. A. (2012). FACS Purification and Transcriptome Analysis of Drosophila Neural Stem Cells Reveals a Role for Klumpfuss in Self-Renewal. *Cell Reports*, *2*(2), 407–418. https://doi.org/10.1016/j.celrep.2012.07.008

Betschinger, J., Mechtler, K., & Knoblich, J. A. (2006). Asymmetric Segregation of the Tumor Suppressor Brat Regulates Self-Renewal in Drosophila Neural Stem Cells. *Cell*, *124*(6), 1241–1253. https://doi.org/10.1016/j.cell.2006.01.038

Bilder, D. (2004). Epithelial polarity and proliferation control: Links from the *Drosophila* neoplastic tumor suppressors. *Genes & Development*, *18*(16), 1909–1925. https://doi.org/10.1101/gad.1211604

Blanchard, D. P., Georlette, D., Antoszewski, L., & Botchan, M. R. (2014). Chromatin reader L(3)mbt requires the Myb–MuvB/DREAM transcriptional regulatory complex for chromosomal recruitment. *Proceedings of the National Academy of Sciences*, *111*(40). https://doi.org/10.1073/pnas.1416321111

Blankenship, J. T., Fuller, M. T., & Zallen, J. A. (2007). The *Drosophila* homolog of the Exo84 exocyst subunit promotes apical epithelial identity. *Journal of Cell Science*, *120*(17), 3099–3110. https://doi.org/10.1242/jcs.004770

Boccuni, P., MacGrogan, D., Scandura, J. M., & Nimer, S. D. (2003). The Human L(3)MBT Polycomb Group Protein Is a Transcriptional Repressor and Interacts Physically and Functionally with TEL (ETV6). *Journal of Biological Chemistry*, *278*(17), 15412–15420. https://doi.org/10.1074/jbc.M300592200

Bolus, H., Crocker, K., Boekhoff-Falk, G., & Chtarbanova, S. (2020). Modeling Neurodegenerative Disorders in Drosophila melanogaster. *International Journal of Molecular Sciences*, *21*(9), 3055. https://doi.org/10.3390/ijms21093055

Bonasio, R., Lecona, E., & Reinberg, D. (2010). MBT domain proteins in development and disease. *Seminars in Cell & Developmental Biology*, *21*(2), 221–230. https://doi.org/10.1016/j.semcdb.2009.09.010

Bonnay, F., Veloso, A., Steinmann, V., Köcher, T., Abdusselamoglu, M. D., Bajaj, S., Rivelles, E., Landskron, L., Esterbauer, H., Zinzen, R. P., & Knoblich, J. A. (2020). Oxidative Metabolism Drives Immortalization of Neural Stem Cells during Tumorigenesis. *Cell*, *182*(6), 1490-1507.e19. https://doi.org/10.1016/j.cell.2020.07.039

Boone, J. Q., & Doe, C. Q. (2008). Identification of *Drosophila* type II neuroblast lineages containing transit amplifying ganglion mother cells. *Developmental Neurobiology*, *68*(9), 1185–1195. https://doi.org/10.1002/dneu.20648

Boore, J. L. (1999). Animal mitochondrial genomes. *Nucleic Acids Research*, *27*(8), 1767–1780. https://doi.org/10.1093/nar/27.8.1767

Bornemann, D., Miller, E., & Simon, J. (1996). The Drosophila Polycomb group gene Sex comb on midleg (Scm) encodes a zinc finger protein with similarity to polyhomeotic protein. *Development*, *122*(5), 1621–1630. https://doi.org/10.1242/dev.122.5.1621

Bowman, S. K., Neumüller, R. A., Novatchkova, M., Du, Q., & Knoblich, J. A. (2006). The Drosophila NuMA Homolog Mud Regulates Spindle Orientation in Asymmetric Cell Division. *Developmental Cell*, *10*(6), 731–742. https://doi.org/10.1016/j.devcel.2006.05.005

Bowman, S. K., Rolland, V., Betschinger, J., Kinsey, K. A., Emery, G., & Knoblich, J. A. (2008). The Tumor Suppressors Brat and Numb Regulate Transit-Amplifying Neuroblast Lineages in Drosophila. *Developmental Cell*, *14*(4), 535–546. https://doi.org/10.1016/j.devcel.2008.03.004

Brand, A. H., Manoukian, A. S., & Perrimon, N. (1994). Chapter 33 Ectopic Expression in Drosophila. In *Methods in Cell Biology* (Vol. 44, pp. 635–654). Elsevier. https://doi.org/10.1016/S0091-679X(08)60936-X

Brand, A. H., & Perrimon, N. (1993). Targeted gene expression as a means of altering cell fates and generating dominant phenotypes. *Development*, *118*(2), 401–415. https://doi.org/10.1242/dev.118.2.401

Cabernard, C., Prehoda, K. E., & Doe, C. Q. (2010). A spindle-independent cleavage furrow positioning pathway. *Nature*, *467*(7311), 91–94. https://doi.org/10.1038/nature09334

Cao, R., Wang, L., Wang, H., Xia, L., Erdjument-Bromage, H., Tempst, P., Jones, R. S., & Zhang, Y. (2002). Role of Histone H3 Lysine 27 Methylation in Polycomb-Group

Silencing. *Science*, *298*(5595), 1039–1043. https://doi.org/10.1126/science.1076997

Carney, T. D., Miller, M. R., Robinson, K. J., Bayraktar, O. A., Osterhout, J. A., & Doe, C. Q. (2012). Functional genomics identifies neural stem cell sub-type expression profiles and genes regulating neuroblast homeostasis. *Developmental Biology*, *361*(1), 137–146. https://doi.org/10.1016/j.ydbio.2011.10.020

Castellanos, E., Dominguez, P., & Gonzalez, C. (2008). Centrosome Dysfunction in Drosophila Neural Stem Cells Causes Tumors that Are Not Due to Genome Instability. *Current Biology*, *18*(16), 1209–1214. https://doi.org/10.1016/j.cub.2008.07.029

Caussinus, E., & Gonzalez, C. (2005). Induction of tumor growth by altered stem-cell asymmetric division in Drosophila melanogaster. *Nature Genetics*, *37*(10), 1125–1129. https://doi.org/10.1038/ng1632

Caussinus, E., & Hirth, F. (2007). Asymmetric Stem Cell Division in Development and Cancer. In A. Macieira-Coelho (Ed.), *Asymmetric Cell Division* (Vol. 45, pp. 205–225). Springer Berlin Heidelberg. https://doi.org/10.1007/978-3-540-69161-7_9

Ceron, J., González, C., & Tejedor, F. J. (2001). Patterns of Cell Division and Expression of Asymmetric Cell Fate Determinants in Postembryonic Neuroblast Lineages of Drosophila. *Developmental Biology*, *230*(2), 125–138. https://doi.org/10.1006/dbio.2000.0110

Chang, L., Ruiz, P., Ito, T., & Sellers, W. R. (2021). Targeting pan-essential genes in cancer: Challenges and opportunities. *Cancer Cell*, *39*(4), 466–479. https://doi.org/10.1016/j.ccell.2020.12.008

Chen, C.-L., Lin, C.-Y., & Kung, H.-J. (2021). Targeting Mitochondrial OXPHOS and Their Regulatory Signals in Prostate Cancers. *International Journal of Molecular Sciences*, *22*(24), 13435. https://doi.org/10.3390/ijms222413435

Chen, G., Kong, J., Tucker-Burden, C., Anand, M., Rong, Y., Rahman, F., Moreno, C. S., Van Meir, E. G., Hadjipanayis, C. G., & Brat, D. J. (2014). Human *Brat* Ortholog *TRIM3* Is a Tumor Suppressor That Regulates Asymmetric Cell Division in Glioblastoma. *Cancer Research*, *74*(16), 4536–4548. https://doi.org/10.1158/0008-5472.CAN-13-3703

Chia, W., Somers, W. G., & Wang, H. (2008). Drosophila neuroblast asymmetric divisions: Cell cycle regulators, asymmetric protein localization, and tumorigenesis. *Journal of Cell Biology*, *180*(2), 267–272. https://doi.org/10.1083/jcb.200708159

Cho, P. F., Gamberi, C., Cho-Park, Y. A., Cho-Park, I. B., Lasko, P., & Sonenberg, N. (2006). Cap-Dependent Translational Inhibition Establishes Two Opposing Morphogen Gradients in Drosophila Embryos. *Current Biology*, *16*(20), 2035–2041. https://doi.org/10.1016/j.cub.2006.08.093

Choksi, S. P., Southall, T. D., Bossing, T., Edoff, K., de Wit, E., Fischer, B. E., van Steensel, B., Micklem, G., & Brand, A. H. (2006). Prospero Acts as a Binary Switch between Self-Renewal and Differentiation in Drosophila Neural Stem Cells. *Developmental Cell*, *11*(6), 775–789. https://doi.org/10.1016/j.devcel.2006.09.015

Clemente-Ruiz, M., Murillo-Maldonado, J. M., Benhra, N., Barrio, L., Pérez, L., Quiroga, G., Nebreda, A. R., & Milán, M. (2016). Gene Dosage Imbalance Contributes to Chromosomal Instability-Induced Tumorigenesis. *Developmental Cell*, *36*(3), 290–302. https://doi.org/10.1016/j.devcel.2016.01.008

Coleman, J. E. (1992). ZINC PROTEINS: Enzymes, Storage Proteins, Transcription Factors, and Replication Proteins. *Annual Review of Biochemistry*, *61*(1), 897–946. https://doi.org/10.1146/annurev.bi.61.070192.004341

Connacher, R. P., & Goldstrohm, A. C. (2021). Molecular and biological functions of TRIM-NHL RNA-BINDING proteins. *WIREs RNA*, *12*(2).

https://doi.org/10.1002/wrna.1620
Coux, R.-X., Teixeira, F. K., & Lehmann, R. (2018). L(3)mbt and the LINT complex safeguard cellular identity in the Drosophila ovary. *Development*. https://doi.org/10.1242/dev.160721
Crabtree, H. G. (1929). Observations on the carbohydrate metabolism of tumours. *Biochemical Journal*, *23*(3), 536–545. https://doi.org/10.1042/bj0230536
Criscuolo, D., Avolio, R., Matassa, D. S., & Esposito, F. (2021). Targeting Mitochondrial Protein Expression as a Future Approach for Cancer Therapy. *Frontiers in Oncology*, *11*, 797265. https://doi.org/10.3389/fonc.2021.797265
Curran, S. P., Wu, X., Riedel, C. G., & Ruvkun, G. (2009). A soma-to-germline transformation in long-lived Caenorhabditis elegans mutants. *Nature*, *459*(7250), 1079–1084. https://doi.org/10.1038/nature08106
D'Andrea, A., Gritti, I., Nicoli, P., Giorgio, M., Doni, M., Conti, A., Bianchi, V., Casoli, L., Sabò, A., Mironov, A., Beznoussenko, G. V., & Amati, B. (2016). The mitochondrial translation machinery as a therapeutic target in Myc-driven lymphomas. *Oncotarget*, *7*(45), 72415–72430. https://doi.org/10.18632/oncotarget.11719
Dar, A. C., Das, T. K., Shokat, K. M., & Cagan, R. L. (2012). Chemical genetic discovery of targets and anti-targets for cancer polypharmacology. *Nature*, *486*(7401), 80–84. https://doi.org/10.1038/nature11127
D'Avino, P. P., & Thummel, C. S. (1999). [7] Ectopic expression systems in Drosophila. In *Methods in Enzymology* (Vol. 306, pp. 129–142). Elsevier. https://doi.org/10.1016/S0076-6879(99)06009-7
DeCamillis, M., Cheng, N. S., Pierre, D., & Brock, H. W. (1992). The polyhomeotic gene of Drosophila encodes a chromatin protein that shares polytene chromosome-binding sites with Polycomb. *Genes & Development*, *6*(2), 223–232. https://doi.org/10.1101/gad.6.2.223
Deng, Q., & Wang, H. (2022). Re-visiting the principles of apicobasal polarity in Drosophila neural stem cells. *Developmental Biology*, *484*, 57–62. https://doi.org/10.1016/j.ydbio.2022.02.006
Dewald, G. W., Schad, C. R., Lilla, V. C., & Jalal, S. M. (1993). Frequency and photographs of HGM11 chromosome anomalies in bone marrow samples from 3,996 patients with malignant hematologic neoplasms. *Cancer Genetics and Cytogenetics*, *68*(1), 60–69. https://doi.org/10.1016/0165-4608(93)90075-W
Dietzl, G., Chen, D., Schnorrer, F., Su, K.-C., Barinova, Y., Fellner, M., Gasser, B., Kinsey, K., Oppel, S., Scheiblauer, S., Couto, A., Marra, V., Keleman, K., & Dickson, B. J. (2007). A genome-wide transgenic RNAi library for conditional gene inactivation in Drosophila. *Nature*, *448*(7150), 151–156. https://doi.org/10.1038/nature05954
Dijk, S. N., Protasoni, M., Elpidorou, M., Kroon, A. M., & Taanman, J.-W. (2020). Mitochondria as target to inhibit proliferation and induce apoptosis of cancer cells: The effects of doxycycline and gemcitabine. *Scientific Reports*, *10*(1), 4363. https://doi.org/10.1038/s41598-020-61381-9
Doe, C. Q., Chu-LaGraff, Q., Wright, D. M., & Scott, M. P. (1991). The prospero gene specifies cell fates in the drosophila central nervous system. *Cell*, *65*(3), 451–464. https://doi.org/10.1016/0092-8674(91)90463-9
Dopazo, J. (2009). Functional Profiling Methods in Cancer. In R. Grützmann & C. Pilarsky (Eds.), *Cancer Gene Profiling* (Vol. 576, pp. 363–374). Humana Press. https://doi.org/10.1007/978-1-59745-545-9_19
Dorsett, D., Eissenberg, J. C., Misulovin, Z., Martens, A., Redding, B., & McKim, K.

(2005). Effects of sister chromatid cohesion proteins on *cut* gene expression during wing development in *Drosophila*. *Development*, *132*(21), 4743–4753. https://doi.org/10.1242/dev.02064

Drăghici, S., Khatri, P., Martins, R. P., Ostermeier, G. C., & Krawetz, S. A. (2003). Global functional profiling of gene expression☆☆This work was funded in part by a Sun Microsystems grant awarded to S.D., NIH Grant HD36512 to S.A.K., a Wayne State University SOM Dean's Post-Doctoral Fellowship, and an NICHD Contraception and Infertility Loan to G.C.O. Support from the WSU MCBI mode is gratefully appreciated. *Genomics*, *81*(2), 98–104. https://doi.org/10.1016/S0888-7543(02)00021-6

Dura, J.-M., Randsholt, N. B., Deatrick, J., Erk, I., Santamaria, P., Freeman, J. D., Freeman, S. J., Weddell, D., & Brock, H. W. (1987). A complex genetic locus, polyhomeotic, is required for segmental specification and epidermal development in D. melanogaster. *Cell*, *51*(5), 829–839. https://doi.org/10.1016/0092-8674(87)90106-1

Edwards, T. A. (2003). Model of the Brain Tumor-Pumilio translation repressor complex. *Genes & Development*, *17*(20), 2508–2513. https://doi.org/10.1101/gad.1119403

Egger, B., Boone, J. Q., Stevens, N. R., Brand, A. H., & Doe, C. Q. (2007). Regulation of spindle orientation and neural stem cell fate in the Drosophila optic lobe. *Neural Development*, *2*(1), 1. https://doi.org/10.1186/1749-8104-2-1

Egger, B., Chell, J. M., & Brand, A. H. (2008). Insights into neural stem cell biology from flies. *Philosophical Transactions of the Royal Society B: Biological Sciences*, *363*(1489), 39–56. https://doi.org/10.1098/rstb.2006.2011

Egger, B., Gold, K. S., & Brand, A. H. (2010). Notch regulates the switch from symmetric to asymmetric neural stem cell division in the *Drosophila* optic lobe. *Development*, *137*(18), 2981–2987. https://doi.org/10.1242/dev.051250

Egger, B., Gold, K. S., & Brand, A. H. (2011). Regulating the balance between symmetric and asymmetric stem cell division in the developing brain. *Fly*, *5*(3), 237–241. https://doi.org/10.4161/fly.5.3.15640

Enomoto, M., Siow, C., & Igaki, T. (2018). Drosophila As a Cancer Model. In M. Yamaguchi (Ed.), *Drosophila Models for Human Diseases* (Vol. 1076, pp. 173–194). Springer Singapore. https://doi.org/10.1007/978-981-13-0529-0_10

Escobar-Alvarez, S., Gardner, J., Sheth, A., Manfredi, G., Yang, G., Ouerfelli, O., Heaney, M. L., & Scheinberg, D. A. (2010). Inhibition of Human Peptide Deformylase Disrupts Mitochondrial Function. *Molecular and Cellular Biology*, *30*(21), 5099–5109. https://doi.org/10.1128/MCB.00469-10

Fantin, V. R., St-Pierre, J., & Leder, P. (2006). Attenuation of LDH-A expression uncovers a link between glycolysis, mitochondrial physiology, and tumor maintenance. *Cancer Cell*, *9*(6), 425–434. https://doi.org/10.1016/j.ccr.2006.04.023

Feichtinger, J., Larcombe, L., & McFarlane, R. J. (2014). Meta-analysis of expression of l(3)mbt tumor-associated germline genes supports the model that a soma-to-germline transition is a hallmark of human cancers. *International Journal of Cancer*, *134*(10), 2359–2365. https://doi.org/10.1002/ijc.28577

Fernández-Hernández, I., Scheenaard, E., Pollarolo, G., & Gonzalez, C. (2016). The translational relevance of *Drosophila* in drug discovery. *EMBO Reports*, *17*(4), 471–472. https://doi.org/10.15252/embr.201642080

Figueroa-Clarevega, A., & Bilder, D. (2015). Malignant Drosophila Tumors Interrupt Insulin Signaling to Induce Cachexia-like Wasting. *Developmental Cell*, *33*(1), 47–55. https://doi.org/10.1016/j.devcel.2015.03.001

Francis, N. J., Kingston, R. E., & Woodcock, C. L. (2004). Chromatin Compaction by a Polycomb Group Protein Complex. *Science*, *306*(5701), 1574–1577. https://doi.org/10.1126/science.1100576

Frank, D. J., Edgar, B. A., & Roth, M. B. (2002). The *Drosophila melanogaster* gene *brain tumor* negatively regulates cell growth and ribosomal RNA synthesis. *Development*, *129*(2), 399–407. https://doi.org/10.1242/dev.129.2.399

Furrer, M., Balbi, M., Albarca-Aguilera, M., Gallant, M., Herr, W., & Gallant, P. (2010). Drosophila Myc Interacts with Host Cell Factor (dHCF) to Activate Transcription and Control Growth. *Journal of Biological Chemistry*, *285*(51), 39623–39636. https://doi.org/10.1074/jbc.M110.140467

García-Escudero, R., & Paramio, J. M. (2008). Gene expression profiling as a tool for basic analysis and clinical application of human cancer. *Molecular Carcinogenesis*, *47*(8), 573–579. https://doi.org/10.1002/mc.20430

Gateff, E. (1978). Malignant Neoplasms of Genetic Origin in *Drosophila melanogaster*: Some developmental genes that control differentiation can also cause malignant neoplasms when mutated. *Science*, *200*(4349), 1448–1459. https://doi.org/10.1126/science.96525

Gateff, E. (1994). Tumor suppressor and overgrowth suppressor genes of Drosophila melanogaster: Developmental aspects. *The International Journal of Developmental Biology*, *38*(4), 565–590.

Gateff, E., Löffler, T., & Wismar, J. (1993). A temperature-sensitive brain tumor suppressor mutation of Drosophila melanogaster: Developmental studies and molecular localization of the gene. *Mechanisms of Development*, *41*(1), 15–31. https://doi.org/10.1016/0925-4773(93)90052-Y

Gaudet, P., Livstone, M. S., Lewis, S. E., & Thomas, P. D. (2011). Phylogenetic-based propagation of functional annotations within the Gene Ontology consortium. *Briefings in Bioinformatics*, *12*(5), 449–462. https://doi.org/10.1093/bib/bbr042

Genovese, S., Clément, R., Gaultier, C., Besse, F., Narbonne-Reveau, K., Daian, F., Foppolo, S., Luis, N. M., & Maurange, C. (2019). Coopted temporal patterning governs cellular hierarchy, heterogeneity and metabolism in Drosophila neuroblast tumors. *ELife*, *8*, e50375. https://doi.org/10.7554/eLife.50375

Georlette, D., Ahn, S., MacAlpine, D. M., Cheung, E., Lewis, P. W., Beall, E. L., Bell, S. P., Speed, T., Manak, J. R., & Botchan, M. R. (2007). Genomic profiling and expression studies reveal both positive and negative activities for the *Drosophila* Myb–MuvB/dREAM complex in proliferating cells. *Genes & Development*, *21*(22), 2880–2896. https://doi.org/10.1101/gad.1600107

Gladstone, M., & Su, T. T. (2011). Chemical genetics and drug screening in Drosophila cancer models. *Journal of Genetics and Genomics*, *38*(10), 497–504. https://doi.org/10.1016/j.jgg.2011.09.003

Golub, T. R., Barker, G. F., Lovett, M., & Gilliland, D. G. (1994). Fusion of PDGF receptor β to a novel ets-like gene, tel, in chronic myelomonocytic leukemia with t(5;12) chromosomal translocation. *Cell*, *77*(2), 307–316. https://doi.org/10.1016/0092-8674(94)90322-0

Golubovsky, M. D., Weisman, N. Y., Arbeev, K. G., Ukraintseva, S. V., & Yashin, A. I. (2006). Decrease in the lgl tumor suppressor dose in Drosophila increases survival and longevity in stress conditions. *Experimental Gerontology*, *41*(9), 819–827. https://doi.org/10.1016/j.exger.2006.06.035

Gönczy, P. (2008). Mechanisms of asymmetric cell division: Flies and worms pave the way. *Nature Reviews Molecular Cell Biology*, *9*(5), 355–366. https://doi.org/10.1038/nrm2388

Gonzalez and Glover. (1993). Techniques for studying mitosis in Drosophila. *The Cell Cycle: A Practical Approach. Oxford University Press*, *143–175*.

Gonzalez, C. (2007). Spindle orientation, asymmetric division and tumour suppression in Drosophila stem cells. *Nature Reviews Genetics*, *8*(6), 462–472. https://doi.org/10.1038/nrg2103

Gonzalez, C. (2013). Drosophila melanogaster: A model and a tool to investigate malignancy and identify new therapeutics. *Nature Reviews Cancer*, *13*(3), 172–183. https://doi.org/10.1038/nrc3461

Götz, M., & Huttner, W. B. (2005). The cell biology of neurogenesis. *Nature Reviews Molecular Cell Biology*, *6*(10), 777–788. https://doi.org/10.1038/nrm1739

Graham, P., & Pick, L. (2017). Drosophila as a Model for Diabetes and Diseases of Insulin Resistance. In *Current Topics in Developmental Biology* (Vol. 121, pp. 397–419). Elsevier. https://doi.org/10.1016/bs.ctdb.2016.07.011

Gramates, L. S., Agapite, J., Attrill, H., Calvi, B. R., Crosby, M. A., dos Santos, G., Goodman, J. L., Goutte-Gattat, D., Jenkins, V. K., Kaufman, T., Larkin, A., Matthews, B. B., Millburn, G., Strelets, V. B., the FlyBase Consortium, Perrimon, N., Gelbart, S. R., Agapite, J., Broll, K., … Lovato, T. (2022). FlyBase: A guided tour of highlighted features. *Genetics*, *220*(4), iyac035. https://doi.org/10.1093/genetics/iyac035

Gui, H., Li, M.-L., & Tsai, C.-C. (2011). A Tale of Tailless. *Developmental Neuroscience*, *33*(1), 1–13. https://doi.org/10.1159/000321585

Guillermin, O., Perruchoud, B., Sprecher, S. G., & Egger, B. (2015). Characterization of tailless functions during Drosophila optic lobe formation. *Developmental Biology*, *405*(2), 202–213. https://doi.org/10.1016/j.ydbio.2015.06.011

Gurvich, N., Perna, F., Farina, A., Voza, F., Menendez, S., Hurwitz, J., & Nimer, S. D. (2010). L3MBTL1 polycomb protein, a candidate tumor suppressor in del(20q12) myeloid disorders, is essential for genome stability. *Proceedings of the National Academy of Sciences*, *107*(52), 22552–22557. https://doi.org/10.1073/pnas.1017092108

Hakes, A. E., & Brand, A. H. (2020). Tailless/TLX reverts intermediate neural progenitors to stem cells driving tumourigenesis via repression of asense/ASCL1. *ELife*, *9*. https://doi.org/10.7554/eLife.53377

Hales, K. G., Korey, C. A., Larracuente, A. M., & Roberts, D. M. (2015). Genetics on the Fly: A Primer on the *Drosophila* Model System. *Genetics*, *201*(3), 815–842. https://doi.org/10.1534/genetics.115.183392

Halligan, D. L., & Keightley, P. D. (2006). Ubiquitous selective constraints in the *Drosophila* genome revealed by a genome-wide interspecies comparison. *Genome Research*, *16*(7), 875–884. https://doi.org/10.1101/gr.5022906

Hanash, S. (2003). Disease proteomics. *Nature*, *422*(6928), 226–232. https://doi.org/10.1038/nature01514

Hardin, P. E., Hall, J. C., & Rosbash, M. (1990). Feedback of the Drosophila period gene product on circadian cycling of its messenger RNA levels. *Nature*, *343*(6258), 536–540. https://doi.org/10.1038/343536a0

Harnish, J. M., Link, N., & Yamamoto, S. (2021). Drosophila as a Model for Infectious Diseases. *International Journal of Molecular Sciences*, *22*(5), 2724. https://doi.org/10.3390/ijms22052724

Harris, R. E., Pargett, M., Sutcliffe, C., Umulis, D., & Ashe, H. L. (2011). Brat Promotes Stem Cell Differentiation via Control of a Bistable Switch that Restricts BMP Signaling. *Developmental Cell*, *20*(1), 72–83. https://doi.org/10.1016/j.devcel.2010.11.019

Harrison, D. A., Binari, R., Nahreini, T. S., Gilman, M., & Perrimon, N. (1995). Activation of a Drosophila Janus kinase (JAK) causes hematopoietic neoplasia and developmental defects. *The EMBO Journal*, *14*(12), 2857–2865. https://doi.org/10.1002/j.1460-2075.1995.tb07285.x

Hartenstein, V., Spindler, S., Pereanu, W., & Fung, S. (2008). The Development of the Drosophila Larval Brain. In G. M. Technau (Ed.), *Brain Development in Drosophila melanogaster* (Vol. 628, pp. 1–31). Springer New York. https://doi.org/10.1007/978-0-387-78261-4_1

Hatakeyama, S. (2017). TRIM Family Proteins: Roles in Autophagy, Immunity, and Carcinogenesis. *Trends in Biochemical Sciences*, *42*(4), 297–311. https://doi.org/10.1016/j.tibs.2017.01.002

Hofbauer, A., & Campos-Ortega, J. A. (1990). Proliferation pattern and early differentiation of the optic lobes in Drosophila melanogaster. *Roux's Archives of Developmental Biology*, *198*(5), 264–274. https://doi.org/10.1007/BF00377393

Hoffmann, J. A., & Reichhart, J.-M. (2002). Drosophila innate immunity: An evolutionary perspective. *Nature Immunology*, *3*(2), 121–126. https://doi.org/10.1038/ni0202-121

Homem, C. C. F., & Knoblich, J. A. (2012). *Drosophila* neuroblasts: A model for stem cell biology. *Development*, *139*(23), 4297–4310. https://doi.org/10.1242/dev.080515

Homem, C. C. F., Repic, M., & Knoblich, J. A. (2015). Proliferation control in neural stem and progenitor cells. *Nature Reviews Neuroscience*, *16*(11), 647–659. https://doi.org/10.1038/nrn4021

Homem, C. C. F., Steinmann, V., Burkard, T. R., Jais, A., Esterbauer, H., & Knoblich, J. A. (2014). Ecdysone and Mediator Change Energy Metabolism to Terminate Proliferation in Drosophila Neural Stem Cells. *Cell*, *158*(4), 874–888. https://doi.org/10.1016/j.cell.2014.06.024

Hsu, Y.-C., Chern, J. J., Cai, Y., Liu, M., & Choi, K.-W. (2007). Drosophila TCTP is essential for growth and proliferation through regulation of dRheb GTPase. *Nature*, *445*(7129), 785–788. https://doi.org/10.1038/nature05528

Huang, D. W., Sherman, B. T., & Lempicki, R. A. (2009). Systematic and integrative analysis of large gene lists using DAVID bioinformatics resources. *Nature Protocols*, *4*(1), 44–57. https://doi.org/10.1038/nprot.2008.211

Hulsen, T., de Vlieg, J., & Alkema, W. (2008). BioVenn – a web application for the comparison and visualization of biological lists using area-proportional Venn diagrams. *BMC Genomics*, *9*(1), 488. https://doi.org/10.1186/1471-2164-9-488

Humbert, P., Russell, S., & Richardson, H. (2003). Dlg, Scribble and Lgl in cell polarity, cell proliferation and cancer. *BioEssays*, *25*(6), 542–553. https://doi.org/10.1002/bies.10286

Ikeshima-Kataoka, H., Skeath, J. B., Nabeshima, Y., Doe, C. Q., & Matsuzaki, F. (1997). Miranda directs Prospero to a daughter cell during Drosophila asymmetric divisions. *Nature*, *390*(6660), 625–629. https://doi.org/10.1038/37641

Irion, U., Adams, J., Chang, C.-W., & St Johnston, D. (2006). Miranda couples oskar mRNA/Staufen complexes to the bicoid mRNA localization pathway. *Developmental Biology*, *297*(2), 522–533. https://doi.org/10.1016/j.ydbio.2006.05.029

Izumi, Y., Ohta, N., Hisata, K., Raabe, T., & Matsuzaki, F. (2006). Drosophila Pins-binding protein Mud regulates spindle-polarity coupling and centrosome organization. *Nature Cell Biology*, *8*(6), 586–593. https://doi.org/10.1038/ncb1409

Izumi, Y., Ohta, N., Itoh-Furuya, A., Fuse, N., & Matsuzaki, F. (2004). Differential functions of G protein and Baz–aPKC signaling pathways in Drosophila neuroblast

asymmetric division. *Journal of Cell Biology*, *164*(5), 729–738. https://doi.org/10.1083/jcb.200309162

Janic, A., Mendizabal, L., Llamazares, S., Rossell, D., & Gonzalez, C. (2010). Ectopic Expression of Germline Genes Drives Malignant Brain Tumor Growth in Drosophila. *Science*, *330*(6012), 1824–1827. https://doi.org/10.1126/science.1195481

Janssens, D. H., Komori, H., Grbac, D., Chen, K., Koe, C. T., Wang, H., & Lee, C.-Y. (2014). Earmuff restricts progenitor cell potential by attenuating the competence to respond to self-renewal factors. *Development*, *141*(5), 1036–1046. https://doi.org/10.1242/dev.106534

Januschke, J., & Gonzalez, C. (2008). Drosophila asymmetric division, polarity and cancer. *Oncogene*, *27*(55), 6994–7002. https://doi.org/10.1038/onc.2008.349

Januschke, J., & Gonzalez, C. (2010). The interphase microtubule aster is a determinant of asymmetric division orientation in Drosophila neuroblasts. *Journal of Cell Biology*, *188*(5), 693–706. https://doi.org/10.1083/jcb.200905024

Jia, M., Meng, D., Chen, M., Li, T., Zhang, Y. Q., & Yao, A. (2019). Drosophila homolog of the intellectual disability-related long-chain acyl-CoA synthetase 4 is required for neuroblast proliferation. *Journal of Genetics and Genomics*, *46*(1), 5–17. https://doi.org/10.1016/j.jgg.2018.10.006

Jiang, Y., & Reichert, H. (2014). *Drosophila* Neural Stem Cells in Brain Development and Tumor Formation. *Journal of Neurogenetics*, *28*(3–4), 181–189. https://doi.org/10.3109/01677063.2014.898639

Johannes, L., & Popoff, V. (2008). Tracing the Retrograde Route in Protein Trafficking. *Cell*, *135*(7), 1175–1187. https://doi.org/10.1016/j.cell.2008.12.009

Jürgens, G., Wieschaus, E., Nüsslein-Volhard, C., & Kluding, H. (1984). Mutations affecting the pattern of the larval cuticle inDrosophila melanogaster. *Wilhelm Roux's Archives of Developmental Biology*, *193*(5), 283–295.

Jüschke, C., Dohnal, I., Pichler, P., Harzer, H., Swart, R., Ammerer, G., Mechtler, K., & Knoblich, J. A. (2013). Transcriptome and proteome quantification of a tumor model provides novel insights into post-transcriptional gene regulation. *Genome Biology*, *14*(11), r133. https://doi.org/10.1186/gb-2013-14-11-r133

Kaltschmidt, J. A., Davidson, C. M., Brown, N. H., & Brand, A. H. (2000). Rotation and asymmetry of the mitotic spindle direct asymmetric cell division in the developing central nervous system. *Nature Cell Biology*, *2*(1), 7–12. https://doi.org/10.1038/71323

Kang, K. H., & Reichert, H. (2015). Control of neural stem cell self-renewal and differentiation in Drosophila. *Cell and Tissue Research*, *359*(1), 33–45. https://doi.org/10.1007/s00441-014-1914-9

Kim, H.-J., Maiti, P., & Barrientos, A. (2017). Mitochondrial ribosomes in cancer. *Seminars in Cancer Biology*, *47*, 67–81. https://doi.org/10.1016/j.semcancer.2017.04.004

Kim, K., Lane, E. A., Saftien, A., Wang, H., Xu, Y., Wirtz-Peitz, F., & Perrimon, N. (2020). *Drosophila* as a model for studying cystic fibrosis pathophysiology of the gastrointestinal system. *Proceedings of the National Academy of Sciences*, *117*(19), 10357–10367. https://doi.org/10.1073/pnas.1913127117

Klymenko, T., Papp, B., Fischle, W., Köcher, T., Schelder, M., Fritsch, C., Wild, B., Wilm, M., & Müller, J. (2006). A Polycomb group protein complex with sequence-specific DNA-binding and selective methyl-lysine-binding activities. *Genes & Development*, *20*(9), 1110–1122. https://doi.org/10.1101/gad.377406

Knoblich, J. A. (2008). Mechanisms of Asymmetric Stem Cell Division. *Cell*, *132*(4),

583–597. https://doi.org/10.1016/j.cell.2008.02.007

Koga, H., Matsui, S., Hirota, T., Takebayashi, S., Okumura, K., & Saya, H. (1999). A human homolog of Drosophila lethal(3)malignant brain tumor (l(3)mbt) protein associates with condensed mitotic chromosomes. *Oncogene*, *18*(26), 3799–3809. https://doi.org/10.1038/sj.onc.1202732

Komori, H., Golden, K. L., Kobayashi, T., Kageyama, R., & Lee, C.-Y. (2018). Multilayered gene control drives timely exit from the stem cell state in uncommitted progenitors during *Drosophila* asymmetric neural stem cell division. *Genes & Development*, *32*(23–24), 1550–1561. https://doi.org/10.1101/gad.320333.118

Komori, H., Xiao, Q., McCartney, B. M., & Lee, C.-Y. (2014). Brain tumor specifies intermediate progenitor cell identity by attenuating β-catenin/Armadillo activity. *Development*, *141*(1), 51–62. https://doi.org/10.1242/dev.099382

Konopka, R. J., & Benzer, S. (1971). Clock Mutants of *Drosophila melanogaster*. *Proceedings of the National Academy of Sciences*, *68*(9), 2112–2116. https://doi.org/10.1073/pnas.68.9.2112

Kraut, R., Chia, W., Jan, L. Y., Jan, Y. N., & Knoblich, J. A. (1996). Role of inscuteable in orienting asymmetric cell divisions in Drosophila. *Nature*, *383*(6595), 50–55. https://doi.org/10.1038/383050a0

Kumari, P., Aeschimann, F., Gaidatzis, D., Keusch, J. J., Ghosh, P., Neagu, A., Pachulska-Wieczorek, K., Bujnicki, J. M., Gut, H., Großhans, H., & Ciosk, R. (2018). Evolutionary plasticity of the NHL domain underlies distinct solutions to RNA recognition. *Nature Communications*, *9*(1), 1549. https://doi.org/10.1038/s41467-018-03920-7

Kurzik-Dumke, U., Phannavong, B., Gundacker, D., & Gateff, E. (1992). Genetic, cytogenetic and developmental analysis of the Drosophila melanogaster tumor suppressor gene lethal(2)tumorous imaginal discs (l(2)tid). *Differentiation*, *51*(2), 91–104. https://doi.org/10.1111/j.1432-0436.1992.tb00685.x

Lachner, M., O'Carroll, D., Rea, S., Mechtler, K., & Jenuwein, T. (2001). Methylation of histone H3 lysine 9 creates a binding site for HP1 proteins. *Nature*, *410*(6824), 116–120. https://doi.org/10.1038/35065132

Lakatos, Z., Benkő, P., Juhász, G., & Lőrincz, P. (2021). Drosophila Rab39 Attenuates Lysosomal Degradation. *International Journal of Molecular Sciences*, *22*(19), 10635. https://doi.org/10.3390/ijms221910635

Landskron, L., Steinmann, V., Bonnay, F., Burkard, T. R., Steinmann, J., Reichardt, I., Harzer, H., Laurenson, A.-S., Reichert, H., & Knoblich, J. A. (2018). The asymmetrically segregating lncRNA cherub is required for transforming stem cells into malignant cells. *ELife*, *7*. https://doi.org/10.7554/eLife.31347

Lauri, A., Fasano, G., Venditti, M., Dallapiccola, B., & Tartaglia, M. (2021). In vivo Functional Genomics for Undiagnosed Patients: The Impact of Small GTPases Signaling Dysregulation at Pan-Embryo Developmental Scale. *Frontiers in Cell and Developmental Biology*, *9*, 642235. https://doi.org/10.3389/fcell.2021.642235

Laver, J. D., Li, X., Ray, D., Cook, K. B., Hahn, N. A., Nabeel-Shah, S., Kekis, M., Luo, H., Marsolais, A. J., Fung, K. Y., Hughes, T. R., Westwood, J. T., Sidhu, S. S., Morris, Q., Lipshitz, H. D., & Smibert, C. A. (2015). Brain tumor is a sequence-specific RNA-binding protein that directs maternal mRNA clearance during the Drosophila maternal-to-zygotic transition. *Genome Biology*, *16*(1). https://doi.org/10.1186/s13059-015-0659-4

Lee, C.-Y., Andersen, R. O., Cabernard, C., Manning, L., Tran, K. D., Lanskey, M. J., Bashirullah, A., & Doe, C. Q. (2006). Drosophila Aurora-A kinase inhibits neuroblast self-renewal by regulating aPKC/Numb cortical polarity and spindle

orientation. *Genes & Development*, *20*(24), 3464–3474. https://doi.org/10.1101/gad.1489406

Lee, C.-Y., Wilkinson, B. D., Siegrist, S. E., Wharton, R. P., & Doe, C. Q. (2006). Brat Is a Miranda Cargo Protein that Promotes Neuronal Differentiation and Inhibits Neuroblast Self-Renewal. *Developmental Cell*, *10*(4), 441–449. https://doi.org/10.1016/j.devcel.2006.01.017

Lee, M. D., She, Y., Soskis, M. J., Borella, C. P., Gardner, J. R., Hayes, P. A., Dy, B. M., Heaney, M. L., Philips, M. R., Bornmann, W. G., Sirotnak, F. M., & Scheinberg, D. A. (2004). Human mitochondrial peptide deformylase, a new anticancer target of actinonin-based antibiotics. *Journal of Clinical Investigation*, *114*(8), 1107–1116. https://doi.org/10.1172/JCI200422269

Lewis, P. W., Beall, E. L., Fleischer, T. C., Georlette, D., Link, A. J., & Botchan, M. R. (2004). Identification of a *Drosophila* Myb-E2F2/RBF transcriptional repressor complex. *Genes & Development*, *18*(23), 2929–2940. https://doi.org/10.1101/gad.1255204

Li, B., Wong, C., Gao, S. M., Zhang, R., Sun, R., Li, Y., & Song, Y. (2018). The retromer complex safeguards against neural progenitor-derived tumorigenesis by regulating Notch receptor trafficking. *ELife*, *7*, e38181. https://doi.org/10.7554/eLife.38181

Li, J., Bench, A. J., Vassiliou, G. S., Fourouclas, N., Ferguson-Smith, A. C., & Green, A. R. (2004). Imprinting of the human *L3MBTL* gene, a polycomb family member located in a region of chromosome 20 deleted in human myeloid malignancies. *Proceedings of the National Academy of Sciences*, *101*(19), 7341–7346. https://doi.org/10.1073/pnas.0308195101

Li, P., Yang, X., Wasser, M., Cai, Y., & Chia, W. (1997). Inscuteable and Staufen Mediate Asymmetric Localization and Segregation of prospero RNA during Drosophila Neuroblast Cell Divisions. *Cell*, *90*(3), 437–447. https://doi.org/10.1016/S0092-8674(00)80504-8

Li, X., Erclik, T., Bertet, C., Chen, Z., Voutev, R., Venkatesh, S., Morante, J., Celik, A., & Desplan, C. (2013). Temporal patterning of Drosophila medulla neuroblasts controls neural fates. *Nature*, *498*(7455), 456–462. https://doi.org/10.1038/nature12319

Liang, L., Haug, J. S., Seidel, C. W., & Gibson, M. C. (2014). Functional Genomic Analysis of the Periodic Transcriptome in the Developing Drosophila Wing. *Developmental Cell*, *29*(1), 112–127. https://doi.org/10.1016/j.devcel.2014.02.018

Liberti, M. V., & Locasale, J. W. (2016). The Warburg Effect: How Does it Benefit Cancer Cells? *Trends in Biochemical Sciences*, *41*(3), 211–218. https://doi.org/10.1016/j.tibs.2015.12.001

Loedige, I., Jakob, L., Treiber, T., Ray, D., Stotz, M., Treiber, N., Hennig, J., Cook, K. B., Morris, Q., Hughes, T. R., Engelmann, J. C., Krahn, M. P., & Meister, G. (2015). The Crystal Structure of the NHL Domain in Complex with RNA Reveals the Molecular Basis of Drosophila Brain-Tumor-Mediated Gene Regulation. *Cell Reports*, *13*(6), 1206–1220. https://doi.org/10.1016/j.celrep.2015.09.068

Loedige, I., Stotz, M., Qamar, S., Kramer, K., Hennig, J., Schubert, T., Loffler, P., Langst, G., Merkl, R., Urlaub, H., & Meister, G. (2014). The NHL domain of BRAT is an RNA-binding domain that directly contacts the hunchback mRNA for regulation. *Genes & Development*, *28*(7), 749–764. https://doi.org/10.1101/gad.236513.113

Loop, T., Leemans, R., Stiefel, U., Hermida, L., Egger, B., Xie, F., Primig, M., Certa, U., Fischbach, K.-F., Reichert, H., & Hirth, F. (2004). Transcriptional signature of an

adult brain tumor in Drosophila. *BMC Genomics*, *5*(1). https://doi.org/10.1186/1471-2164-5-24

Loyer, N., & Januschke, J. (2018). The last-born daughter cell contributes to division orientation of Drosophila larval neuroblasts. *Nature Communications*, *9*(1), 3745. https://doi.org/10.1038/s41467-018-06276-0

Lu, B., Rothenberg, M., Jan, L. Y., & Jan, Y. N. (1998). Partner of Numb Colocalizes with Numb during Mitosis and Directs Numb Asymmetric Localization in Drosophila Neural and Muscle Progenitors. *Cell*, *95*(2), 225–235. https://doi.org/10.1016/S0092-8674(00)81753-5

Lund, J., Tedesco, P., Duke, K., Wang, J., Kim, S. K., & Johnson, T. E. (2002). Transcriptional Profile of Aging in C. elegans. *Current Biology*, *12*(18), 1566–1573. https://doi.org/10.1016/S0960-9822(02)01146-6

Luo, H., Hanratty, W. P., & Dearolf, C. R. (1995). An amino acid substitution in the Drosophila hopTum-l Jak kinase causes leukemia-like hematopoietic defects. *The EMBO Journal*, *14*(7), 1412–1420. https://doi.org/10.1002/j.1460-2075.1995.tb07127.x

Mačinković, I., Theofel, I., Hundertmark, T., Kovač, K., Awe, S., Lenz, J., Forné, I., Lamp, B., Nist, A., Imhof, A., Stiewe, T., Renkawitz-Pohl, R., Rathke, C., & Brehm, A. (2019). Distinct CoREST complexes act in a cell-type-specific manner. *Nucleic Acids Research*, gkz1050. https://doi.org/10.1093/nar/gkz1050

Marín, I. (2012). Origin and Diversification of TRIM Ubiquitin Ligases. *PLoS ONE*, *7*(11), e50030. https://doi.org/10.1371/journal.pone.0050030

Maurange, C., Cheng, L., & Gould, A. P. (2008). Temporal Transcription Factors and Their Targets Schedule the End of Neural Proliferation in Drosophila. *Cell*, *133*(5), 891–902. https://doi.org/10.1016/j.cell.2008.03.034

Maurer-Stroh, S., Dickens, N. J., Hughes-Davies, L., Kouzarides, T., Eisenhaber, F., & Ponting, C. P. (2003). The Tudor domain 'Royal Family': Tudor, plant Agenet, Chromo, PWWP and MBT domains. *Trends in Biochemical Sciences*, *28*(2), 69–74. https://doi.org/10.1016/S0968-0004(03)00004-5

Meier, K., Mathieu, E.-L., Finkernagel, F., Reuter, L. M., Scharfe, M., Doehlemann, G., Jarek, M., & Brehm, A. (2012). LINT, a Novel dL(3)mbt-Containing Complex, Represses Malignant Brain Tumour Signature Genes. *PLoS Genetics*, *8*(5), e1002676. https://doi.org/10.1371/journal.pgen.1002676

Meltzer, H., Marom, E., Alyagor, I., Mayseless, O., Berkun, V., Segal-Gilboa, N., Unger, T., Luginbuhl, D., & Schuldiner, O. (2019). Tissue-specific (ts)CRISPR as an efficient strategy for in vivo screening in Drosophila. *Nature Communications*, *10*(1), 2113. https://doi.org/10.1038/s41467-019-10140-0

Mirzoyan, Z., Sollazzo, M., Allocca, M., Valenza, A. M., Grifoni, D., & Bellosta, P. (2019). Drosophila melanogaster: A Model Organism to Study Cancer. *Frontiers in Genetics*, *10*, 51. https://doi.org/10.3389/fgene.2019.00051

Mollinari, C., Lange, B., & González, C. (2002). Miranda, a protein involved in neuroblast asymmetric division, is associated with embryonic centrosomes of Drosophila melanogaster. *Biology of the Cell*, *94*(1), 1–13. https://doi.org/10.1016/S0248-4900(02)01181-4

Molnar, C., Heinen, J. P., Reina, J., Llamazares, S., Palumbo, E., Breschi, A., Gay, M., Villarreal, L., Vilaseca, M., Pollarolo, G., & Gonzalez, C. (2019). The histone code reader PHD finger protein 7 controls sex-linked disparities in gene expression and malignancy in *Drosophila*. *Science Advances*, *5*(8), eaaw7965. https://doi.org/10.1126/sciadv.aaw7965

Molnar, C., Louzao, A., & Gonzalez, C. (2020). Context-Dependent Tumorigenic Effect

of Testis-Specific Mitochondrial Protein Tiny Tim 2 in Drosophila Somatic Epithelia. *Cells*, *9*(8), 1842. https://doi.org/10.3390/cells9081842

Moreau, Y., Aerts, S., Moor, B. D., Strooper, B. D., & Dabrowski, M. (2003). Comparison and meta-analysis of microarray data: From the bench to the computer desk. *Trends in Genetics*, *19*(10), 570–577. https://doi.org/10.1016/j.tig.2003.08.006

Morgan, T. H., & Bridges, C. B. (1916). *Sex-linked Inheritance in Drosophila*. Carnegie Institution of Washington. https://books.google.es/books?id=JNQGAAAAYAAJ

Morral, C., Stanisavljevic, J., Hernando-Momblona, X., Mereu, E., Álvarez-Varela, A., Cortina, C., Stork, D., Slebe, F., Turon, G., Whissell, G., Sevillano, M., Merlos-Suárez, A., Casanova-Martí, À., Moutinho, C., Lowe, S. W., Dow, L. E., Villanueva, A., Sancho, E., Heyn, H., & Batlle, E. (2020). Zonation of Ribosomal DNA Transcription Defines a Stem Cell Hierarchy in Colorectal Cancer. *Cell Stem Cell*, *26*(6), 845-861.e12. https://doi.org/10.1016/j.stem.2020.04.012

Muller, H. J. (1927). Artificial Transmutation of the Gene. *Science*, *66*(1699), 84–87. https://doi.org/10.1126/science.66.1699.84

Muller, H. J. (1928). THE MEASUREMENT OF GENE MUTATION RATE IN DROSOPHILA, ITS HIGH VARIABILITY, AND ITS DEPENDENCE UPON TEMPERATURE. *Genetics*, *13*(4), 279–357. https://doi.org/10.1093/genetics/13.4.279

Nakayama, J., Rice, J. C., Strahl, B. D., Allis, C. D., & Grewal, S. I. S. (2001). Role of Histone H3 Lysine 9 Methylation in Epigenetic Control of Heterochromatin Assembly. *Science*, *292*(5514), 110–113. https://doi.org/10.1126/science.1060118

Nériec, N., & Desplan, C. (2016). From the Eye to the Brain. In *Current Topics in Developmental Biology* (Vol. 116, pp. 247–271). Elsevier. https://doi.org/10.1016/bs.ctdb.2015.11.032

Neumüller, R. A., Gross, T., Samsonova, A. A., Vinayagam, A., Buckner, M., Founk, K., Hu, Y., Sharifpoor, S., Rosebrock, A. P., Andrews, B., Winston, F., & Perrimon, N. (2013). Conserved Regulators of Nucleolar Size Revealed by Global Phenotypic Analyses. *Science Signaling*, *6*(289). https://doi.org/10.1126/scisignal.2004145

Neumüller, R. A., Richter, C., Fischer, A., Novatchkova, M., Neumüller, K. G., & Knoblich, J. A. (2011). Genome-Wide Analysis of Self-Renewal in Drosophila Neural Stem Cells by Transgenic RNAi. *Cell Stem Cell*, *8*(5), 580–593. https://doi.org/10.1016/j.stem.2011.02.022

Newton, F. G., Harris, R. E., Sutcliffe, C., & Ashe, H. L. (2015). Coordinate post-transcriptional repression of Dpp-dependent transcription factors attenuates signal range during development. *Development*. https://doi.org/10.1242/dev.123273

Ngo, K. T., Wang, J., Junker, M., Kriz, S., Vo, G., Asem, B., Olson, J. M., Banerjee, U., & Hartenstein, V. (2010). Concomitant requirement for Notch and Jak/Stat signaling during neuro-epithelial differentiation in the Drosophila optic lobe. *Developmental Biology*, *346*(2), 284–295. https://doi.org/10.1016/j.ydbio.2010.07.036

Ni, J.-Q., Liu, L.-P., Binari, R., Hardy, R., Shim, H.-S., Cavallaro, A., Booker, M., Pfeiffer, B. D., Markstein, M., Wang, H., Villalta, C., Laverty, T. R., Perkins, L. A., & Perrimon, N. (2009). A Drosophila Resource of Transgenic RNAi Lines for Neurogenetics. *Genetics*, *182*(4), 1089–1100. https://doi.org/10.1534/genetics.109.103630

Northcott, P. A., Fernandez-L, A., Hagan, J. P., Ellison, D. W., Grajkowska, W., Gillespie, Y., Grundy, R., Van Meter, T., Rutka, J. T., Croce, C. M., Kenney, A. M., & Taylor, M. D. (2009). The miR-17/92 Polycistron Is Up-regulated in Sonic Hedgehog–Driven Medulloblastomas and Induced by N-myc in Sonic Hedgehog–Treated Cerebellar Neural Precursors. *Cancer Research*, *69*(8), 3249–3255.

https://doi.org/10.1158/0008-5472.CAN-08-4710
Noselli, S., & Agnès, F. (1999). Roles of the JNK signaling pathway in Drosophila morphogenesis. *Current Opinion in Genetics & Development*, *9*(4), 466–472. https://doi.org/10.1016/S0959-437X(99)80071-9
Ohshiro, T., Yagami, T., Zhang, C., & Matsuzaki, F. (2000). Role of cortical tumour-suppressor proteins in asymmetric division of Drosophila neuroblast. *Nature*, *408*(6812), 593–596. https://doi.org/10.1038/35046087
O'Neil, N. J., Bailey, M. L., & Hieter, P. (2017). Synthetic lethality and cancer. *Nature Reviews Genetics*, *18*(10), 613–623. https://doi.org/10.1038/nrg.2017.47
Otsuki, L., & Brand, A. H. (2018). Cell cycle heterogeneity directs the timing of neural stem cell activation from quiescence. *Science*, *360*(6384), 99–102. https://doi.org/10.1126/science.aan8795
Parisi, F., Riccardo, S., Daniel, M., Saqcena, M., Kundu, N., Pession, A., Grifoni, D., Stocker, H., Tabak, E., & Bellosta, P. (2011). Drosophila insulin and target of rapamycin (TOR) pathways regulate GSK3 beta activity to control Myc stability and determine Myc expression in vivo. *BMC Biology*, *9*(1), 65. https://doi.org/10.1186/1741-7007-9-65
Parmentier, M.-L., Woods, D., Greig, S., Phan, P. G., Radovic, A., Bryant, P., & O'Kane, C. J. (2000). Rapsynoid/Partner of Inscuteable Controls Asymmetric Division of Larval Neuroblasts in *Drosophila*. *The Journal of Neuroscience*, *20*(14), RC84–RC84. https://doi.org/10.1523/JNEUROSCI.20-14-j0003.2000
Peng, C.-Y., Manning, L., Albertson, R., & Doe, C. Q. (2000). The tumour-suppressor genes lgl and dlg regulate basal protein targeting in Drosophila neuroblasts. *Nature*, *408*(6812), 596–600. https://doi.org/10.1038/35046094
Perkins, L. A., Holderbaum, L., Tao, R., Hu, Y., Sopko, R., McCall, K., Yang-Zhou, D., Flockhart, I., Binari, R., Shim, H.-S., Miller, A., Housden, A., Foos, M., Randkelv, S., Kelley, C., Namgyal, P., Villalta, C., Liu, L.-P., Jiang, X., … Perrimon, N. (2015). The Transgenic RNAi Project at Harvard Medical School: Resources and Validation. *Genetics*, *201*(3), 843–852. https://doi.org/10.1534/genetics.115.180208
Peterson, A. J., Kyba, M., Bornemann, D., Morgan, K., Brock, H. W., & Simon, J. (1997). A domain shared by the Polycomb group proteins Scm and ph mediates heterotypic and homotypic interactions. *Molecular and Cellular Biology*, *17*(11), 6683–6692. https://doi.org/10.1128/MCB.17.11.6683
Petronczki, M., & Knoblich, J. A. (2001). DmPAR-6 directs epithelial polarity and asymmetric cell division of neuroblasts in Drosophila. *Nature Cell Biology*, *3*(1), 43–49. https://doi.org/10.1038/35050550
Pielage, J., Kippert, A., Zhu, M., & Klämbt, C. (2004). The Drosophila transmembrane protein Fear-of-intimacy controls glial cell migration. *Developmental Biology*, *275*(1), 245–257. https://doi.org/10.1016/j.ydbio.2004.07.039
Pimenta-Marques, A., Tostões, R., Marty, T., Barbosa, V., Lehmann, R., & Martinho, R. G. (2008). Differential requirements of a mitotic acetyltransferase in somatic and germ line cells. *Developmental Biology*, *323*(2), 197–206. https://doi.org/10.1016/j.ydbio.2008.08.021
Piper, M. D. W., & Partridge, L. (2018). Drosophila as a model for ageing. *Biochimica et Biophysica Acta (BBA) - Molecular Basis of Disease*, *1864*(9), 2707–2717. https://doi.org/10.1016/j.bbadis.2017.09.016
Ponting, C. P. (1995). SAM: A novel motif in yeast sterile and *drosophila* polyhomeotic proteins. *Protein Science*, *4*(9), 1928–1930. https://doi.org/10.1002/pro.5560040927
Port, F., Kuster, M., Herr, P., Furger, E., Bänziger, C., Hausmann, G., & Basler, K. (2008). Wingless secretion promotes and requires retromer-dependent cycling of

Wntless. *Nature Cell Biology*, *10*(2), 178–185. https://doi.org/10.1038/ncb1687

Portela, M., Mitchell, T., & Casas-Tintó, S. (2020). Cell to cell communication mediates glioblastoma progression in *Drosophila*. *Biology Open*, bio.053405. https://doi.org/10.1242/bio.053405

Protasoni, M., Kroon, A. M., & Taanman, J.-W. (2018). Mitochondria as oncotarget: A comparison between the tetracycline analogs doxycycline and COL-3. *Oncotarget*, *9*(73), 33818–33831. https://doi.org/10.18632/oncotarget.26107

Prüßing, K., Voigt, A., & Schulz, J. B. (2013). Drosophila melanogaster as a model organism for Alzheimer's disease. *Molecular Neurodegeneration*, *8*(1), 35. https://doi.org/10.1186/1750-1326-8-35

Qin, J., Van Buren, D., Huang, H.-S., Zhong, L., Mostoslavsky, R., Akbarian, S., & Hock, H. (2010). Chromatin Protein L3MBTL1 Is Dispensable for Development and Tumor Suppression in Mice. *Journal of Biological Chemistry*, *285*(36), 27767–27775. https://doi.org/10.1074/jbc.M110.115410

Ramos, A., Grünert, S., Adams, J., Micklem, D. R., Proctor, M. R., Freund, S., Bycroft, M., St Johnston, D., & Varani, G. (2000). RNA recognition by a Staufen double-stranded RNA-binding domain. *The EMBO Journal*, *19*(5), 997–1009. https://doi.org/10.1093/emboj/19.5.997

Read, R. D., Cavenee, W. K., Furnari, F. B., & Thomas, J. B. (2009). A Drosophila Model for EGFR-Ras and PI3K-Dependent Human Glioma. *PLoS Genetics*, *5*(2), e1000374. https://doi.org/10.1371/journal.pgen.1000374

Rebollo, E., & González, C. (2000). Visualizing the spindle checkpoint in *Drosophila* spermatocytes. *EMBO Reports*, *1*(1), 65–70. https://doi.org/10.1093/embo-reports/kvd011

Rebollo, E., Sampaio, P., Januschke, J., Llamazares, S., Varmark, H., & González, C. (2007). Functionally Unequal Centrosomes Drive Spindle Orientation in Asymmetrically Dividing Drosophila Neural Stem Cells. *Developmental Cell*, *12*(3), 467–474. https://doi.org/10.1016/j.devcel.2007.01.021

Reddy, B. V. V. G., Rauskolb, C., & Irvine, K. D. (2010). Influence of Fat-Hippo and Notch signaling on the proliferation and differentiation of *Drosophila* optic neuroepithelia. *Development*, *137*(14), 2397–2408. https://doi.org/10.1242/dev.050013

Regan, J. C., Khericha, M., Dobson, A. J., Bolukbasi, E., Rattanavirotkul, N., & Partridge, L. (2016). Sex difference in pathology of the ageing gut mediates the greater response of female lifespan to dietary restriction. *ELife*, *5*, e10956. https://doi.org/10.7554/eLife.10956

Reichardt, I., Bonnay, F., Steinmann, V., Loedige, I., Burkard, T. R., Meister, G., & Knoblich, J. A. (2018). The tumor suppressor Brat controls neuronal stem cell lineages by inhibiting Deadpan and Zelda. *EMBO Reports*, *19*(1), 102–117. https://doi.org/10.15252/embr.201744188

Richards, C., Pantanowitz, L., & Dezube, B. J. (2011). Antimicrobial and non-antimicrobial tetracyclines in human cancer trials. *Pharmacological Research*, *63*(2), 151–156. https://doi.org/10.1016/j.phrs.2010.10.008

Richardson, H. E., Cordero, J. B., & Grifoni, D. (2020). Basic and Translational Models of Cooperative Oncogenesis. *International Journal of Molecular Sciences*, *21*(16), 5919. https://doi.org/10.3390/ijms21165919

Richardson, H. E., & Portela, M. (2018). Modelling Cooperative Tumorigenesis in *Drosophila*. *BioMed Research International*, *2018*, 1–29. https://doi.org/10.1155/2018/4258387

Richter, C., Oktaba, K., Steinmann, J., Müller, J., & Knoblich, J. A. (2011). The tumour

suppressor L(3)mbt inhibits neuroepithelial proliferation and acts on insulator elements. *Nature Cell Biology*, *13*(9), 1029–1039. https://doi.org/10.1038/ncb2306

Richter, U., Lahtinen, T., Marttinen, P., Myöhänen, M., Greco, D., Cannino, G., Jacobs, H. T., Lietzén, N., Nyman, T. A., & Battersby, B. J. (2013). A Mitochondrial Ribosomal and RNA Decay Pathway Blocks Cell Proliferation. *Current Biology*, *23*(6), 535–541. https://doi.org/10.1016/j.cub.2013.02.019

Rolls, M. M., Albertson, R., Shih, H.-P., Lee, C.-Y., & Doe, C. Q. (2003). Drosophila aPKC regulates cell polarity and cell proliferation in neuroblasts and epithelia. *Journal of Cell Biology*, *163*(5), 1089–1098. https://doi.org/10.1083/jcb.200306079

Ross-Elliott, T. J., Watkins, J., Shan, X., Lou, F., Dreyer, B., Tunc-Ozdemir, M., Jia, H., Yang, J., Wu, L., Trusov, Y., Krysan, P., & Jones, A. M. (2019). *Biased Signaling: Distinct Ligand-directed Plasma Membrane Signalosomes Using a Common RGS/G protein Core* [Preprint]. Plant Biology. https://doi.org/10.1101/666578

Rossi, F., & Gonzalez, C. (2015). Studying tumor growth in Drosophila using the tissue allograft method. *Nature Protocols*, *10*(10), 1525–1534. https://doi.org/10.1038/nprot.2015.096

Rossi, F., Molnar, C., Hashiyama, K., Heinen, J. P., Pampalona, J., Llamazares, S., Reina, J., Hashiyama, T., Rai, M., Pollarolo, G., Fernández-Hernández, I., & Gonzalez, C. (2017). An *in vivo* genetic screen in *Drosophila* identifies the orthologue of human cancer/testis gene *SPO11* among a network of targets to inhibit *lethal(3)malignant brain tumour* growth. *Open Biology*, *7*(8), 170156. https://doi.org/10.1098/rsob.170156

Roy, K. (2004). The Tlx Gene Regulates the Timing of Neurogenesis in the Cortex. *Journal of Neuroscience*, *24*(38), 8333–8345. https://doi.org/10.1523/JNEUROSCI.1148-04.2004

Rusan, N. M., & Peifer, M. (2007). A role for a novel centrosome cycle in asymmetric cell division. *Journal of Cell Biology*, *177*(1), 13–20. https://doi.org/10.1083/jcb.200612140

Saavedra, P., & Perrimon, N. (2019). Drosophila as a Model for Tumor-Induced Organ Wasting. In W.-M. Deng (Ed.), *The Drosophila Model in Cancer* (Vol. 1167, pp. 191–205). Springer International Publishing. https://doi.org/10.1007/978-3-030-23629-8_11

Salomon, R. N., & Jackson, F. R. (2008). Tumors of the testis and midgut in aging flies. *Fly*, *2*(6), 265–268. https://doi.org/10.4161/fly.7396

Sara, H., Kallioniemi, O., & Nees, M. (2009). A Decade of Cancer Gene Profiling: From Molecular Portraits to Molecular Function. In R. Grützmann & C. Pilarsky (Eds.), *Cancer Gene Profiling* (Vol. 576, pp. 61–87). Humana Press. https://doi.org/10.1007/978-1-59745-545-9_5

Schaefer, M., Shevchenko, A., Shevchenko, A., & Knoblich, J. A. (2000). A protein complex containing Inscuteable and the Gα-binding protein Pins orients asymmetric cell divisions in Drosophila. *Current Biology*, *10*(7), 353–362. https://doi.org/10.1016/S0960-9822(00)00401-2

Schneider, C. A., Rasband, W. S., & Eliceiri, K. W. (2012). NIH Image to ImageJ: 25 years of image analysis. *Nature Methods*, *9*(7), 671–675. https://doi.org/10.1038/nmeth.2089

Schneider, D. T., Zahn, S., Sievers, S., Alemazkour, K., Reifenberger, G., Wiestler, O. D., Calaminus, G., Göbel, U., & Perlman, E. J. (2006). Molecular genetic analysis of central nervous system germ cell tumors with comparative genomic hybridization. *Modern Pathology*, *19*(6), 864–873. https://doi.org/10.1038/modpathol.3800607

Schober, M., Schaefer, M., & Knoblich, J. A. (1999). Bazooka recruits Inscuteable to orient asymmetric cell divisions in Drosophila neuroblasts. *Nature*, *402*(6761), 548–551. https://doi.org/10.1038/990135

Shahzad, U., Taccone, M. S., Kumar, S. A., Okura, H., Krumholtz, S., Ishida, J., Mine, C., Gouveia, K., Edgar, J., Smith, C., Hayes, M., Huang, X., Derry, W. B., Taylor, M. D., & Rutka, J. T. (2021). Modeling human brain tumors in flies, worms, and zebrafish: From proof of principle to novel therapeutic targets. *Neuro-Oncology*, *23*(5), 718–731. https://doi.org/10.1093/neuonc/noaa306

Shen, C.-P., Jan, L. Y., & Jan, Y. N. (1997). Miranda Is Required for the Asymmetric Localization of Prospero during Mitosis in Drosophila. *Cell*, *90*(3), 449–458. https://doi.org/10.1016/S0092-8674(00)80505-X

Sherman, B. T., Hao, M., Qiu, J., Jiao, X., Baseler, M. W., Lane, H. C., Imamichi, T., & Chang, W. (2022). DAVID: A web server for functional enrichment analysis and functional annotation of gene lists (2021 update). *Nucleic Acids Research*, *50*(W1), W216–W221. https://doi.org/10.1093/nar/gkac194

Shim, H., Chun, Y. S., Lewis, B. C., & Dang, C. V. (1998). A unique glucose-dependent apoptotic pathway induced by c-Myc. *Proceedings of the National Academy of Sciences*, *95*(4), 1511–1516. https://doi.org/10.1073/pnas.95.4.1511

Shohayeb, B., Mitchell, N., Millard, S. S., Quinn, L. M., & Ng, D. C. H. (2020). Elevated levels of Drosophila Wdr62 promote glial cell growth and proliferation through AURKA signalling to AKT and MYC. *Biochimica et Biophysica Acta (BBA) - Molecular Cell Research*, *1867*(7), 118713. https://doi.org/10.1016/j.bbamcr.2020.118713

Siller, K. H., Cabernard, C., & Doe, C. Q. (2006). The NuMA-related Mud protein binds Pins and regulates spindle orientation in Drosophila neuroblasts. *Nature Cell Biology*, *8*(6), 594–600. https://doi.org/10.1038/ncb1412

Simpson, A. J. G., Caballero, O. L., Jungbluth, A., Chen, Y.-T., & Old, L. J. (2005). Cancer/testis antigens, gametogenesis and cancer. *Nature Reviews Cancer*, *5*(8), 615–625. https://doi.org/10.1038/nrc1669

Škrtić, M., Sriskanthadevan, S., Jhas, B., Gebbia, M., Wang, X., Wang, Z., Hurren, R., Jitkova, Y., Gronda, M., Maclean, N., Lai, C. K., Eberhard, Y., Bartoszko, J., Spagnuolo, P., Rutledge, A. C., Datti, A., Ketela, T., Moffat, J., Robinson, B. H., … Schimmer, A. D. (2011). Inhibition of Mitochondrial Translation as a Therapeutic Strategy for Human Acute Myeloid Leukemia. *Cancer Cell*, *20*(5), 674–688. https://doi.org/10.1016/j.ccr.2011.10.015

Slaidina, M., & Lehmann, R. (2014). Translational control in germline stem cell development. *Journal of Cell Biology*, *207*(1), 13–21. https://doi.org/10.1083/jcb.201407102

Song, Y., & Lu, B. (2011). Regulation of cell growth by Notch signaling and its differential requirement in normal vs. Tumor-forming stem cells in *Drosophila*. *Genes & Development*, *25*(24), 2644–2658. https://doi.org/10.1101/gad.171959.111

Sonoda, J. (2001). Drosophila Brain Tumor is a translational repressor. *Genes & Development*, *15*(6), 762–773. https://doi.org/10.1101/gad.870801

Sonoshita, M., & Cagan, R. L. (2017). Modeling Human Cancers in Drosophila. In *Current Topics in Developmental Biology* (Vol. 121, pp. 287–309). Elsevier. https://doi.org/10.1016/bs.ctdb.2016.07.008

Southall, T. D., & Brand, A. H. (2009). Neural stem cell transcriptional networks highlight genes essential for nervous system development. *The EMBO Journal*, *28*(24), 3799–3807. https://doi.org/10.1038/emboj.2009.309

Southall, T. D., Davidson, C. M., Miller, C., Carr, A., & Brand, A. H. (2014).

Dedifferentiation of Neurons Precedes Tumor Formation in lola Mutants. *Developmental Cell*, *28*(6), 685–696. https://doi.org/10.1016/j.devcel.2014.01.030

Southall, T. D., Gold, K. S., Egger, B., Davidson, C. M., Caygill, E. E., Marshall, O. J., & Brand, A. H. (2013). Cell-Type-Specific Profiling of Gene Expression and Chromatin Binding without Cell Isolation: Assaying RNA Pol II Occupancy in Neural Stem Cells. *Developmental Cell*, *26*(1), 101–112. https://doi.org/10.1016/j.devcel.2013.05.020

Sprangers, R., Groves, M. R., Sinning, I., & Sattler, M. (2003). High-resolution X-ray and NMR Structures of the SMN Tudor Domain: Conformational Variation in the Binding Site for Symmetrically Dimethylated Arginine Residues. *Journal of Molecular Biology*, *327*(2), 507–520. https://doi.org/10.1016/S0022-2836(03)00148-7

St Johnston, D., Beuchle, D., & Nüsslein-Volhard, C. (1991). Staufen, a gene required to localize maternal RNAs in the Drosophila egg. *Cell*, *66*(1), 51–63. https://doi.org/10.1016/0092-8674(91)90138-O

Stathakis, D. G., Pentz, E. S., Freeman, M. E., Kullman, J., Hankins, G. R., Pearlson, N. J., & Wright, T. R. (1995). The genetic and molecular organization of the Dopa decarboxylase gene cluster of Drosophila melanogaster. *Genetics*, *141*(2), 629–655. https://doi.org/10.1093/genetics/141.2.629

Stork, T., Sheehan, A., Tasdemir-Yilmaz, O. E., & Freeman, M. R. (2014). Neuron-Glia Interactions through the Heartless FGF Receptor Signaling Pathway Mediate Morphogenesis of Drosophila Astrocytes. *Neuron*, *83*(2), 388–403. https://doi.org/10.1016/j.neuron.2014.06.026

Strecker, T. R., Kongsuwan, K., Lengyel, J. A., & Merriam, J. R. (1986). The zygotic mutant tailless affects the anterior and posterior ectodermal regions of the Drosophila embryo. *Developmental Biology*, *113*(1), 64–76. https://doi.org/10.1016/0012-1606(86)90108-9

Stuelten, C. H., Parent, C. A., & Montell, D. J. (2018). Cell motility in cancer invasion and metastasis: Insights from simple model organisms. *Nature Reviews Cancer*, *18*(5), 296–312. https://doi.org/10.1038/nrc.2018.15

Sundareshan, T. (2003). Deletion of 6q23 as sole abnormality in acute myelocytic leukemia. *Cancer Genetics and Cytogenetics*, *143*(1), 87–88. https://doi.org/10.1016/S0165-4608(02)00822-1

Teleman, A. A., Hietakangas, V., Sayadian, A. C., & Cohen, S. M. (2008). Nutritional Control of Protein Biosynthetic Capacity by Insulin via Myc in Drosophila. *Cell Metabolism*, *7*(1), 21–32. https://doi.org/10.1016/j.cmet.2007.11.010

Tennessen, J. M., & Thummel, C. S. (2011). Coordinating Growth and Maturation—Insights from Drosophila. *Current Biology*, *21*(18), R750–R757. https://doi.org/10.1016/j.cub.2011.06.033

Thummel, C. S. (1996). Flies on steroids—Drosophila metamorphosis and the mechanisms of steroid hormone action. *Trends in Genetics*, *12*(8), 306–310. https://doi.org/10.1016/0168-9525(96)10032-9

Tio, M., Udolph, G., Yang, X., & Chia, W. (2001). Cdc2 links the Drosophila cell cycle and asymmetric division machineries. *Nature*, *409*(6823), 1063–1067. https://doi.org/10.1038/35059124

Trojer, P., Li, G., Sims, R. J., Vaquero, A., Kalakonda, N., Boccuni, P., Lee, D., Erdjument-Bromage, H., Tempst, P., Nimer, S. D., Wang, Y.-H., & Reinberg, D. (2007). L3MBTL1, a Histone-Methylation-Dependent Chromatin Lock. *Cell*, *129*(5), 915–928. https://doi.org/10.1016/j.cell.2007.03.048

Ugur, B., Chen, K., & Bellen, H. J. (2016). *Drosophila* tools and assays for the study of

human diseases. *Disease Models & Mechanisms*, *9*(3), 235–244. https://doi.org/10.1242/dmm.023762

Usui, H., Ichikawa, T., Kobayashi, K., & Kumanishi, T. (2000). Cloning of a novel murine gene Sfmbt, Scm-related gene containing four mbt domains, structurally belonging to the Polycomb group of genes. *Gene*, *248*(1–2), 127–135. https://doi.org/10.1016/S0378-1119(00)00131-1

van den Ameele, J., & Brand, A. H. (2019). Neural stem cell temporal patterning and brain tumour growth rely on oxidative phosphorylation. *ELife*, *8*. https://doi.org/10.7554/eLife.47887

Velazquez-Ulloa, N. A. (2017). A Drosophila model for developmental nicotine exposure. *PLOS ONE*, *12*(5), e0177710. https://doi.org/10.1371/journal.pone.0177710

Wang, H., Ouyang, Y., Somers, W. G., Chia, W., & Lu, B. (2007). Polo inhibits progenitor self-renewal and regulates Numb asymmetry by phosphorylating Pon. *Nature*, *449*(7158), 96–100. https://doi.org/10.1038/nature06056

Wang, H., Somers, G. W., Bashirullah, A., Heberlein, U., Yu, F., & Chia, W. (2006). Aurora-A acts as a tumor suppressor and regulates self-renewal of Drosophila neuroblasts. *Genes & Development*, *20*(24), 3453–3463. https://doi.org/10.1101/gad.1487506

Wang, J.-H. (2010). *Drosophila* as a model for antiviral immunity. *World Journal of Biological Chemistry*, *1*(5), 151. https://doi.org/10.4331/wjbc.v1.i5.151

Wang, W. K., Tereshko, V., Boccuni, P., MacGrogan, D., Nimer, S. D., & Patel, D. J. (2003). Malignant Brain Tumor Repeats. *Structure*, *11*(7), 775–789. https://doi.org/10.1016/S0969-2126(03)00127-8

Wang, W., Liu, W., Wang, Y., Zhou, L., Tang, X., & Luo, H. (2011). Notch signaling regulates neuroepithelial stem cell maintenance and neuroblast formation in Drosophila optic lobe development. *Developmental Biology*, *350*(2), 414–428. https://doi.org/10.1016/j.ydbio.2010.12.002

Warburg, O. (1925). The Metabolism of Carcinoma Cells. *The Journal of Cancer Research*, *9*(1), 148–163. https://doi.org/10.1158/jcr.1925.148

Wasylyk, B., Hahn, S. L., & Giovane, A. (1994). The Ets family of transcription factors. In P. Christen & E. Hofmann, *EJB Reviews 1993* (pp. 7–18). Springer Berlin Heidelberg. https://doi.org/10.1007/978-3-642-78757-7_2

Watson, K. L., Justice, R. W., & Bryant, P. J. (1994). *Drosophila* in cancer research: The first fifty tumor suppressor genes. *Journal of Cell Science*, *1994*(Supplement_18), 19–33. https://doi.org/10.1242/jcs.1994.Supplement_18.4

Weng, M., Haenfler, J. M., & Lee, C.-Y. (2012). Changes in *Notch* signaling coordinates maintenance and differentiation of the *Drosophila* larval optic lobe neuroepithelia. *Developmental Neurobiology*, *72*(11), 1376–1390. https://doi.org/10.1002/dneu.20995

Wieschaus, E., & Nüsslein-Volhard, C. (2016). The Heidelberg Screen for Pattern Mutants of *Drosophila*: A Personal Account. *Annual Review of Cell and Developmental Biology*, *32*(1), 1–46. https://doi.org/10.1146/annurev-cellbio-113015-023138

Wismar, J., Löffler, T., Habtemichael, N., Vef, O., Geißen, M., Zirwes, R., Altmeyer, W., Sass, H., & Gateff, E. (1995). The Drosophila melanogaster tumor suppressor gene lethal(3)malignant brain tumor encodes a proline-rich protein with a novel zinc finger. *Mechanisms of Development*, *53*(1), 141–154. https://doi.org/10.1016/0925-4773(95)00431-9

Wissel, S., Harzer, H., Bonnay, F., Burkard, T. R., Neumüller, R. A., & Knoblich, J. A.

(2018). Time-resolved transcriptomics in neural stem cells identifies a v-ATPase/Notch regulatory loop. *Journal of Cell Biology*, *217*(9), 3285–3300. https://doi.org/10.1083/jcb.201711167

Witte, H. T., Jeibmann, A., Klämbt, C., & Paulus, W. (2009). Modeling Glioma Growth and Invasion in Drosophila melanogaster. *Neoplasia*, *11*(9), 882–888. https://doi.org/10.1593/neo.09576

Wodarz, A. (2005). Molecular control of cell polarity and asymmetric cell division in Drosophila neuroblasts. *Current Opinion in Cell Biology*, *17*(5), 475–481. https://doi.org/10.1016/j.ceb.2005.08.005

Wodarz, A., Ramrath, A., Kuchinke, U., & Knust, E. (1999). Bazooka provides an apical cue for Inscuteable localization in Drosophila neuroblasts. *Nature*, *402*(6761), 544–547. https://doi.org/10.1038/990128

Woodhouse, E., Hersperger, E., & Shearn, A. (1998). Growth, metastasis, and invasiveness of Drosophila tumors caused by mutations in specific tumor suppressor genes. *Development Genes and Evolution*, *207*(8), 542–550. https://doi.org/10.1007/s004270050145

Wright, T. R. F., Beermann, W., Marsh, J. L., Bishop, C. P., Steward, R., Black, B. C., Tomsett, A. D., & Wright, E. Y. (1981). The genetics of dopa decarboxylase in Drosophila melanogaster: IV. The genetics and cytology of the 37B10-37D1 region. *Chromosoma*, *83*(1), 45–58. https://doi.org/10.1007/BF00286015

Xiao, Q., Komori, H., & Lee, C.-Y. (2012). *Klumpfuss* distinguishes stem cells from progenitor cells during asymmetric neuroblast division. *Development*, *139*(15), 2670–2680. https://doi.org/10.1242/dev.081687

Yasugi, T., Umetsu, D., Murakami, S., Sato, M., & Tabata, T. (2008). *Drosophila* optic lobe neuroblasts triggered by a wave of proneural gene expression that is negatively regulated by JAK/STAT. *Development*, *135*(8), 1471–1480. https://doi.org/10.1242/dev.019117

Yohn, C. B., Pusateri, L., Barbosa, V., & Lehmann, R. (2003). *L(3)malignant brain tumor* and Three Novel Genes Are Required for Drosophila Germ-Cell Formation. *Genetics*, *165*(4), 1889–1900. https://doi.org/10.1093/genetics/165.4.1889

Yu, F., Kuo, C. T., & Jan, Y. N. (2006). Drosophila Neuroblast Asymmetric Cell Division: Recent Advances and Implications for Stem Cell Biology. *Neuron*, *51*(1), 13–20. https://doi.org/10.1016/j.neuron.2006.06.016

Zhang, Q., Shalaby, N. A., & Buszczak, M. (2014). Changes in rRNA Transcription Influence Proliferation and Cell Fate Within a Stem Cell Lineage. *Science*, *343*(6168), 298–301. https://doi.org/10.1126/science.1246384

Zhang, W., Yu, Y., Hertwig, F., Thierry-Mieg, J., Zhang, W., Thierry-Mieg, D., Wang, J., Furlanello, C., Devanarayan, V., Cheng, J., Deng, Y., Hero, B., Hong, H., Jia, M., Li, L., Lin, S. M., Nikolsky, Y., Oberthuer, A., Qing, T., … Fischer, M. (2015). Comparison of RNA-seq and microarray-based models for clinical endpoint prediction. *Genome Biology*, *16*(1), 133. https://doi.org/10.1186/s13059-015-0694-1

Zhou, L., & Luo, H. (2013). Replication Protein A Links Cell Cycle Progression and the Onset of Neurogenesis in Drosophila Optic Lobe Development. *Journal of Neuroscience*, *33*(7), 2873–2888. https://doi.org/10.1523/JNEUROSCI.3357-12.2013

Zisi, A., Bartek, J., & Lindström, M. S. (2022). Targeting Ribosome Biogenesis in Cancer: Lessons Learned and Way Forward. *Cancers*, *14*(9), 2126. https://doi.org/10.3390/cancers14092126

8. Appendix

Appendix A

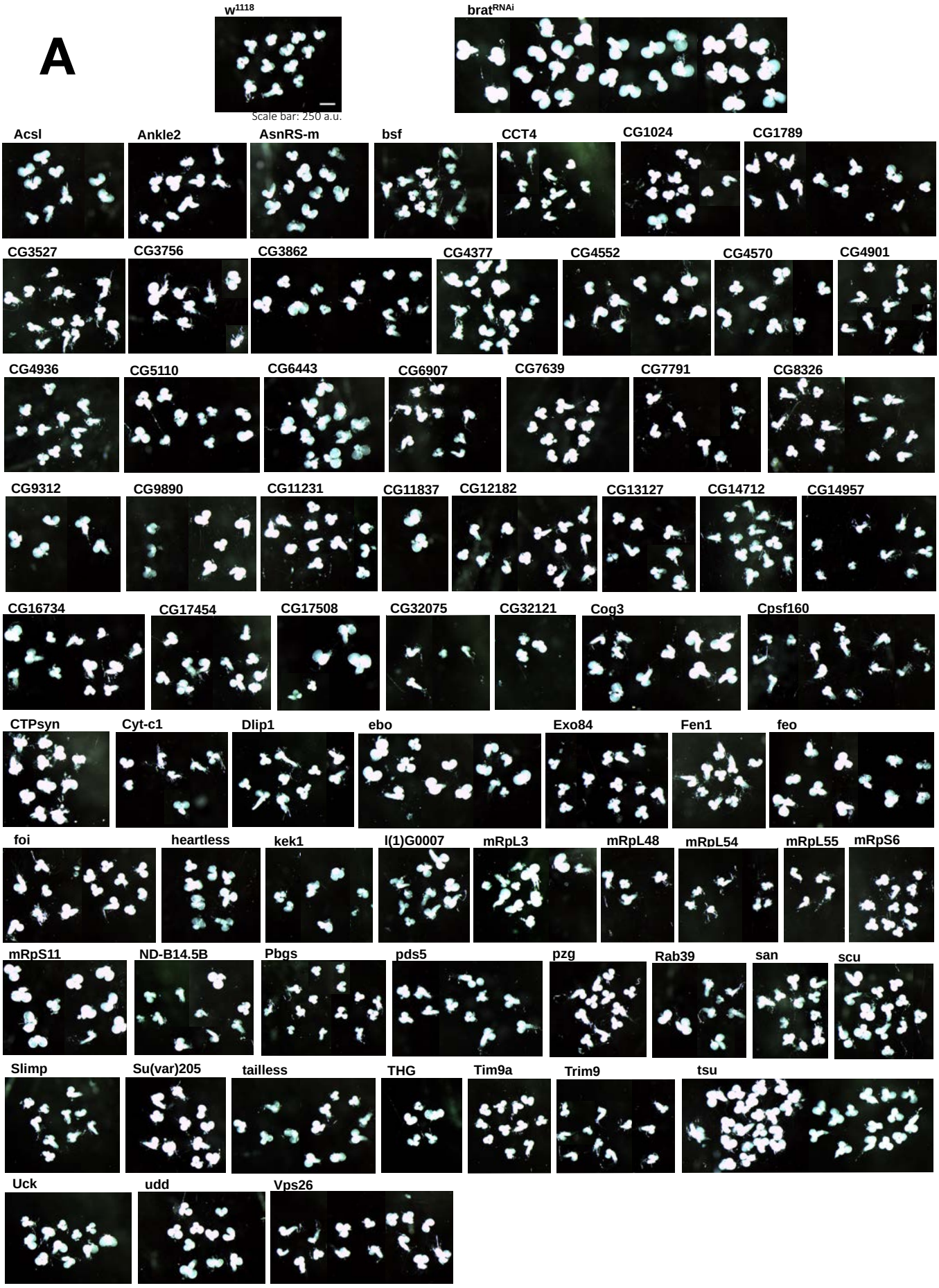
A
w1118
bratRNAi
Scale bar: 250 a.u.
Acsl
Ankle2
AsnRS-m
bsf
CCT4
CG1024
CG1789
CG3527
CG3756
CG3862
CG4377
CG4552
CG4570
CG4901
CG4936
CG5110
CG6443
CG6907
CG7639
CG7791
CG8326
CG9312
CG9890
CG11231
CG11837
CG12182
CG13127
CG14712
CG14957
CG16734
CG17454
CG17508
CG32075
CG32121
Cog3
Cpsf160
CTPsyn
Cyt-c1
Dlip1
ebo
Exo84
Fen1
feo
foi
heartless
kek1
l(1)G0007
mRpL3
mRpL48
mRpL54
mRpL55
mRpS6
mRpS11
ND-B14.5B
Pbgs
pds5
pzg
Rab39
san
scu
Slimp
Su(var)205
tailless
THG
Tim9a
Trim9
tsu
Uck
udd
Vps26

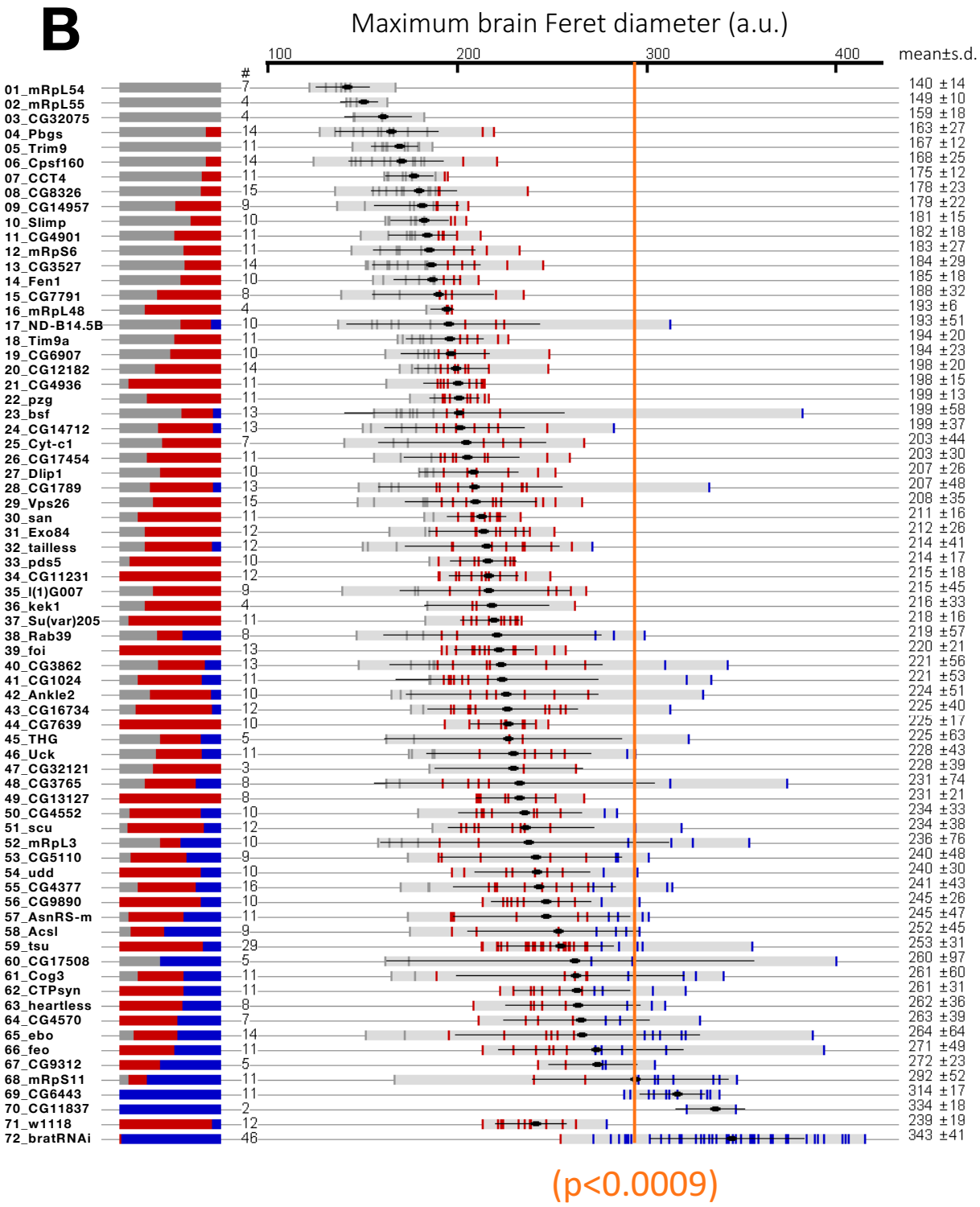

Appendix A. Results from the high content screen for brat-SPRs (A) Panels showing larval brains from each if the RNAi lines analysed. **(B)** Plot of larval brain sizes. Each vertical bar corresponds to one brain. Colour code: smaller than wild type=grey, wild-type size =red, and tumour size =blue. The corresponding mean and s.d. values are shown on the right.

Appendix B

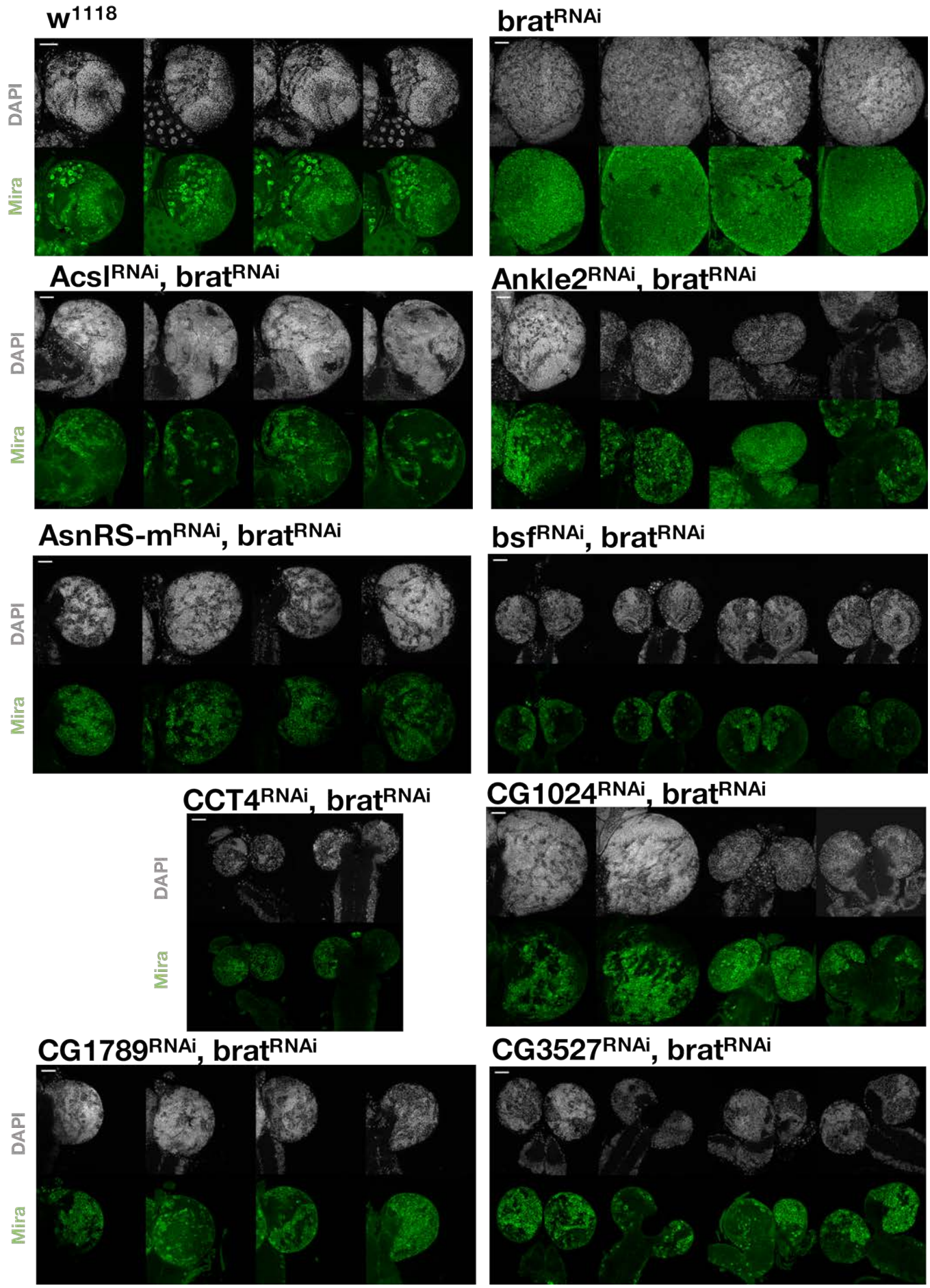
w1118
bratRNAi
AcsIRNAi, bratRNAi
Ankle2RNAi, bratRNAi
AsnRS-mRNAi, bratRNAi
bsfRNAi, bratRNAi
CCT4RNAi, bratRNAi
CG1024RNAi, bratRNAi
CG1789RNAi, bratRNAi
CG3527RNAi, bratRNAi
DAPI
Mira

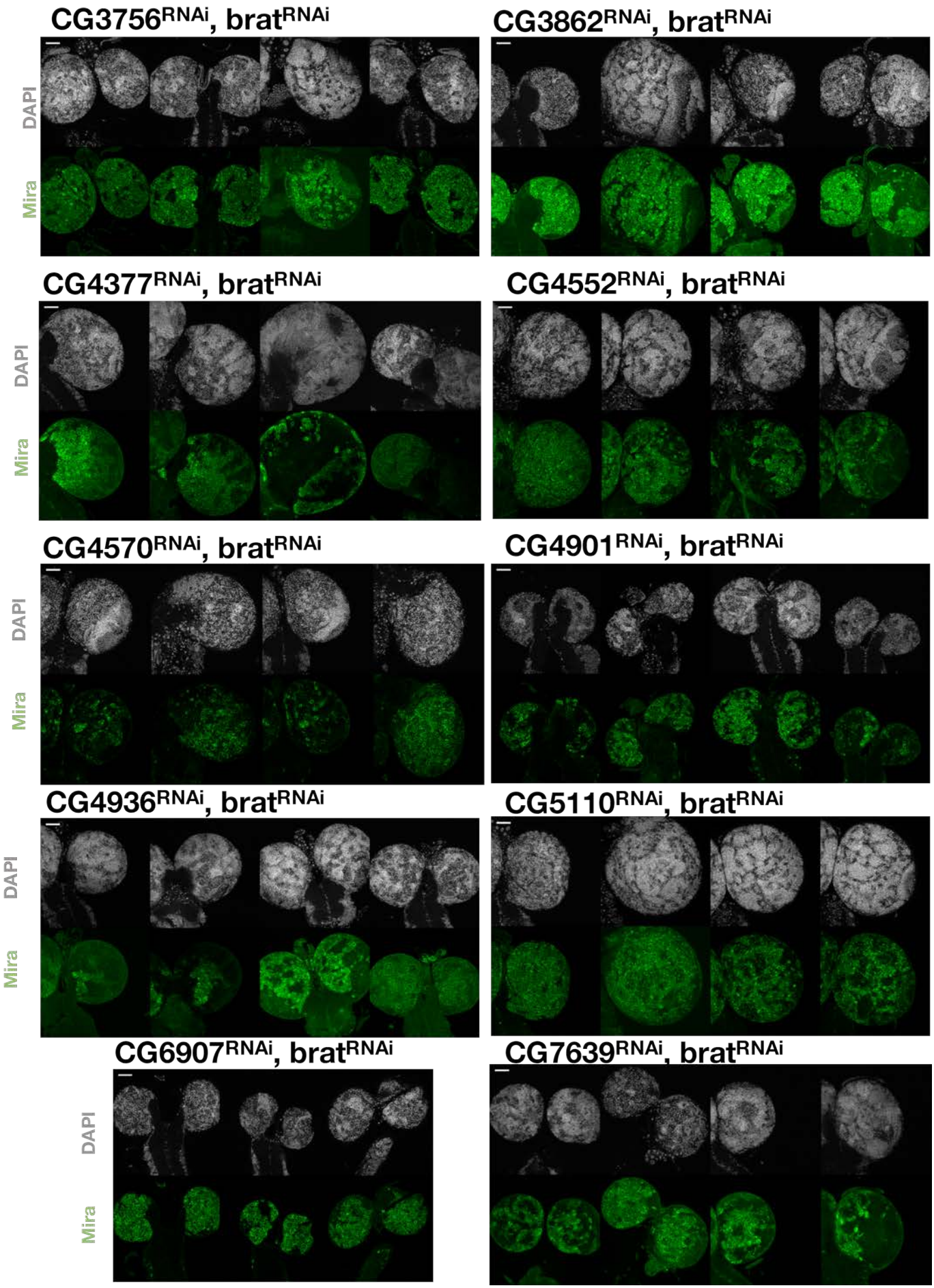
CG3756RNAi, bratRNAi
CG3862RNAi, bratRNAi
CG4377RNAi, bratRNAi
CG4552RNAi, bratRNAi
CG4570RNAi, bratRNAi
CG4901RNAi, bratRNAi
CG4936RNAi, bratRNAi
CG5110RNAi, bratRNAi
CG6907RNAi, bratRNAi
CG7639RNAi, bratRNAi
DAPI
Mira

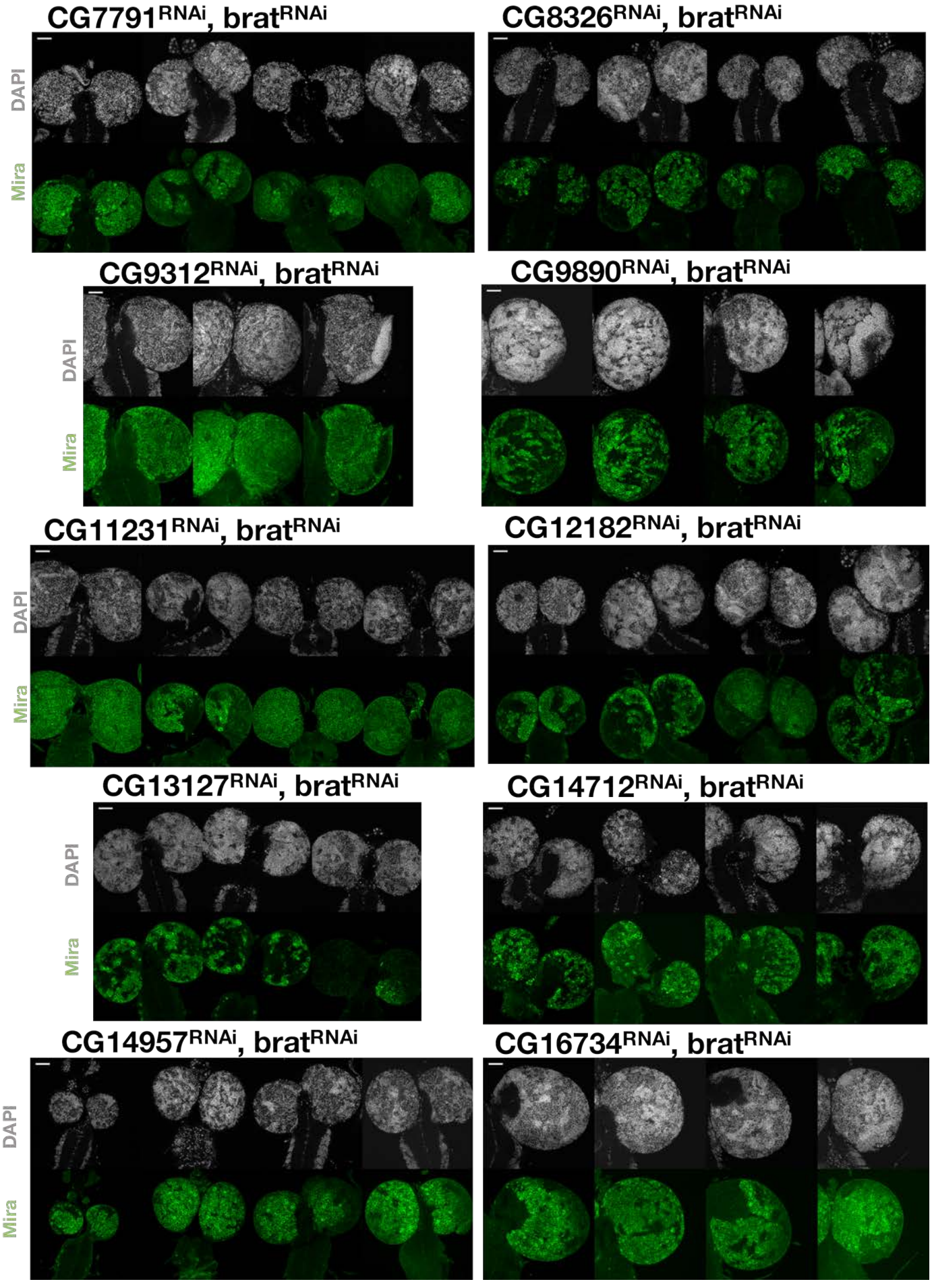
CG7791RNAi, bratRNAi
CG8326RNAi, bratRNAi
CG9312RNAi, bratRNAi
CG9890RNAi, bratRNAi
CG11231RNAi, bratRNAi
CG12182RNAi, bratRNAi
CG13127RNAi, bratRNAi
CG14712RNAi, bratRNAi
CG14957RNAi, bratRNAi
CG16734RNAi, bratRNAi
DAPI
Mira

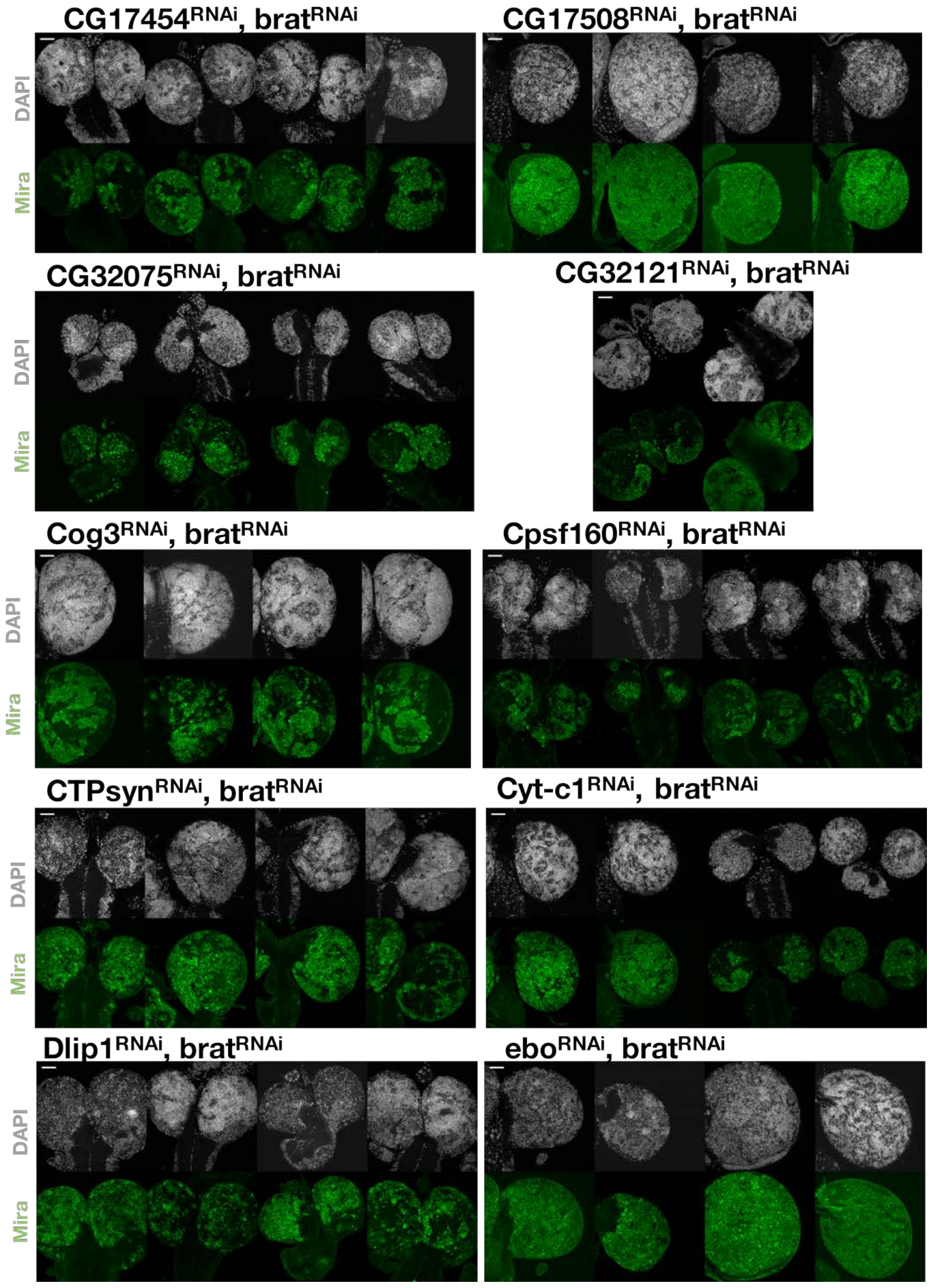
CG17454RNAi, bratRNAi
CG17508RNAi, bratRNAi
CG32075RNAi, bratRNAi
CG32121RNAi, bratRNAi
Cog3RNAi, bratRNAi
Cpsf160RNAi, bratRNAi
CTPsynRNAi, bratRNAi
Cyt-c1RNAi, bratRNAi
Dlip1RNAi, bratRNAi
eboRNAi, bratRNAi
DAPI
Mira

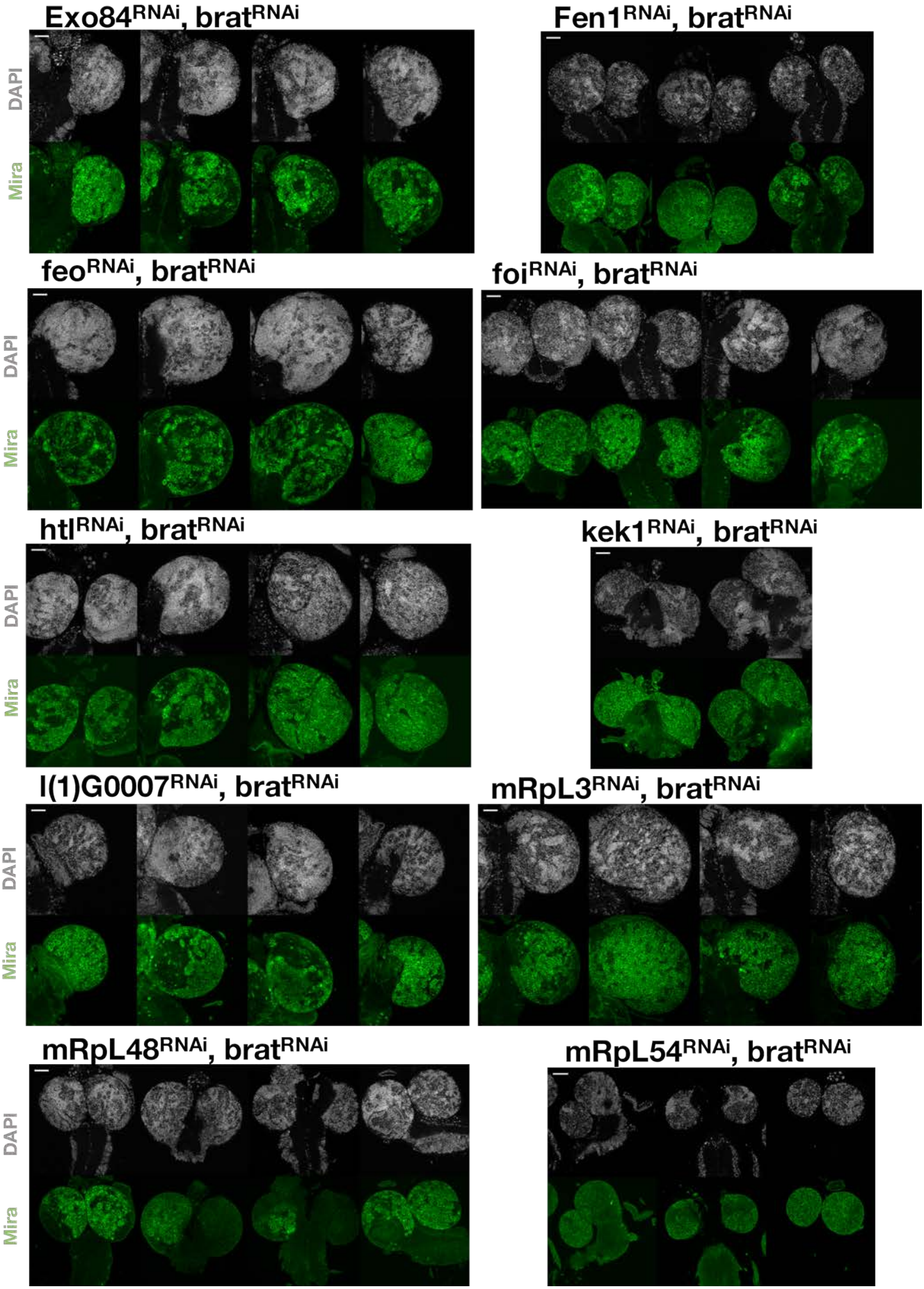
Exo84RNAi, bratRNAi
Fen1RNAi, bratRNAi
feoRNAi, bratRNAi
foiRNAi, bratRNAi
htlRNAi, bratRNAi
kek1RNAi, bratRNAi
l(1)G0007RNAi, bratRNAi
mRpL3RNAi, bratRNAi
mRpL48RNAi, bratRNAi
mRpL54RNAi, bratRNAi
DAPI
Mira

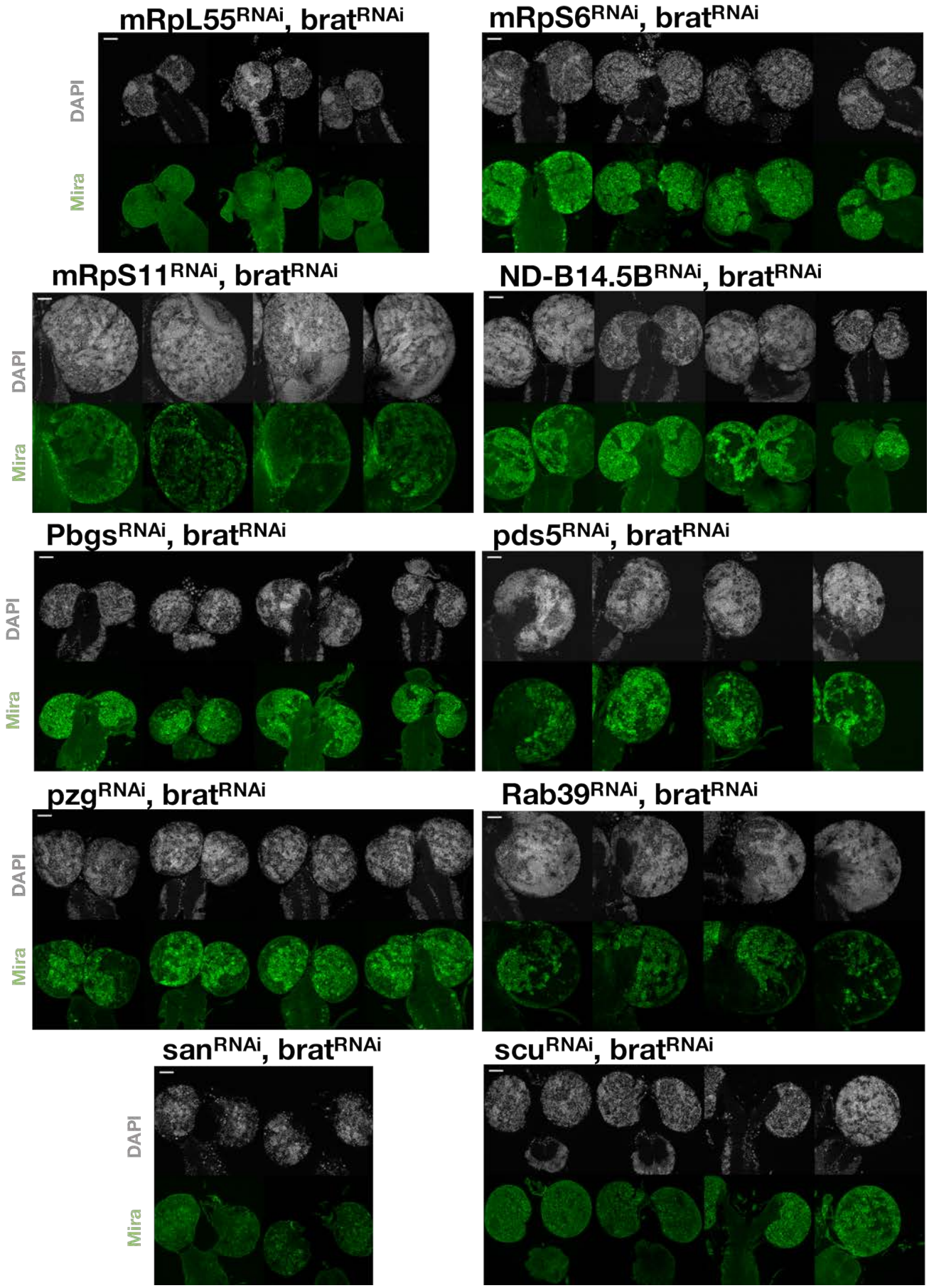
mRpL55RNAi, bratRNAi
mRpS6RNAi, bratRNAi
mRpS11RNAi, bratRNAi
ND-B14.5BRNAi, bratRNAi
PbgsRNAi, bratRNAi
pds5RNAi, bratRNAi
pzgRNAi, bratRNAi
Rab39RNAi, bratRNAi
sanRNAi, bratRNAi
scuRNAi, bratRNAi
DAPI
Mira

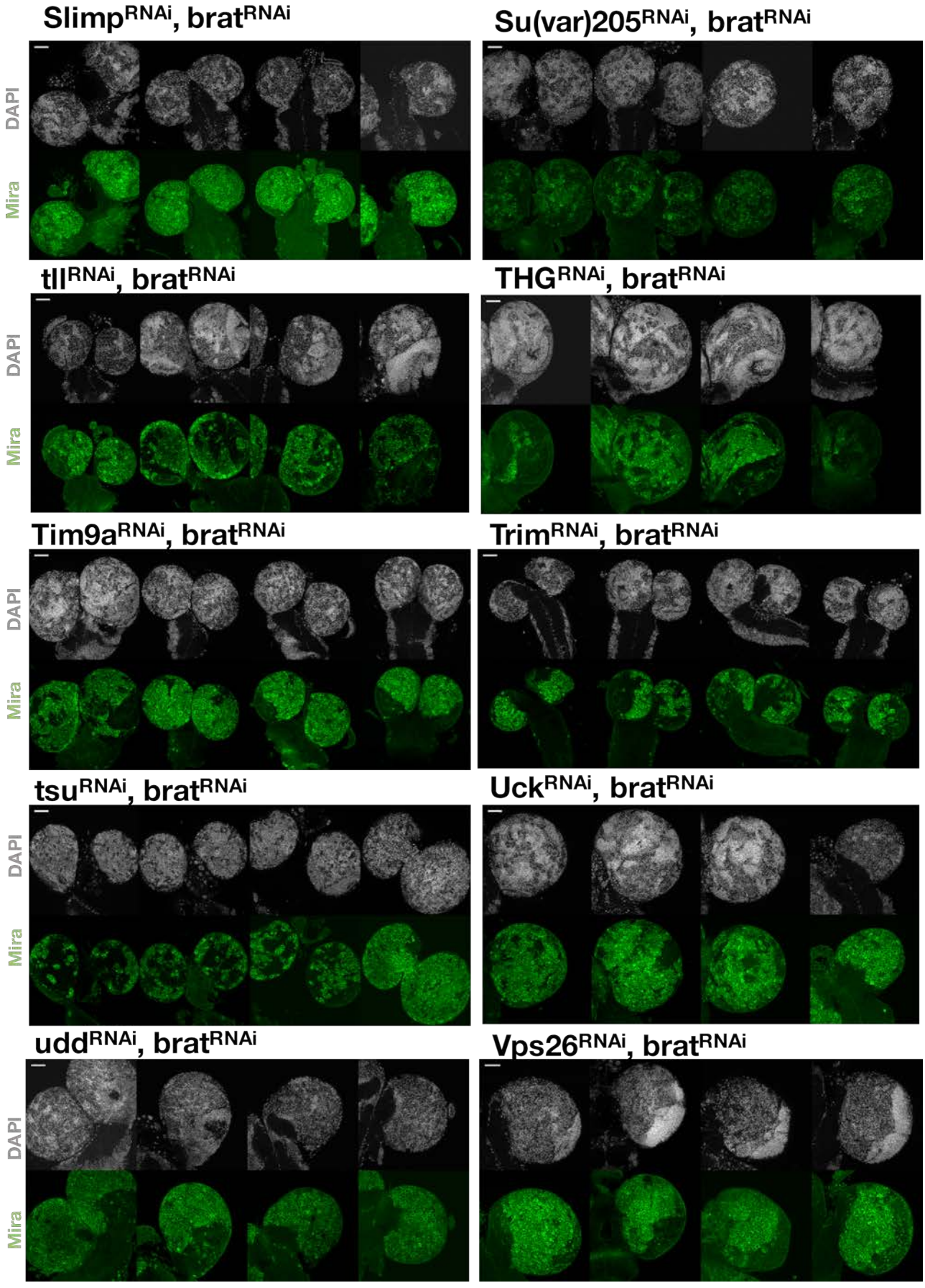
Slimp^RNAi, brat^RNAi
Su(var)205^RNAi, brat^RNAi
tll^RNAi, brat^RNAi
THG^RNAi, brat^RNAi
Tim9a^RNAi, brat^RNAi
Trim^RNAi, brat^RNAi
tsu^RNAi, brat^RNAi
Uck^RNAi, brat^RNAi
udd^RNAi, brat^RNAi
Vps26^RNAi, brat^RNAi
DAPI
Mira

Appendix B. Phenotype of brat tumours suppressed with each brat-SPR. Panels showing dorsal sections of suppressed brat brain lobes from each brat-SPR stained with DAPI (grey) and Mira (green), to reveal morphology and NB distribution. Mira levels have been digitally enhanced.

Appendix C

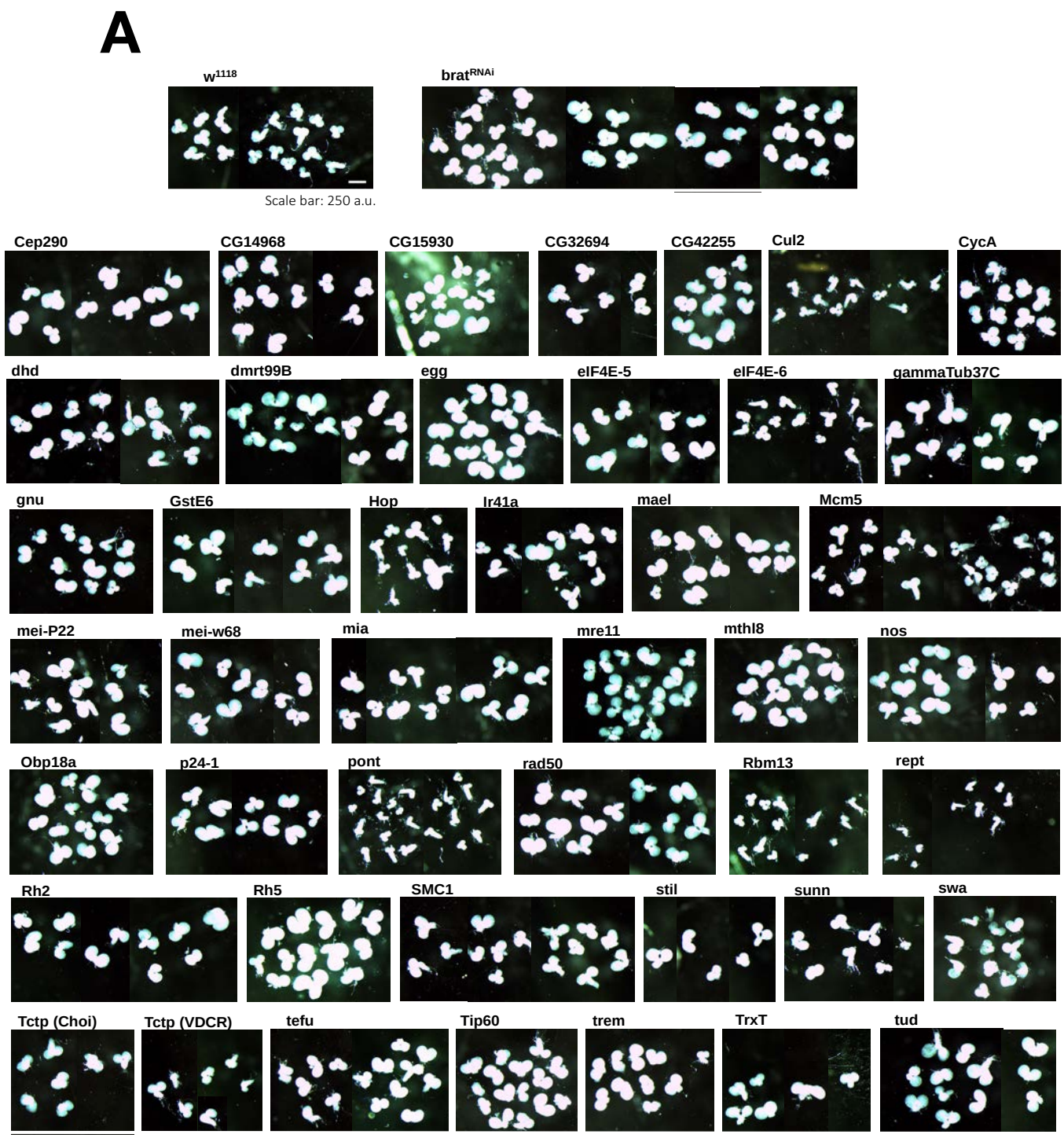
A
w1118
bratRNAi
Scale bar: 250 a.u.
Cep290
CG14968
CG15930
CG32694
CG42255
Cul2
CycA
dhd
dmrt99B
egg
eIF4E-5
eIF4E-6
gammaTub37C
gnu
GstE6
Hop
Ir41a
mael
Mcm5
mei-P22
mei-w68
mia
mre11
mthl8
nos
Obp18a
p24-1
pont
rad50
Rbm13
rept
Rh2
Rh5
SMC1
stil
sunn
swa
Tctp (Choi)
Tctp (VDCR)
tefu
Tip60
trem
TrxT
tud

B

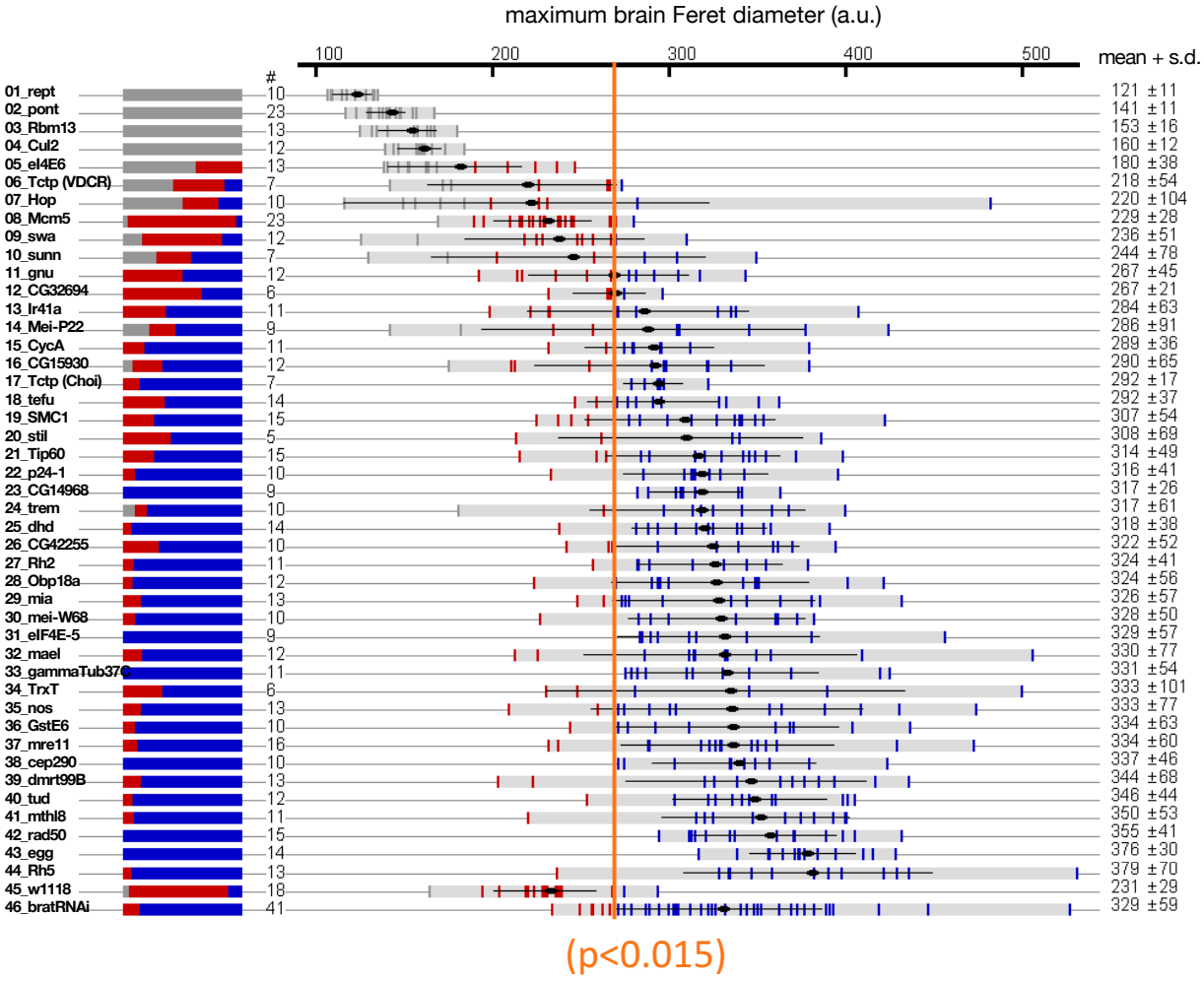

Appendix C. Results for depletion of mbt-biased SPRs in brat background. (A) Panels showing larval brains from each of the RNAi lines analysed. **(B)** Plot of larval brain sizes. Each vertical bar corresponds to one brain. Colour code: smaller than wild type=grey, wild-type size =red, and tumour size =blue. The corresponding mean and s.d. values are shown on the right.

Appendix D

D1.

Excel file: Results from high content screen (4300 VDRC lines) (file "Supplementary_Thesis_Brat_screening" on CD).

D2.

Excel file: Gene expression values and differential expression results from Affymetrix analysis (file"Supplementary_Thesis_Brat_Transcriptome_Affymetrix" on CD).